Development of a novel bioassay and portable spectrometer to assess inorganic arsenic bioavailability in the environment

Martin Pothier

August, 2020

Thesis submitted to the University of Ottawa
in partial Fulfillment of the requirements for the
Doctorate in Philosophy Biology
Specialization in Chemical and Environmental Toxicology

Department of Biology
Faculty of Science
University of Ottawa

ABSTRACT

Purpose

Arsenic is a notorious poison due to its high toxicity, worldwide distribution, and lack of any taste and colour once dissolved. The abundance of arsenic in Earth's crust makes that it can naturally find its way into food and drinking water. Rapid and reliable detection of arsenic, directly in the field, is critical to support evidence-based decision-making in choosing irrigation or drinking water sources. Current cost-effective colourimetric techniques are associated with poor accuracy, health risks, and unacceptable levels of false negatives. Arsenic-specific cellular sensors, or biosensors, may present an inexpensive, safe, and renewable alternative, yet they have long been criticized for unsatisfactory sensing performance, and inconsistency of the outcome. This, in addition to the lack of suitable instruments capable of measuring the signals produced by these biosensors, has led to very few solutions reaching market. The goal of my thesis research was to test hypotheses that improve our fundamental understanding of As species biogeochemistry in simple and complex environmental matrices to then develop a new arsenic monitoring interface, one that would be both simple and accessible to the general public.

Contributions

Using a combination of wild-type and mutant strains, I managed to detail both the internal regulation of arsenic, and the external drivers of arsenic bioavailability. I started by designing a defined exposure protocol that achieved, for the first time, equimolar uptake of over 94% of the added As(III) and As(V) into the cells. By developing this control early into my thesis, I then worked to reintroduce commonly found constituents of environmental waters that are thought to impact arsenic uptake. This direct testing approach uncovered fundamentals of environmental arsenic redox chemistry such as As(III) photooxidation in solution, environmental ligand exchanges, and biological transport pathways.

Applications

Simplifying a complex exposure protocol for use by the general public required automation of the data analysis steps. This consists of several hundred lines of code, capable of analyzing, normalizing and stabilizing biosensor output to improve the consistency and robustness of this system. These algorithms were then integrated into a new arsenic monitoring interface, one that was built and designed specifically for dehydrated biosensors. This portable, low-cost spectrometer achieved a fluorescent detection range that rivals expensive and sophisticated laboratory equipment at a fraction of the price, and without the need for a computer to compile the measurements. In contrast to highly criticized colorimetric techniques, the biosensor exposure protocol exceeds in operational use, reliability and detection limit. At its core, my thesis research provides a new and complete arsenic testing solution, one capable of measuring both As(III) and As(V) at levels relevant to the World Health Organization and Canadian guidelines for arsenic content in water (10 µg/L). It also provides a new method capable of selectively discriminating between arsenic species, thereby providing an inexpensive and high-throughput arsenic speciation method. I hope this work will help kickstart development of a marketable solution that empowers individuals to test and to monitor the quality of their water sources.

RÉSUMÉ

Objectif

L'arsenic est un poison notoire en raison de sa toxicité élevée, sa distribution mondiale et son absence de gout et couleur une fois dissout. L'abondance d'arsenic dans la croûte terrestre lui permet de se retrouver naturellement dans les aliments et l'eau potable. La détection rapide et fiable d'arsenic directement sur le terrain, est donc essentielle pour soutenir la prise de décision fondée sur les données probantes en considération du choix de l'eau potable. Présentement, les techniques colorimétriques les plus rentables présentent un risque pour la santé est largement associé à une mauvaise précision, et à des taux inacceptables de faux négatifs. Les capteurs cellulaires spécifiques à l'arsenic, ou biocapteurs, peuvent s'avérer très utiles pour le dépistage, ou pour la détection rapide d'arsenic de façon économique, sécuritaire et renouvelable. Ceci dit, ces biocapteurs sont souvent reprochés pour leurs performances de détection insatisfaisante et pour une incohérence dans les résultats. Il y a également un manque d'instruments adaptés pour mesurer les signaux produits par ces biocapteurs, ce qui a abouti à très peu de solutions qui ont atteint le marché. Le but de ma thèse était de remettre en question les hypothèses qui pourraient améliorer notre compréhension fondamentale de la biogéochimie d'arsenic dans les matrices environnementales simples et complexes pour ensuite développer une nouvelle interface de surveillance d'arsenic, une qui serait facilement accessible au public.

Contribution

En utilisant une combinaison de souches sauvages et mutantes, j'ai réussi à préciser la régulation interne d'arsenic ainsi que les facteurs externes de biodisponibilité. J'ai commencé par développer un média dont les composantes sont précises et défini, ce qui m'a permis d'atteindre, pour la première fois, une absorption équimolaire de plus de 94% d'As(III) et d'As(V) ajoutés à travers les membranes cellulaires de ces

capteurs cellulaires. Ayant établi ce contrôle au début de ma thèse, j'ai ensuite travaillé à réintroduire certains constituants d'eaux environnementales, qui ont souvent été soupçonnés d'avoir un impact sur la prise en charge d'arsenic. Cette approche de mesure et d'analyse directe a permis de découvrir les principes fondamentaux de la chimie redox d'arsenic, les échanges environnementaux de ligands et les voies de transport biologiques.

Applications

La simplification d'un protocole d'exposition complexe, pour l'utilisation générale auprès du public, a nécessité l'automatisation des étapes d'analyses des données. Cela consiste de plusieurs centaines de lignes de code, qui analysent, normalisent et stabilisent le signal produit par ces biocapteurs. À l'aide d'une nouvelle interface, le cheminement de ces algorithmes a permis la conception d'un instrument adapté pour la détection de signaux provenant de biocapteurs déshydratés. Ce spectromètre portable et peu couteux, a atteint une plage de détection fluorescente qui fait compétition avec les équipements de laboratoire couteux et sophistiqué, sans avoir besoin d'ordinateur pour compiler les mesures. À la base, ma recherche fournit une solution complète et robuste qui permet de mesurer à la fois, As(III) et As(V) à des niveaux pertinents aux critères fixés par l'Organisation mondiale de la Santé et aux recommandations canadiennes pour la quantité d'arsenic trouvé dans l'eau potable (10 µg/L). À l'aide d'un milieu d'exposition sélectif, cette solution peut également fournir en tant qu'une méthode de spéciation d'arsenic peu couteuse, et à haut débit. Ensemble, j'espère que ma recherche pourra servir à expédier le développement d'une solution commercialisable qui permettra aux individus de tester et de surveiller la qualité des sources d'eau.

ACKNOWLEDGEMENTS

A great supervisor has an innate ability to tailor a support system that reaches each student individually. Dr. Poulain, you have offered me opportunities that no other has. You took the time to listen, provided me with guidance while working through solutions, then built an education plan that was perfectly fitted to my goals. I hope this journey was as meaningful and fulfilling to you as it was for me – I thank you.

When exploring a topic that touches on a number of disciplines, I quickly realized the importance of surrounding myself with research experts who are not afraid to challenge every aspect of the work. To my committee members and examiners, Dr. Jules Blais, Dr. Nadia Mykytczuk, Dr. Jesse Vermaire, Dr. Danielle Fortin and Dr. Scott Smith, your advice and guidance has helped focus my research objectives so that they maintain relevance to the fields while also avoiding the rabbit holes (at least I think it did). For these reasons and many more - I thank you.

Another important recognition only made itself apparent to me after embarking on in this endeavour. It starts with the network of people in my day-to-day activities, my lab mates Ben, Dr. Dan, Galen, Jess, Mija, Phil and many more. I thank you all for helping me ride the waves, especially those who helped filter out my frivolous ideas. This also includes the support staff Aaron (writing), Dave (Yellowknife) and Emmanuel (ICP). Likewise, I must acknowledge the internationals, Clément, Benjamin, Véronique and Cédric; thank you for immediately making Toulon feel like my second home. My time among you led me to explore exciting new opportunities and to foster lifelong relationships. I have also had the privilege to train and work with remarkable students. Charlotte, thanks for the long hours, enthusiasm and dedication you brought to the project. Justin and Steve, thank you for finding the time to introduce and guide the microbiologist to the mechanical engineering world.

Finally, to my friends and family. It is sometimes difficult to separate professional from personal support needs, especially when the work hours reach far into the night. This doctoral research was a long process, one where I had the opportunity to travel while I transitioned from a young student, into a loving husband and father. Thank you to the Pothier, Hammer and Kitchen families, and specially to my new wife and son. You mean the world to me.

TABLE OF CONTENTS

LIST OF FIGURES

LIST OF SUPPLEMENTAL FIGURES

LIST OF SUPPLEMENTAL TABLES

LIST OF SUPPLEMENTAL PROTOCOLS

LIST OF ABBREVIATIONS

[x]	Concentration of compound x;
ADC	Analog to digital converter;
As	Arsenic;
As(III)	Arsenite;
As(M)	Methylated arsenic;
As(T)	Total inorganic arsenic;
As(V)	Arsenate;
BMS	Battery management system;
DOC	Dissolved organic carbon;
DMA(III)	Dimethylarsinous acid;
DMA(V)	Dimethylarsinic acid;
DOM	Dissolved organic matter;
e-	Electron;
EDTA	Ethylenediaminetetraacetic acid
EM	Electromagnetic;
EPA	Environmental protection agency;
ESFA	Elliott soil fulvic acid;
FBMS	Field biosensor mixed salts;
HDPE	High density polyethylene;
HPLC	High performance liquid chromatography;
ICP-MS	Inductively coupled plasma - mass spectroscopy;
LB	Lysogeny Broth;
MGP	Mops glycerophosphate;
MIP	Mops Inorganic Phosphate;
MMA(III)	Monomethylarsinous acid;
MMA(V)	Monomethylarsonic acid;
MOPS	3-(N-morpholino)-propanesulphonic acid;
NOM	Natural organic matter;
NSERC	Natural sciences and engineering research council of Canada;
OD_{600}	Optical density at 600 nm;
PCB	Polychlorinated biphenyl;
pe	Concentration of electrons (-log[e-]);
pH	Concentration of protons (-log[H^+]);
PLA	Polylactic acid;
Pi	Inorganic phosphate;
pMP01	Arsenic biosensor;
RDA	redundancy analysis;
RFU	Relative fluorescent units;
SRFA	Suwannee river fulvic acid;
SRHA	Suwannee river humic acid.
TIA	Transimpedance amplifier;
UNEP	United nations environmental programme;
WHO	World health organization;

Chapter 1 – Introduction

1.1 Arsenic in the environment

From home remedies to witchcraft to poisons, arsenic has a rich and convoluted past. Occurring naturally, arsenic is a metalloid with the symbol As and the atomic number of 33. Arsenic is a redox active oxyanion, and, in certain situations, it is essential to life by serving as an electron acceptor during respiration and as an electron donor during photosynthesis (**Section 1.2.2**, **page 9**). While its uses are limited by its toxicity, it does have some applications in alloys, electronic manufacturing (semi-conductors), LEDs, pesticides, herbicides, insecticides and in cancer treatments. In the environment, As is found in water, soil, food and air. It is the 20th most abundant element and has been identified in over 300 minerals (*69*) making it one of the most prevalent and widely distributed elements on the Earth's crust (*21*).

1.1.1 Abundance, distribution and extraction

Arsenic is naturally found in water, soil, food and air with only one known stable isotope (^{75}As). The presence of As in food and drinking water is closely linked to its occurrence in minerals (*9*), making it possible to predict geographical patterns of exposure (*65*). The steady release of As in the environment is typically of natural origin, but can be exacerbated by anthropogenic activities.

1.1.1.1 Natural processes

With an estimated average abundance of 1.8 ppm (g/tonne) in crustal rocks (*30*), arsenic does not represent a major component but is often localized in abundance in

the form of minerals. Arsenides (i.e., NiAs), arsenates (i.e., $FeAsO_4 \cdot 2H_2O$), sulphides (i.e., FeAsS) and oxides (i.e., As_2O_3) are primary As minerals that are sensitive to changes in pH and redox potential. There are no permanent nor stable forms of storing arsenic. Volcanoes, forest fires and mineral erosion are some of the main routes of natural As redistribution. Once deposited, solid phase sorption (*e.g.* complexation onto oxide minerals) is the governing parameter controlling As concentration and therefore range of transportation.

In Canada, oxidation/reduction potential readily changes throughout the seasons which can lead to rapid mobilization of As to groundwater (*6, 69*). Bacteria are also dominant remobilizers of As in natural systems (*9*). Researchers have shown that, under laboratory conditions, even scorodite ($FeAsO_4 \cdot 2H_2O$), considered to be a common and stable secondary arsenate mineral, is subject to the Fe/As reductive dissolution by microbes (*67, 105*). Here, release of highly soluble inorganic As into soils and aquifers is a result of both natural weathering and biologically mediated dissolution of As; accessible for human consumption.

1.1.1.2 Anthropogenic processes

For centuries, sulphide ores containing high levels of As have been exploited for these frequently contain traces of gold, silver, iron, cobalt, nickel and more (*101*). When heated, As sublimes and oxidizes and becomes volatile with a garlic-like odour (*30*). During mining operations, the high temperatures of gold roasters and base metal smelters can lead the unintentional yet major releases of As in the air, and onto the surrounding landscape (*59, 64, 69*).

However, in many cases, a mixture of both natural and anthropogenic activities will exacerbate this release. An example is the low pH and metal(oid)s mine drainage that can occur during/after mine operations due to the combination of physiochemical weathering, and microbially assisted dissolution of As and from sulphide minerals

(*54, 61, 84*). Once released, the highly soluble inorganic As is subject to diverse modes of transportation before eventual consumption.

1.1.2 Speciation

Arsenic is highly susceptible to changes in redox potential (*50*), resulting in four possible valence states: +5 (arsenate), +3 (arsenite), -3 (arsine) and 0 (elemental) (*40*). In natural waters, As is mostly found as trivalent As(III) (H_3AsO_3), and pentavalent As(V) ($H_2AsO_4^-$) species where its charge, protonation and oxidation will depend on water pH and redox potential (**Figure 1.1**) (*21, 32*).

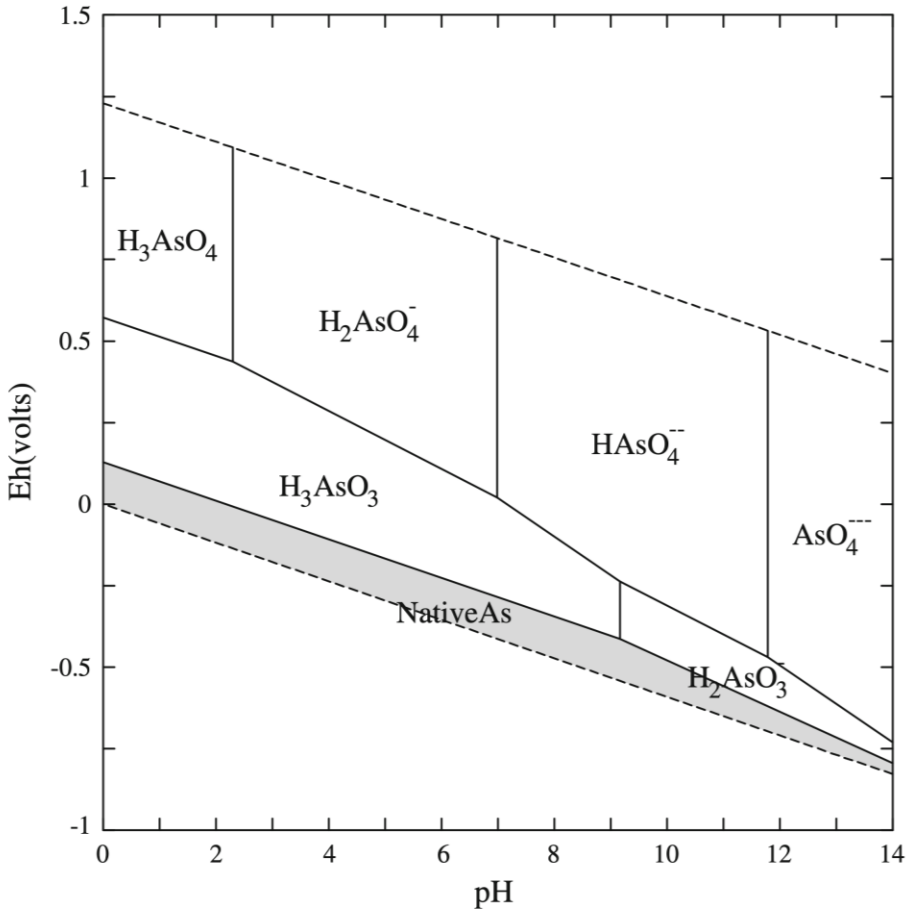

Fig. 1 Eh–pH diagram for the system As–O–H at 25°C and 1 bar. $\sum$As is set at 10^{-6} M. *Gray shaded area* denotes the solid phase

Figure 1.1 | How redox and pH conditions drive As speciation. Reprinted by permission from Springer Nature Customer Service Centre GmbH (the Licensor): Springer Nature, Environmental Earth Sciences '*Arsenic Eh-pH diagrams at 25ºC and 1 bar*', by Lu and Zhu (*50*). Copyright Springer-Verlag 2010.

The chemical/physical forms and oxidation states of As, better known as speciation, are properties which dictate its behaviour and ultimately play a crucial role in determining its transport, fate, and environmental consequences (*16, 42, 49, 65*).

i) **Concentration** – the presence of secondary As minerals (*e.g.,* amorphous iron or aluminum oxides) can reduce human exposure by binding As during precipitation events (*2, 23, 33*). Removal of As from water is also possible through precipitation processes such as ferric chloride (*e.g.*, $FeCl_3$).

ii) **Mobility** – neutrally charged As species are thought to travel longer distances in groundwater due to reduced solid phase interactions (*56*). It has been suggested that charged/dissolved As complexes are more likely to sorb onto solid phase minerals than neutral complexes (*111*), thus resulting in reduced mobility (*14*). Dissolved As concentrations have also been linked to increased phosphate amendments (*14*) and tend to follow calcium, ammonium and carbon profiles (*31*) (**Section 1.2.1**). Although some evidence is emerging (*76*), little is known of the mobility of methylated As compounds. This information is important to gather considering increased mobility means longer travel distances and therefore increased risk of human contact.

iii) **Toxicity** – following its injection, arsenic species present drastic differences in modes of toxic actions (**Section 1.1.3**).

1.1.3 Implications of arsenic speciation on human health

Arsenic exposure has been associated with a number of diseases including diabetes, hypertension, neurological disorders and more (*22*). It is also a well-established human carcinogen (*39*), yet it does not have a clear, unidirectional, adverse outcome pathway (*26*) (**Figure 1.2**).

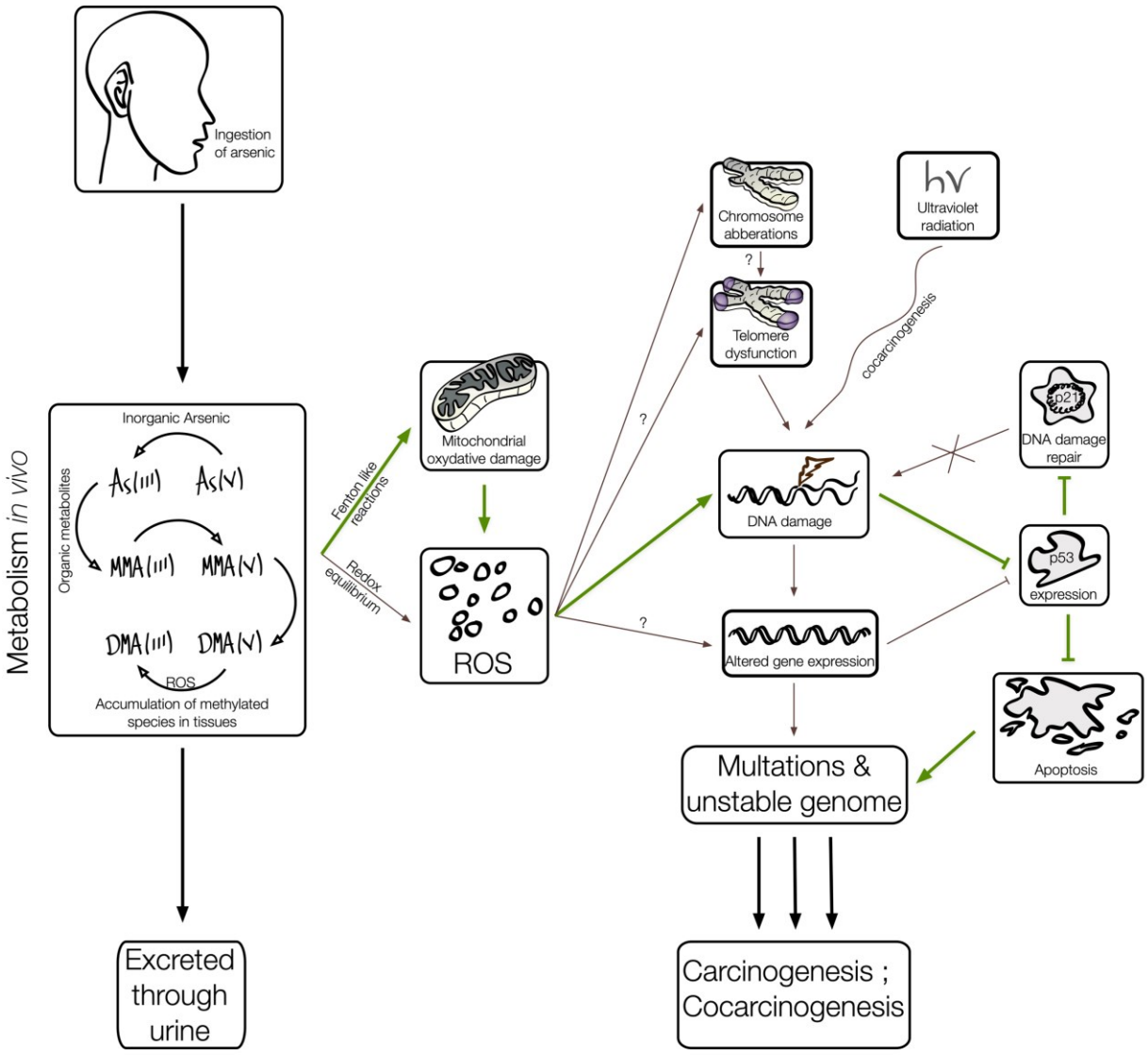

Figure 1.2 | Diagram showing the multiple possible mechanisms involved in As-induced carcinogenesis. All associations were gathered from a metanalysis of published scientific literature and summarized in the text (**Sections 1.1.3** and **1.1.4**). Pointed arrows denote activation or outcome of the pathway, while arrows with flat ends represent inhibition or a consequence. Pathways with common denominations among studies are highlighted in green while question marks present associations that require further research. **Abbreviations**: As(V), arsenate; As(III), arsenite; MMA(III), monomethylarsinous acid; MMA(V), monomethylarsonic acid; DMA(V), dimethylarsinic acid; DMA(III), dimethylarsinous acid; ROS, reactive oxygen species.

Both humans and mammals excrete organic As in their urine when only inorganic As was ingested (*10*). The result is rapid excretion of the metabolites through urine (*4*). Although this process does result in less overall As in the system,

these methylated metabolites have been shown to exert stronger cytotoxicity than its inorganic counterparts (*5*). Here, both DMA(V) and DMA(III) are reported to induce oxidative damage via production of reactive oxygen species (*89*). The result is altered gene expression (*40*), DNA oxidative damage (*74*), telomere dysfunction (*48*), genomic instability (*40, 48*), cytotoxicity, apoptosis (*106*), glutathione depletion at the mitochondrial wall (*106*), and more. ROS may even inhibit DNA repair signalling/mechanisms once damage has occurred (*41, 98*). Overall, As-induced carcinogenesis is thought to result from an accumulation of mutations from various sources that ultimately drives genetic alteration towards gross genomic instability, transforming a natural cell to a pre-cancerous state (*8*).

1.1.4 Species of interest

Studying the toxicokinetics of As in animal models has proven ineffective at exposure relevant concentrations (*26*) and has left an open and active debate regarding the most toxic species of As to humans. The bladder is a target tissue for As (*20*). Using EJ-1 human bladder cancer cells, current understanding places the order of cytotoxicity as DMA(III) > As(III) >> As(V) > MMA(V) > DMA(V) (*53*). Note that this information is subject to change as new findings emerge. That said, of the two dominant As species found in the environment, As(V) is shown to be far less cytotoxic than As(III) (*95*).

What is seemingly clear is that the speciation of As strongly affects its toxicity and mode of toxic action. Although exposure risk to As varies by local circumstances (*e.g.*, air, food, water and soil), the most pressing concern is typically when As is found in water (*15, 92*). There, it is odourless and tasteless and can enter food supply in high concentrations when irrigating crops with untreated water (*55, 114*).

1.2 Arsenic release and mobility

1.2.1 Biogeochemical cycle

The occurrence of As in lakes and groundwater is closely linked to geological sources and mostly derived from the interactions between groundwater and sediments (*92*). Crucial in the cycling of As in the environment is the complex biogeochemistry involved in mobilizing, transporting, and precipitating this contaminant. These relations are complex and have been summarized (**Figure 1.3**).

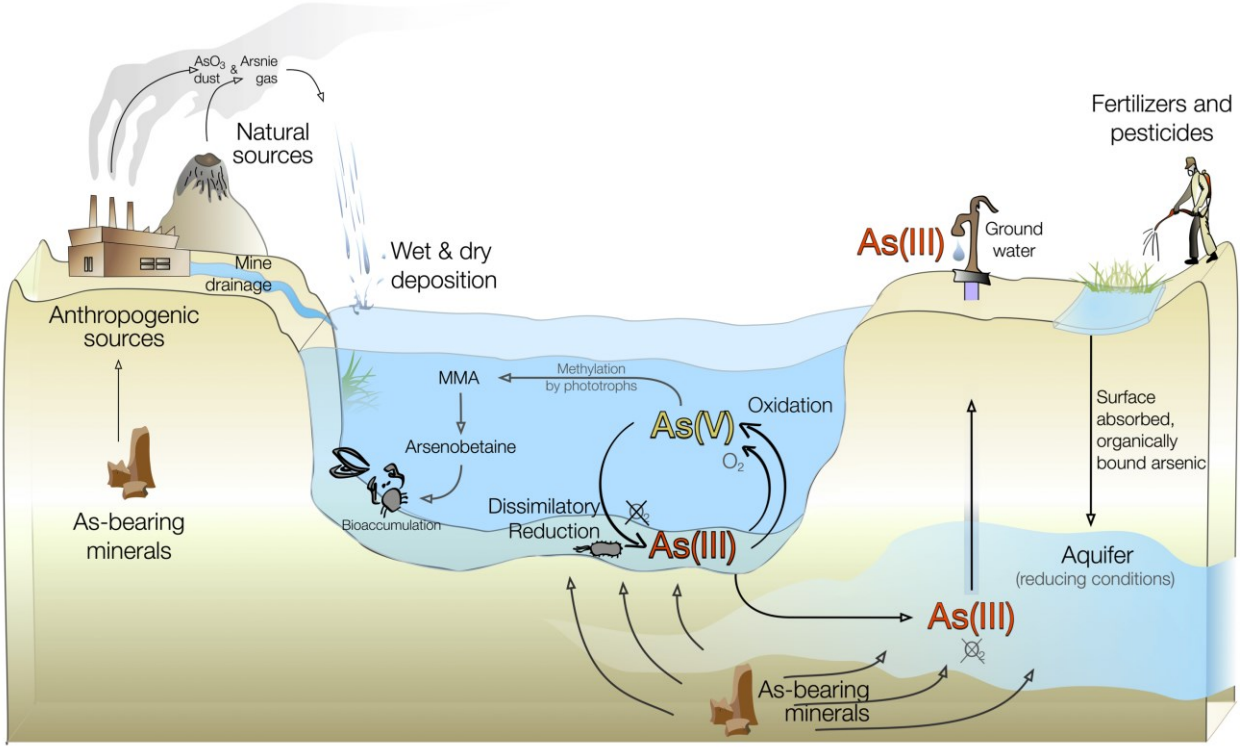

Figure 1.3 | Sources and distribution of arsenic species in the environment. Oxidized inorganic arsenate (As(V)) is the dominant species found in oxygenated surface waters while reduced inorganic arsenite (As(III)) is primarily found in anoxic groundwater.

Whether of natural or anthropogenic origin, release of As into a system can be quickly adsorbed back into solid forms thereby decreasing As concentration in that water body (*24*). This makes studying interactions between water and sediments difficult considering the complex set of biogeochemical processes that occur simultaneously across organic and inorganic particles and each transpiring at different reaction kinetics (*109*). Moreover, As interactions with solid phase minerals

will depend on the type of As-specific surface areas of the mineral phase (*e.g.*, amorphous iron oxides (HFO), goethite or magnetite (*24*)), and on the quantity of charged surface species (*111*). Finally, the biogeochemical cycle of As is also affected by other elements, namely:

i) **Carbon:** Dissolved organic matter (DOM) is a ubiquitous sorbent for As (*51*) that is strongly associated with As concentrations in sediments (*3*). There is a growing body of evidence pointing towards DOM as a governing factor in regulating the mobility and bioavailability of As by direct interactions (sorption/ligands) (*11, 97*) and through changes in reductive dissolution (*45, 51*). Surprisingly, little is known of the mechanisms involved in As-DOM interactions (*51, 93*).

ii) **Iron:** The precipitation of secondary iron (Fe) minerals greatly limits the dissolved concentration of As in the environment (*23*). For instance, Fe speciation can indirectly affect As concentration due to the numerous arsenic/phosphate specific sorption sites on the surface of hydrous ferric oxides (HFO) (*85*). In contrast, bacterial dissimilatory reduction and reductive dissolution of Fe oxides leads to the release of As in aquifers (*1, 67, 68*).

iii) **Sulphur:** In sediments, production of sulphide can reduce As(V) and mineralize As(III) in an iron-sulphur mineral (*75*). The speciation and charge of these sulphur complexes depend on the redox state. Microbially mediated sulphate reduction is, alone, unlikely to release As (*75*). In solution, sulphide released by sulphate-reducing bacteria acts in a similar fashion as it can precipitate or co-precipitate As from solution (*43*). In systems where sulphate concentrations are limited, dissolved As(III) can accumulate to high concentrations (*58*). In anoxic environments where sulphide concentrations are elevated, iron(II) sulphide minerals are pervasive and strongly govern the geochemical cycling of As (*111*).

iv) **Nitrogen:** Frequently found in agricultural runoffs, excess nitrate can lead to an eutrophic (hypoxic/anoxic) system and drive both Fe(II) (*107*) and As(III) oxidation (*34*) while also inhibiting arsenate dissimilatory reduction (*52*). Nitrate is a form of nitrogen that can serve as a strong oxidant of As(III) when oxygen is absent (*115*). Like sulphides, nitrate-dependent Fe(II) oxidation may limit As mobility in groundwater and sediments (*115*).

v) **Phosphate:** Phosphate is ubiquitous in environmental waters, sourced both from bedrocks and agricultural runoffs (*81, 82*). In many respects, As bares close similarities to phosphorous as both share the same valence and columns in the periodic table. Overall, phosphate has been shown to competitively desorb As in soils (*102*), clays (*62*), humic acids (*88*), metal hydroxides (*57*), and in minerals (*35*), thereby increasing the concentration of As in groundwater (*29*) and in plants (*14*). These findings, although limited, are indicative of major disruptions in the natural cycling of As in environmental waters. The impact of inorganic phosphate on the uptake of As in microbes was assessed in Chapter 2, and its impact on As-DOM interactions was assessed in Chapter 3.

1.2.2 The role of microbes

Many of the heavier elements that comprise Earth's crust are thought to be synthesized in the high temperature nuclear fusion processes of imploding-exploding stars (*103*). While the particular chemical processes that create As remains unclear (*60*), its presence in the universe (and therefore in crustal rocks) is ubiquitous and ancient. Thus, microbes have been exposed to As for several billion years (*86*) and evolved a complex set of genetic determinants that support As transformation pathways. These have been categorized into five groups (*28*):

i) As(V) cytoplasmic reduction and As(III) extrusion (*ars* operon), for detoxification (*112*).
ii) As(V) used as a terminal electron acceptor during anaerobic respiration (*arr* operon) (*77*).
iii) As(III) oxidation (*aio* operon, *aso* (*91*) and *aox* gene clusters (*13, 79*)).
iv) As(III) extrusion genes (*acr*3-*ars*C-*ars*R) (*79*).
v) As(III) methylation (*ars*M, ArArsM (*37, 63*)).

These genetic determinants offer microbes the ability to significantly affect the stability of the primary and secondary As minerals (*25, 59, 67, 69*). New emerging evidence is linking land use (*e.g.*, pumping of aquifers) to the seasonal fluctuations of As in groundwater (*7, 27, 80*). This suggests an interplay between human activities and the stimulation of microbial communities responsible for releasing As into the environment. How and why these activities are linked remain unclear, but are worth further investigations. As illustrated in **Figure 1.4**, the work presented here defines bioavailability as the fraction of As that can be internalized by microbes. Because these organisms serve as dominant environmental mobilizers of As, drivers of As bioavailability are the subject of frequent discussion but has remained difficult to directly test, experimentally.

One reason for this gap of knowledge may be the complex synergies involved between hydrology, geology and microbiology. Rapid and reliable detection of bioavailable As, directly in the field, is critical to better understand how microbes

affect its fate and support evidence-based decision-making in choosing irrigation or drinking water sources. One promising approach to assess the biologically relevant fraction of As in the environment relies on microbial sensor systems.

1.2.3 As bioavailability and the use of biosensors

Over the past three decades, whole-cell biosensors have been engineered to detect the presence and quantify a variety of chemicals and toxic metals (*38*). Whole cell biosensors typically have a genetically engineered regulatory/sensory circuitry comprised of a target promoter and associated reporter genes hosted in a microbial chassis (*44*). As-specific biosensors have been designed to quantify the concentration of As(III) at environmentally relevant concentrations (*18, 19, 99, 100*). Genetic engineering generally consists of the *ars*R transcriptional regulator and a reporter protein based either on luminescence or fluorescence. Because these biological sensors are comprised of the entire bacterial cell, dissolved As must therefore cross biological membranes before reaching the As-specific sensors in the cytoplasm. Thus, the signal produced over time is generally regarded to represent the bioavailable fraction of As in that solution, both in the laboratory and in the field (*19, 90, 99*) (**Figure 1.4**).

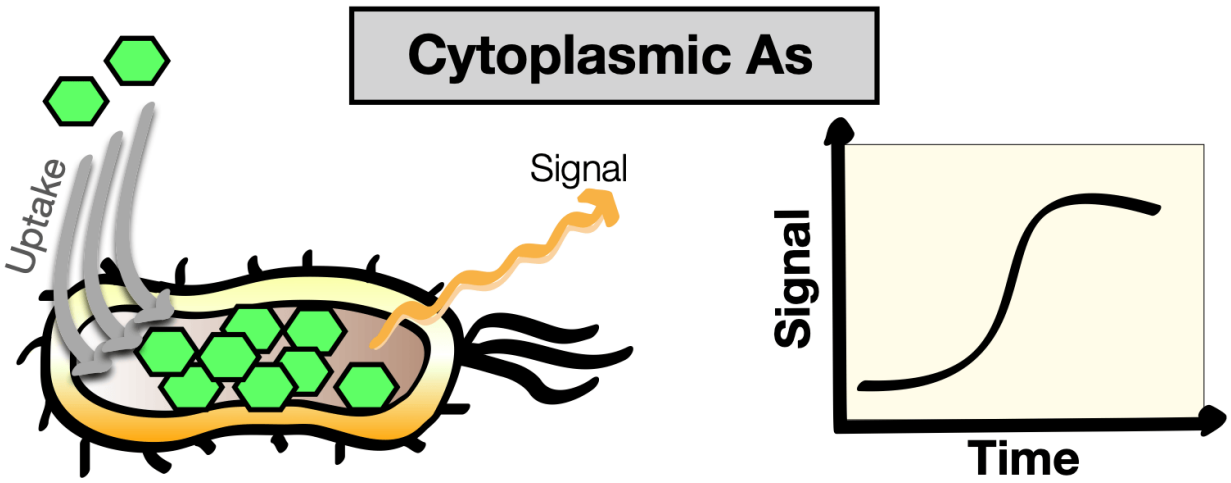

Figure 1.4 | Cytoplasmic As is the bioavailable fraction of dissolved inorganic As that can be detected by As-specific biosensors. These microbes are engineered to produce a quantifiable signal that typically increases over time and is proportional to the quantity of As that enters the cytoplasm.

Bacterial sensors are customizable and reliable for measuring the biologically relevant fraction of contaminants. They have been adapted to work as a light emitting biosensor (*ars*R-lux) (*96, 99, 113*), fluorescent sensors (*ars*R-gfp) (*94*) or as colourimetric sensors (*ars*R-lacZ) (*19, 83*). Although promising technology, they have largely remained a laboratory instrument since little effort has gone into enhancing the portability of these biological systems. With recent advancements in microcontrollers and 3D printers, the technological hurdles limiting the transition of biosensors to the field may soon be eliminated.

1.3 Thesis structure

1.3.1 Thesis goal and outline

The goal of my thesis research was to develop, to validate and to test a new bioanalytical instrument and associated protocol to assess the bioavailability of inorganic As species in the environment. The **first objective** of this work was to develop an improved assay for the quantification of inorganic As species in natural waters. The **second objective** of was to apply the newly developed bioassay to address an important knowledge gaps in As biogeochemistry, that is the role of dissolved organic matter in controlling As species bioavailability. Finally, the **last objective** of this thesis was to design and to build a compact, easy to use, and customizable instruments to enable deployment of the bioassay in the field. My hope was that users that may need it the most, such as individuals relying on groundwater for drinking and irrigation, will be able to access and to use this technology to improve their access to clean water.

Solving this problematic required a multidisciplinary research approach combining microbiology, photonics and electrical engineering. My contributions were separated into three research chapters. In Chapter 2, I present an As biosensor assays capable of rapidly quantifying and determining the speciation of inorganic As at concentrations five times below the World Health Organization's (WHO) guidelines

for As in drinking water. In Chapter 3, I used the biosensor assay developed in Chapter 2 to assess the role of dissolved organic matter on As bioavailability. In Chapter 4, I described how to build a portable spectrometer (fluorometer + photometer) for use in the quantification of inorganic As species *in situ*, and present how this system could be used for field measurements.

1.3.2 Rationale, objectives and hypothesis

Chapter 2. Biosensor assay design

I started my research by investigating why some As biosensor studies report detection of both As(III) and As(V) (*12, 36, 47*) while others (even very recent studies) report biosensor response to As(III) only (*104*). Researchers have highlighted and speculated this knowledge gap for nearly two decades (*70, 87*), with little to no conclusive explanation offered since. The inconsistencies among studies, also extend to the limits of detection where the range reported in the literature can vary by an order of magnitude. Without the ability to discriminate between As(III) and As(V), it is difficult to start addressing the fate of each species in the environment. I therefore focused the first research chapter of my doctoral thesis on designing a reliable exposure medium along with associated bioassay aimed to minimize possible interferences on As species uptake.

Rationale: **As(III):** Research has suggested that ca. 90% of As(III) enters the cytoplasm through an inner-membrane glycerol uptake facilitator channel (GlpF in *E. coli*) (*71, 78*). This transporter is encoded by the *glp* operon that has been shown sensitive to catabolite repression by glucose (*108*).

Hypothesis 1: The presence of glucose in exposure media will limit uptake of As(III) into the cytoplasm. I predicted that cells grown on glucose as their sole carbon source would take up less As(III) than cells grown on glycerol due to the glucose catabolite repression of the glycerol uptake facilitator channels (*glp*F).

Rationale: **<u>As(V):</u>** Bearing close similarities to the phosphate ($H_2PO_4^-$), evidence for As(V) uptake pathway is thought to enter the cells through the high capacity inorganic phosphate transport system (Pit) (*72, 110*).

Hypothesis 2: Inorganic phosphate controls cytoplasmic As(V) concentration. Uptake of As(V) is reduced when the presence of Pi in the periplasm competitively excludes As(V) transport.

By manipulating carbon and phosphate sources in the growth and exposure media, I achieved equal uptake/detection of As(III) and of As(V). I also estimated that the total bioavailable content of As in the exposure media to be over 94%. Finally, I also used the knowledge gained from this research to establish an As speciation protocol that works through selective inhibition of As(V) uptake into the cells. These advances served as an important control and a platform on which I performed a follow-up series of experiments, addressing the environmental drivers of As bioavailability.

Chapter 3. Environmental drivers of arsenic bioavailability

As described in **Section 1.2.2**, microbes can greatly affect mineral stability and consequently, the concentration and speciation of As in water. Thus, the major controls of As bioavailability in the environment are subject to frequent discussion but have remained difficult to directly test, experimentally. This gap in knowledge has also been highlighted long ago (*66*), where it was noted as a limitation of biosensor system that must be fully understood for calibration purposes. In Chapter 3, my primary focus was studying As-DOM interactions, DOM photoreactivity, and the influence of ionic strength on binding affinity between As and DOM.

Rationale: The presence of dissolved organic matter (DOM) in surface waters is ubiquitous, yet its interaction with As is poorly understood. There is a growing body of evidence pointing towards DOM as a governing factor in regulating the mobility and bioavailability of As by direct interactions (sorption/ligands) (*11, 97*) and by reductive dissolution of metal-(hydr)oxides (*45, 51*). DOM is utilized by microbes as carbon and energy sources (*73*). Acting as a chelating agent, it is usually accepted that DOM inhibits metal(oid) uptake by decreasing bioavailable fraction in solution. There is now spectroscopic evidence of As(III)-DOM interactions (*45*), and evidence of indirect binding between As(V) and DOM through cationic bridges (*46*). This interaction is reduced when SRHA was pretreated with a monovalent cation (i.e.: Na^+) (*46*).

Hypothesis 3: DOM controls both As(V) ($H_2AsO_4^-$) and As(III) (H_3AsO_3) bioavailability. Specifically, I predict that As(V) bioavailability will decrease as the concentration of divalent cations increases because of increased cationic bridge formations between DOM and As(V). In contrast, direct binding of As(III) to DOM should not be affected by the presence of cations and therefore pose little effect on As(III) bioavailability.

In exploring the nature of As-DOM interactions, I found that the commonly held knowledge that DOM-bound metal(oid)s are inaccessible to microbes to be partially inaccurate in the case of As. Specifically, I found that a large fraction of environmental As is in a form that is available to microbes. While this study highlights the importance of accounting for environmental controls of As bioavailability, it also helps validate the use of bacterial sensors in the context of environmental monitoring for oxyanions.

Chapter 4. Portability of the bioassay

Current techniques capable of determining the speciation of As in drinking water require sensitive but expensive equipment that is typically only operated by highly qualified staff (*e.g.,* HPLC-ICP-MS). In this chapter, I focused on developing a new As monitoring interface which would provide the accuracy of traditional analytical instruments to users directly in the field and achieve a price point more accessible to the end user (<$100 USD). This required construction of an affordable yet ultrasensitive spectrometer capable of absorbance and fluorescence measurements in the field.

Achieving this goal has only recently been possible due to the major rise in the use of “smart” devices as environmental probes. The newly available high-end, yet low-cost microcircuitry components now makes it possible to surmount the barriers that have previously limited the construction of sensitive yet inexpensive detection equipment that is suitable for field use. In recent years, there has been a push for instruments that allow for direct engagement with the end user by way of citizen science (*17*). Unfortunately, many “smart” monitoring devices in these early days are in a race to market and remain untested by the time they reach consumer hands.

Whole-cell microbial sensors offer a safe and affordable alternative but often require costly/fragile instruments to measure their signals. My goal throughout the conception and design of this instrument was to simplify and to minimize end-user interactions. Using lyophilized biosensor cultures, I managed to accurately detect As concentrations at nM levels relevant to the World Health Organization guidelines. Together, this combination of biosensors and the small footprint of the instrument present an inexpensive and portable on-site As-detection solution with an accuracy that rivals HPLC-ICP-MS. My hope is for this solution to one day contribute to education campaigns that encourage uptake by individuals who need it the most. For instance, farmers requiring the need to make rapid decisions about the quality of irrigation waters; thus, building local capacity and addressing a crippling, global problem of access to clean water, free of inorganic As.

1.4 Bibliography – Chapter 1

1. M. Al-Sid-Cheikh *et al.*, Interactions between natural organic matter, sulfur, arsenic and iron oxides in re-oxidation compounds within riparian wetlands: NanoSIMS and X-ray adsorption spectroscopy evidences. *Science of the Total Environment* **515**, 118-128 (2015).
2. C. N. Alpers, Secondary minerals and acid mine-water chemistry, In Environmental geochemistry of sulfide minewastes. *Short-Course* **22**, 247-270 (1994).
3. H. M. Anawar *et al.*, Geochemical occurrence of arsenic in groundwater of Bangladesh: sources and mobilization processes. *Journal of Geochemical Exploration* **77**, 109-131 (2003).
4. H. V. Aposhian *et al.*, DMPS-arsenic challenge test. II. Modulation of arsenic species, including monomethylarsonous acid (MMA(III)), excreted in human urine. *Toxicology and Applied Pharmacology* **165**, 74-83 (2000).
5. M. Bartel, F. Ebert, L. Leffers, U. Karst, T. Schwerdtle, Toxicological characterization of the inorganic and organic arsenic metabolite Thio- DMA V in cultured human lung cells. *Journal of Toxicology* **2011**, (2011).
6. S. Beauchemin, Y. T. J. Kwong, Impact of redox conditions on arsenic mobilization from tailings in a wetland with neutral drainage. *Environmental Science and Technology* **40**, 6297-6303 (2006).
7. S. Benner, Anthropogenic arsenic. *Nature Geoscience* **3**, 5-6 (2010).
8. P. Bhattacharjee, M. Banerjee, A. K. Giri, Role of genomic instability in arsenic-induced carcinogenicity. A review. *Environment international* **53**, 29-40 (2013).
9. P. Bhattacharya *et al.* (Elsevier, 2007).
10. J.-P. Buchet, R. Lauwerys, H. Roels, Comparison of the urinary excretion of arsenic metabolites after a single oral dose of sodium arsenite, monomethylarsonate, or dimethylarsinate in man. *International archives of occupational and environmental health* **48**, 71-79 (1981).
11. J. Buschmann *et al.*, Arsenite and arsenate binding to dissolved humic acids: Influence of pH, type of humic acid, and aluminum. *Environmental science & technology* **40**, 6015-6020 (2006).
12. J. Cai, M. S. DuBow, Use of a luminescent bacterial biosensor for biomonitoring and characterization of arsenic toxicity of chromated copper arsenate (CCA). *Biodegradation* **8**, 105-111 (1997).
13. L. Cai, C. Rensing, X. Li, G. Wang, Novel gene clusters involved in arsenite oxidation and resistance in two arsenite oxidizers: Achromobacter sp. SY8 and Pseudomonas sp. TS44. *Applied microbiology and biotechnology* **83**, 715-725 (2009).
14. X. Cao, L. Q. Ma, A. Shiralipour, Effects of compost and phosphate amendments on arsenic mobility in soils and arsenic uptake by the hyperaccumulator, Pteris vittata L. *Environmental Pollution* **126**, 157-167 (2003).
15. P. C. Chan, J. Huff, Arsenic carcinogenesis in animals and in humans: Mechanistic, experimental, and epidemiological evidence. *Journal of Environmental Science and Health - Part C Environmental Carcinogenesis and Ecotoxicology Reviews* **15**, 83-122 (1997).
16. J. S. Chang, Y. H. Kim, K. W. Kim, The ars genotype characterization of arsenic-resistant bacteria from arsenic-contaminated gold-silver mines in the Republic of Korea. *Applied Microbiology and Biotechnology* **80**, 155-165 (2008).
17. C. C. Conrad, K. G. Hilchey, A review of citizen science and community-based environmental monitoring: issues and opportunities. *Environmental monitoring and assessment* **176**, 273-291 (2011).
18. P. Corbisier, G. Ji, G. Nuyts, M. Mergeay, S. Silver, luxAB gene fusions with the arsenic and cadmium resistance operons of Staphylococcus aureus plasmid pI258. *FEMS microbiology letters* **110**, 231-238 (1993).

19. F. Cortés-Salazar, S. Beggah, J. R. van der Meer, H. H. Girault, Electrochemical As(III) whole-cell based biochip sensor. *Biosensors and Bioelectronics* **47**, 237-242 (2013).
20. N. R. Council, *Arsenic in drinking water*. (National Academies Press, 1999).
21. W. R. Cullen, K. J. Reimer, Arsenic speciation in the environment. *Chemical Reviews* **89**, 713-764 (1989).
22. A. De Vizcaya-Ruiz, O. Barbier, R. Ruiz-Ramos, M. E. Cebrian, Biomarkers of oxidative stress and damage in human populations exposed to arsenic. *Mutation Research - Genetic Toxicology and Environmental Mutagenesis* **674**, 85-92 (2009).
23. S. L. DeSisto, H. E. Jamieson, M. B. Parsons, Influence of hardpan layers on arsenic mobility in historical gold mine tailings. *Applied Geochemistry* **26**, 2004-2018 (2011).
24. S. Dixit, J. G. Hering, Comparison of arsenic (V) and arsenic (III) sorption onto iron oxide minerals: implications for arsenic mobility. *Environmental science & technology* **37**, 4182-4189 (2003).
25. P. Drahota, M. Filippi, Secondary arsenic minerals in the environment: a review. *Environment international* **35**, 1243-1255 (2009).
26. F. Ebert *et al.*, Arsenicals affect base excision repair by several mechanisms. *Mutation Research - Fundamental and Molecular Mechanisms of Mutagenesis* **715**, 32-41 (2011).
27. L. E. Erban, S. M. Gorelick, H. A. Zebker, S. Fendorf, Release of arsenic to deep groundwater in the Mekong Delta, Vietnam, linked to pumping-induced land subsidence. *Proceedings of the National Academy of Sciences* **110**, 13751-13756 (2013).
28. L. V. Escudero, E. O. Casamayor, G. Chong, C. Pedrós-Alió, C. Demergasso, Distribution of microbial arsenic reduction, oxidation and extrusion genes along a wide range of environmental arsenic concentrations. *PLoS One* **8**, e78890 (2013).
29. X. Gao, Y. Wang, Q. Hu, C. Su, Effects of anion competitive adsorption on arsenic enrichment in groundwater. *Journal of Environmental Science and Health, Part A* **46**, 471-479 (2011).
30. N. N. Greenwood, A. Earnshaw, *Chemistry of the Elements*. (Elsevier, 2012).
31. C. F. Harvey *et al.*, Arsenic mobility and groundwater extraction in Bangladesh. *Science* **298**, 1602-1606 (2002).
32. H. Hasegawa *et al.*, Seasonal changes of arsenic speciation in lake waters in relation to eutrophication. *Science of the Total Environment* **408**, 1684-1690 (2010).
33. J. G. Hering, P. Y. Chen, J. A. Wilkie, M. Elimelech, S. Liang, Arsenic removal by ferric chloride. *Journal / American Water Works Association* **88**, 155-167 (1996).
34. S. E. Hoeft, F. o. Lucas, J. T. Hollibaugh, R. S. Oremland, Characterization of microbial arsenate reduction in the anoxic bottom waters of Mono Lake, California. *Geomicrobiology Journal* **19**, 23-40 (2002).
35. Z. Hongshao, R. Stanforth, Competitive adsorption of phosphate and arsenate on goethite. *Environmental Science & Technology* **35**, 4753-4757 (2001).
36. Q. Hu *et al.*, Construction of WCB-11: A novel phiYFP arsenic-resistant whole-cell biosensor. *Journal of Environmental Sciences* **22**, 1469-1474 (2010).
37. K. Huang *et al.*, Efficient arsenic methylation and volatilization mediated by a novel bacterium from an arsenic-contaminated paddy soil. *Environmental science & technology* **50**, 6389-6396 (2016).
38. A. Hynninen, M. Virta, in *Advances in Biochemical Engineering/Biotechnology*. (2010), vol. 118, pp. 31-64.
39. IARC, *Working Group on the Evaluation of Carcinogenic Risks to Humans. Some drinking-water disinfectants and contaminants, including arsenic*. WHO, Ed., (IARC, Lyon, France, 2004), vol. 84.
40. IARC, Arsenic and Arsenic Compounds. *IARC Monographs*, 52 (2013).
41. A. Insinga, A. Cicalese, P. G. Pelicci, DNA damage response in adult stem cells. *Blood Cells, Molecules, and Diseases* **52**, 147-151 (2014).

42. X. Jiang, C. Chen, W. Zhao, Z. Zhang, Sodium arsenite and arsenic trioxide differently affect the oxidative stress, genotoxicity and apoptosis in A549 cells: An implication for the paradoxical mechanism. *Environmental Toxicology and Pharmacology* **36**, 891-902 (2013).
43. M. F. Kirk *et al.*, Bacterial sulfate reduction limits natural arsenic contamination in groundwater. *Geology* **32**, 953-956 (2004).
44. A. Kuppardt, A. Chatzinotas, U. Breuer, J. R. Van Der Meer, H. Harms, Optimization of preservation conditions of As (III) bioreporter bacteria. *Applied Microbiology and Biotechnology* **82**, 785-792 (2009).
45. P. Langner, C. Mikutta, R. Kretzschmar, Arsenic sequestration by organic sulphur in peat. *Nature Geoscience* **5**, 66-73 (2012).
46. V. Lenoble *et al.*, Evaluation and modelling of dissolved organic matter reactivity toward AsIII and AsV - Implication in environmental arsenic speciation. *Talanta* **134**, 530-537 (2015).
47. V. H. C. Liao, K. L. Ou, Development and testing of a green fluorescent protein - based bacterial biosensor for measuring bioavailable arsenic in contaminated groundwater samples. *Environmental Toxicology and Chemistry: An International Journal* **24**, 1624-1631 (2005).
48. L. Liu, J. R. Trimarchi, P. Navarro, M. A. Blasco, D. L. Keefe, Oxidative stress contributes to arsenic-induced telomere attrition, chromosome instability, and apoptosis. *Journal of Biological Chemistry* **278**, 31998-32004 (2003).
49. S. Lofts, E. Tipping, Assessing WHAM/Model VII against field measurements of free metal ion concentrations: model performance and the role of uncertainty in parameters and inputs. *Environ Chem* **8**, 501-516 (2011).
50. P. Lu, C. Zhu, Arsenic Eh-pH diagrams at 25°C and 1 bar. *Environmental Earth Sciences* **62**, 1673-1683 (2011).
51. C. Mikutta, R. Kretzschmar, Spectroscopic evidence for ternary complex formation between arsenate and ferric iron complexes of humic substances. *Environmental science & technology* **45**, 9550-9557 (2011).
52. J. N. Murphy, C. W. Saltikov, The ArsR repressor mediates arsenite-dependent regulation of arsenate respiration and detoxification operons of Shewanella sp. strain ANA-3. *Journal of Bacteriology* **191**, 6722-6731 (2009).
53. H. Naranmandura *et al.*, Comparative toxicity of arsenic metabolites in human bladder cancer EJ-1 cells. *Chemical Research in Toxicology* **24**, 1586-1596 (2011).
54. K. A. Natarajan, Microbial aspects of acid mine drainage and its bioremediation. *Transactions of Nonferrous Metals Society of China (English Edition)* **18**, 1352-1360 (2008).
55. M. F. Naujokas *et al.*, The broad scope of health effects from chronic arsenic exposure: update on a worldwide public health problem. *Environmental health perspectives* **121**, 295-302 (2013).
56. C. W. Neil, Y. J. Yang, Y.-S. Jun, Arsenic mobilization and attenuation by mineral–water interactions: implications for managed aquifer recharge. *Journal of Environmental Monitoring* **14**, 1772-1788 (2012).
57. G. Neupane, R. J. Donahoe, Y. Arai, Kinetics of competitive adsorption/desorption of arsenate and phosphate at the ferrihydrite–water interface. *Chemical Geology* **368**, 31-38 (2014).
58. P. A. O'Day, D. Vlassopoulos, R. Root, N. Rivera, The influence of sulfur and iron on dissolved arsenic concentrations in the shallow subsurface under changing redox conditions. *Proceedings of the National Academy of Sciences of the United States of America* **101**, 13703-13708 (2004).
59. D. Paktunc, in *Australasian Institute of Mining and Metallurgy Publication Series*. (2008), pp. 343-348.

60. H. Palme, K. Lodders, A. Jones, Solar system abundances of the elements. *Planets, Asteriods, Comets and The Solar System, Volume 2 of Treatise on Geochemistry (Second Edition). Edited by Andrew M. Davis. Elsevier, 2014., p. 15-36* **2**, (2014).
61. L. P. Pereyra, S. R. Hiibel, A. Pruden, K. F. Reardon, Comparison of microbial community composition and activity in sulfate-reducing batch systems remediating mine drainage. *Biotechnology and Bioengineering* **101**, 702-713 (2008).
62. F. Peryea, R. Kammereck, Phosphate-enhanced movement of arsenic out of lead arsenate-contaminated topsoil and through uncontaminated subsoil. *Water, Air, and Soil Pollution* **93**, 243-254 (1997).
63. J. Qin *et al.*, Arsenic detoxification and evolution of trimethylarsine gas by a microbial arsenite S-adenosylmethionine methyltransferase. *Proceedings of the National Academy of Sciences of the United States of America* **103**, 2075-2080 (2006).
64. A. Rajoria, L. Lucena, S. Das, M. Szatkowski, I. Wilkomirsky, in *2014 SME Annual Meeting and Exhibit, SME 2014: Leadership in Uncertain Times*. (2014), pp. 359-365.
65. R. J. Reeder, M. A. A. Schoonen, A. Lanzirotti, in *Reviews in Mineralogy and Geochemistry*. (2006), vol. 64, pp. 59-113.
66. C. Rensing, R. M. Maier, Issues underlying use of biosensors to measure metal bioavailability. *Ecotoxicology and environmental safety* **56**, 140-147 (2003).
67. E. Revesz, D. Fortin, D. Paktunc, Reductive dissolution of scorodite in the presence of Shewanella sp. CN32 and Shewanella sp. ANA-3. *Applied Geochemistry* **63**, 347-356 (2015).
68. E. Revesz, D. Fortin, D. Paktunc, Reductive dissolution of arsenical ferrihydrite by bacteria. *Applied Geochemistry* **66**, 129-139 (2016).
69. P. A. Riveros, J. E. Dutrizac, P. Spencer, Arsenic disposal practices in the metallurgical industry. *Canadian Metallurgical Quarterly* **40**, 395-420 (2001).
70. F. F. Roberto, J. M. Barnes, D. F. Bruhn, Evaluation of a GFP reporter gene construct for environmental arsenic detection. *Talanta* **58**, 181-188 (2002).
71. B. P. Rosen, M. J. Tamás, Arsenic transport in prokaryotes and eukaryotic microbes. *Adv. Exp. Med. Biol* **679**, 47-55 (2010).
72. H. Rosenberg, R. Gerdes, K. Chegwidden, Two systems for the uptake of phosphate in Escherichia coli. *Journal of bacteriology* **131**, 505-511 (1977).
73. R. A. Royer *et al.*, Enhancement of hematite bioreduction by natural organic matter. *Environmental science & technology* **36**, 2897-2904 (2002).
74. R. Ruiz-Ramos, L. Lopez-Carrillo, A. D. Rios-Perez, A. De Vizcaya-Ruíz, M. E. Cebrian, Sodium arsenite induces ROS generation, DNA oxidative damage, HO-1 and c-Myc proteins, NF-κB activation and cell proliferation in human breast cancer MCF-7 cells. *Mutation Research - Genetic Toxicology and Environmental Mutagenesis* **674**, 109-115 (2009).
75. S. L. Saalfield, B. C. Bostick, Changes in iron, sulfur, and arsenic speciation associated with bacterial sulfate reduction in ferrihydrite-rich systems. *Environmental science & technology* **43**, 8787-8793 (2009).
76. M. A. Sabur, S. Goldberg, A. Gale, N. Kabengi, H. A. Al-Abadleh, Temperature-dependent infrared and calorimetric studies on arsenicals adsorption from solution to hematite nanoparticles. *Langmuir* **31**, 2749-2760 (2015).
77. C. W. Saltikov, D. K. Newman, Genetic identification of a respiratory arsenate reductase. *Proceedings of the National Academy of Sciences* **100**, 10983-10988 (2003).
78. O. I. Sanders, C. Rensing, M. Kuroda, B. Mitra, B. P. Rosen, Antimonite is accumulated by the glycerol facilitator GlpF in Escherichia coli. *Journal of bacteriology* **179**, 3365-3367 (1997).
79. J. M. Santini, R. N. vanden Hoven, Molybdenum-containing arsenite oxidase of the chemolithoautotrophic arsenite oxidizer NT-26. *Journal of Bacteriology* **186**, 1614-1619 (2004).

80. M. V. Schaefer *et al.*, Redox controls on arsenic enrichment and release from aquifer sediments in central Yangtze River Basin. *Geochimica et Cosmochimica Acta* **204**, 104-119 (2017).
81. D. Schindler, E. Fee, Experimental lakes area: whole-lake experiments in eutrophication. *Journal of the Fisheries Board of Canada* **31**, 937-953 (1974).
82. D. W. Schindler *et al.*, Eutrophication of lakes cannot be controlled by reducing nitrogen input: results of a 37-year whole-ecosystem experiment. *Proceedings of the National Academy of Sciences* **105**, 11254-11258 (2008).
83. D. L. Scott, S. Ramanathan, W. Shi, B. P. Rosen, S. Daunert, Genetically engineered bacteria: electrochemical sensing systems for antimonite and arsenite. *Analytical chemistry* **69**, 16-20 (1997).
84. H. Seidel, K. Görsch, K. Amstätter, J. Mattusch, Immobilization of arsenic in a tailings material by ferrous iron treatment. *Water Research* **39**, 4073-4082 (2005).
85. D. B. Senn, H. F. Hemond, Nitrate controls on iron and arsenic in an urban lake. *Science* **296**, 2373-2376 (2002).
86. M. C. Sforna *et al.*, Evidence for arsenic metabolism and cycling by microorganisms 2.7 billion years ago. *Nature Geoscience* **7**, 811 (2014).
87. P. Sharma, S. Asad, A. Ali, Bioluminescent bioreporter for assessment of arsenic contamination in water samples of India. *Journal of Biosciences* **38**, 251-258 (2013).
88. P. Sharma, A. Kappler, Desorption of arsenic from clay and humic acid-coated clay by dissolved phosphate and silicate. *Journal of contaminant hydrology* **126**, 216-225 (2011).
89. Y. Shimoda *et al.*, Proposal for novel metabolic pathway of highly toxic dimethylated arsenics accompanied by enzymatic sulfuration, desulfuration and oxidation. *Journal of Trace Elements in Medicine and Biology* **30**, 129-136 (2015).
90. K. Siegfried *et al.*, Field testing of arsenic in groundwater samples of Bangladesh using a test kit based on lyophilized bioreporter bacteria. *Environmental Science and Technology* **46**, 3281-3287 (2012).
91. S. Silver, L. T. Phung, Genes and enzymes involved in bacterial oxidation and reduction of inorganic arsenic. *Applied and Environmental Microbiology* **71**, 599-608 (2005).
92. P. Smedley, D. G. Kinniburgh, in *Essentials of medical geology*. (Springer, 2013), pp. 279-310.
93. D. S. Smith, R. A. Bell, J. R. Kramer, Metal speciation in natural waters with emphasis on reduced sulfur groups as strong metal binding sites. *Comparative Biochemistry and Physiology Part C: Toxicology & Pharmacology* **133**, 65-74 (2002).
94. J. Stocker *et al.*, Development of a set of simple bacterial biosensors for quantitative and rapid measurements of arsenite and arsenate in potable water. *Environmental Science and Technology* **37**, 4743-4750 (2003).
95. M. Styblo *et al.*, Comparative toxicity of trivalent and pentavalent inorganic and methylated arsenicals in rat and human cells. *Archives of Toxicology* **74**, 289-299 (2000).
96. S. Tauriainen, M. Karp, W. Chang, M. Virta, Recombinant luminescent bacteria for measuring bioavailable arsenite and antimonite. *Applied and environmental microbiology* **63**, 4456-4461 (1997).
97. P. Thanabalasingam, W. Pickering, Arsenic sorption by humic acids. *Environmental Pollution Series B, Chemical and Physical* **12**, 233-246 (1986).
98. H.-P. Tran, A. S. Prakash, R. Barnard, B. Chiswell, J. C. Ng, Arsenic inhibits the repair of DNA damage induced by benzo (a) pyrene. *Toxicology letters* **133**, 59-67 (2002).
99. P. T. K. Trang, M. Berg, P. H. Viet, N. Van Mui, J. R. Van Der Meer, Bacterial bioassay for rapid and accurate analysis of arsenic in highly variable groundwater samples. *Environmental Science and Technology* **39**, 7625-7630 (2005).
100. F. Truffer *et al.*, Compact portable biosensor for arsenic detection in aqueous samples with Escherichia coli bioreporter cells. *Review of Scientific Instruments* **85**, (2014).

101. A. Valenzuela, Université Laval, (2000).
102. A. Violante, M. Pigna, Competitive sorption of arsenate and phosphate on different clay minerals and soils. *Soil Science Society of America Journal* **66**, 1788-1796 (2002).
103. R. V. Wagoner, W. A. Fowler, F. Hoyle, On the synthesis of elements at very high temperatures. *The Astrophysical Journal* **148**, 3 (1967).
104. X. Wan *et al.*, Cascaded amplifying circuits enable ultrasensitive cellular sensors for toxic metals. *Nature chemical biology* **15**, 540 (2019).
105. Y. Wang, X. H. Liu, Y. B. Si, R. F. Wang, Release and transformation of arsenic from As-bearing iron minerals by Fe-reducing bacteria. *Chemical Engineering Journal* **295**, 29-38 (2016).
106. Y. Wang *et al.*, Arsenic induces mitochondria-dependent apoptosis by reactive oxygen species generation rather than glutathione depletion in Chang human hepatocytes. *Archives of toxicology* **83**, 899-908 (2009).
107. K. A. Weber, F. W. Picardal, E. E. Roden, Microbially catalyzed nitrate-dependent oxidation of biogenic solid-phase Fe (II) compounds. *Environmental Science & Technology* **35**, 1644-1650 (2001).
108. D. L. Weissenborn, N. Wittekindt, T. J. Larson, Structure and regulation of the glpFK operon encoding glycerol diffusion facilitator and glycerol kinase of Escherichia coli K-12. *Journal of Biological Chemistry* **267**, 6122-6131 (1992).
109. A. H. Welch, K. G. Stollenwerk, *Arsenic in ground water: geochemistry and occurrence*. (Springer Science & Business Media, 2003).
110. G. R. Willsky, M. H. Malamy, Effect of arsenate on inorganic phosphate transport in Escherichia coli. *Journal of Bacteriology* **144**, 366-374 (1980).
111. M. Wolthers, L. Charlet, C. H. van Der Weijden, P. R. Van der Linde, D. Rickard, Arsenic mobility in the ambient sulfidic environment: Sorption of arsenic (V) and arsenic (III) onto disordered mackinawite. *Geochimica et Cosmochimica Acta* **69**, 3483-3492 (2005).
112. J. Wu, B. Rosen, Metalloregulated expression of the ars operon. *Journal of Biological Chemistry* **268**, 52-58 (1993).
113. Y. B. Zhang *et al.*, ArsR arsenic-resistance regulatory protein from Cupriavidus metallidurans CH34. *Antonie van Leeuwenhoek, International Journal of General and Molecular Microbiology* **96**, 161-170 (2009).
114. Y.-G. Zhu, P. N. Williams, A. A. Meharg, Exposure to inorganic arsenic from rice: a global health issue? *Environmental pollution* **154**, 169-171 (2008).
115. Y.-G. Zhu, X.-M. Xue, A. Kappler, B. P. Rosen, A. A. Meharg, Linking genes to microbial biogeochemical cycling: lessons from arsenic. *Environmental Science & Technology*, (2017).

Chapter 2 – Biosensor assay design

OPEN ACCESS – ORIGINAL RESEARCH

Insights into arsenite and arsenate uptake pathways using a whole cell biosensor

Martin P. Pothier[1]*, Aaron J. Hinz*[1]*, Alexandre J. Poulain*[1]

[1] *Biology Department, University of Ottawa, 30 Marie Curie, Ottawa, ON, K1N 6N5, Canada*

Highlights:

i) When compared to ICP-MS, legacy As contamination is accurately quantified by biosensors and presents high bioavailability.

ii) Selective inhibition of As(V) uptake using inorganic phosphate determines As speciation.

iii) Glucose delays As(III) entry, and reduces the extent of As(III) uptake.

iv) DOC is a component of the water matrix that may control the fraction of As that enters bacterial cells.

Contributions to the field:

i) New method to determine the speciation of As using biosensors.

ii) Detailed exposure conditions that enable *ars*R biosensors to detect As(V) at the same rate and limit of detection as As(III).

iii) Linked central bacterial carbon metabolism to the uptake of As(III).

iv) Linked an *ars*-independent reduction pathway to the detection of As(V) by ArsR.

v) Developed exposure protocol that enables use of As-biosensors to analyze the matrix effect of lake water.

vi) First evidence the kinetic control NOM exerts on As(III) and As(V) bioavailability.

A modified version of this manuscript was published online: 02 October 2018
Frontiers in Microbiology **|** *http://doi.org/10.3389/fmicb.2018.02310*

2.1 Abstract

Despite its high toxicity and widespread occurrence in many parts of the world, arsenic (As) concentrations in decentralized water supplies such as domestic wells often remain unquantified. One limitation to effective monitoring is the high cost and lack of portability of current As speciation techniques. Here, we present an As biosensor assay capable of quantifying and determining the bioavailable fraction of As species at environmentally relevant concentrations. First, we found that inorganic phosphate, a buffering agent and nutrient commonly found in most bioassay exposure media, was in fact limiting As(V) uptake, possibly explaining the variability in As(V) detection reported so far. Second, we show that the nature of the carbon source used in the bioassay differentially affects the response of the biosensor to As(III). Finally, our data support the existence of non-specific reduction pathways (non-*ars* encoded) that are responsible for the reduction of As(V) to As(III), allowing its detection by the biosensor. To validate our laboratory approach using field samples, we performed As(III) and As(V) standard additions on natural water samples collected from 17 lakes surrounding Giant Mine in Yellowknife, Canada. We found that legacy As contamination in these lake water samples was accurately quantified by the biosensor. Interestingly, bioavailability of freshly added standards showed signs of matrix interference, indicative of dynamic interactions between As(III) / As(V) and environmental constituents that have yet to be identified. Our results point towards dissolved organic carbon as possibly controlling these interactions, thus altering As bioavailability.

Keywords: arsenic speciation; arsenic uptake; arsenite; arsenate; whole cell biosensor; Giant Mine; water quality

N.B. Supplementary Materials (**Annex A**) are appended at the end of this chapter.

2.2 Introduction

Arsenic contamination of drinking water poses a significant human health risk worldwide (*2*). The occurrence of As in lakes and ground water is closely linked with geologic sources (*5*) and can be exacerbated by anthropogenic activities (*32*). Chronic ingestion of geogenic As from contaminated water increases the risk of several cancers and multisystem diseases (*8, 22, 23*). In efforts to reduce As poisoning, the WHO has set the maximum allowable concentration of As in drinking water to 10 µg/L or 133 nM (*54*).

Despite its high toxicity and widespread occurrence, in many parts of the world (*10, 17, 19*), As concentrations in decentralized water supplies such as domestic wells often remain unquantified. One barrier to effective monitoring is the high cost and lack of portability of analytical techniques (*28*). Commonly used methods of analyzing As in environmental samples involve separation of chemical species by high-performance liquid chromatography (HPLC). Methods for quantification include inductively coupled plasma mass spectrometry (ICP-MS) and atomic fluorescence spectroscopy (AFS). While these techniques reliably provide accurate quantification of As, purchasing and operation costs of these instruments are prohibitive for large-scale monitoring (*28*).

A complementary approach to As quantification involves the use of microbial biosensors (*13, 14, 49, 50*) that produce quantifiable signals in response to As exposure. Most As biosensors are based on regulation of reporter genes by an As sensing transcriptional repressor (ArsR) (*56*). Output signals of reporter genes include light emission (*e.g.*, luciferase) (*48, 49, 59*) and fluorescence (*e.g.*, green fluorescent protein) (*11, 47*). Because production of the signal requires uptake of As by live cells, biosensors quantify, to some extent, the fraction of As that is available to microbes for transformations. This bioavailable fraction cannot be determined by other analytical techniques like HPLC-ICP-MS or chemical test kits. Moreover,

biosensors hold promise for quantifying As in remote locations (*14, 15, 33, 45, 49*) where the use of other analytical methods is impractical.

One potential limitation of previous As biosensors is their inability to distinguish between different chemical species of As. Arsenic in contaminated drinking water is typically inorganic and can exist in two redox states (As(III) and As(V)), which differ in their mobility, bioavailability, and toxicity (*9, 31*). Arsenic speciation is governed by physiochemical conditions of the environment, particularly pH and redox potential (*26*). In anoxic groundwater, As is generally present as As(III), often released by dissolution of As-containing minerals (*51*). Once in contact with oxic surface water, As(III) is oxidized to As(V) (*51*). Microbes also play a key role in controlling As speciation. The genetic determinants involved in As metabolism and cycling are thought to be ancient (*40*) and diverse. Indeed, microbes have been shown to oxidize As(III), [e.g., via the *aio* operon, *aso* or *aox* gene cluster (*7, 38, 46*)], reduce As(V) for catabolic or detoxification purposes (*e.g.*, via the *ars* and *arr* operons (*36, 56*)), as well as catalyze the formation of several organoarsenic species (*e.g.*, via *ars*M (*4, 58*)).

Whereas ArsR-based sensors (i.e., derived from the *ars* operon) have been routinely used to detect inorganic arsenic [As(III) & As(V)] (*15, 43, 45, 47*), output signal is often weaker in response to As(V) (*43, 47*). As(V) detection is likely to require a reduction step to As(III) before binding to ArsR, because As(III) is the only As species known to interact with ArsR (*44, 56*). Thus, the weaker signal has been presumed to result from delayed or inefficient reduction of As(V) by the arsenate specific reductase (ArsC) (*43, 47*). Alternatively, the inability to reliably detect As(V) may stem from differentially reduced bioavailability of As(V) in biosensor exposure assays. These limitations can lead to lower sensitivity and to the underestimation of As concentrations in environmental samples.

We hypothesized that variable responses of As biosensors to As may stem from heterogeneity of exposure conditions that interfere with the bioavailability of inorganic As species. For instance, As(V) complexes ($H_2AsO_4^-$) have similar size, charge and structure to inorganic phosphate (Pi) complexes ($H_2PO_4^-$), and studies have found that Pi transporters are responsible for As(V) uptake (*35, 55*). In contrast, As(III) was found to be transported passively via glycerol uptake facilitator channels (GlpF in *E. coli*) (*34, 37*). Therefore, we predicted that speciation of As can be determined by manipulating media constituents that differentially alter As transport of both inorganic species.

In this study, we evaluated the ability of an *E. coli* ArsR-based biosensor to quantify inorganic As species over a concentration range encompassing the World Health Organization's guideline for As in drinking water. We showed how alteration of media constituents can impact the bioavailability of As species. We identified conditions permissive for the detection of both As(III) and As(V), conditions selective for detection of As(III) alone, and explored mechanisms responsible for species specific detection. We also examined the effects of chemical constituents commonly found in environmental samples that may differentially affect the bioavailability of As species. Finally, we validated our proposed methodology by estimating total inorganic As concentrations in natural lake water samples that cover a wide range of chemical compositions.

2.3 Materials and Methods

2.3.1 Arsenic biosensor construction.

Our biosensing construct was inspired by the design of J. Stocker et al. (*47*), for which two ArsR binding sites were shown to provide optimal detection while minimizing noise (**SI Fig. A2.1**). The sensing-reporting sequence (ArsRBS2-mCherry) was constructed by custom gene synthesis (Integrated DNA Technologies) and cloned into the XmaI and XbaI restriction sites of the high copy pUCP19 shuttle

vector (*6, 39*) upstream of the sequence encoding mCherry (*41, 42*). The reporter plasmid was transformed into *E. coli* NEB10-beta (New England BioLabs) – a level 1, non-pathogenic, non-regulated host. Other than the chromosomal ars operon, *E. coli* NEB10-beta does not carry any other known genetic determinants annotated as involved in As specific transformations.

2.3.2 Construction of the *ars*C deletion mutant.

The chromosomal arsenate-reductase gene (*ars*C) was deleted from the *E. coli* NEB10-beta genome using lambda Red recombination (*16*). The Δ*ars*C mutant from the Keio collection (Strain JW3470), in which the coding sequence is replaced by a kanamycin resistance gene flanked by FLP recognition target (FRT) sequences (*3*), was obtained from the Coli Genetic Stock Center. The FRT-kan cassette and flanking *E. coli* genomic sequences were PCR-amplified from chromosomal DNA isolated from the Δ*ars*C mutant using primers F-Delta-arsC (5'-GTGCTGTTTGTGACGCTGG-3') and R-Delta-arsC (5'-GCGCACTTTTCTAACAACCTGT-3'). Purified PCR products were transformed into electrocompetent NEB10-beta cells induced to express recombination functions from the Red helper plasmid pKD46, as previously described (*16*). Recombinants were selected by plating on LB with 30 μg/mL kanamycin and cured of the temperature-sensitive pKD46 plasmid by incubation at 37ºC. Replacement of the *ars*C gene by the FRT-kan cassette was verified by colony PCR, and plasmid curing was confirmed by testing for ampicillin sensitivity. The kanamycin-resistance gene was subsequently excised by FLP recombination with the plasmid pCP20, as previously described (*16*), followed by plasmid curing, yielding putative Δ*ars*C::FRT mutants susceptible to both kanamycin and ampicillin. Colony PCR with the *ars*C deletion primers yielded a shorter amplicon for the putative Δ*ars*C::FRT mutants in comparison to the wild-type, confirming the deletion of *ars*C sequences. The minimal inhibitory concentrations (MICs) of As(III) and As(V) were determined for both the wild-type and Δ*ars*C strains (**SI Fig. A2.2**). Declines in all mutant fitness measurements (i.e., growth rate, lag time and yield) occurred at an

As(V) concentration 10 fold lower than that of the wild-type (50 µM vs. 500 µM). In contrast, decline in fitness measurements for As(III) were similar for both strains (500 µM). Together, these data confirms that the removal of arsenate reductase from the host genome increases sensitivity to As(V).

2.3.3 Media and reagents.

Ultrapure water was used in all media and reagents. The water purification process involved Milli-Q (Millipore) filtering system, autoclaving and re-filtration at 0.2 µm. Cells hosting the biosensing construct were plated on LB agar (10 g tryptone, 5 g yeast extract, 5 g NaCl and 15 g agar per liter) with 120 µg/mL ampicillin. Before each assay, cells were pre-grown overnight in MGP (Mops Glycero-Phosphate) growth medium, a defined minimal medium free of inorganic phosphates (**SI Table A1.1**). Constituents include 20 mM MOPS as a buffering agent, 1 mM β-glycerophosphate (BGP) as a phosphate source and 30 mM glycerol as the primary carbon source. The growth medium was supplemented with trace elements and amino acids (L-Leucine, L-Isoleucine and Valine) as *E. coli* NEB 10-beta is an auxotrophic strain (Δ(*ara-leu*)) for these compounds (**SI Table A1.1**).

The nonselective As exposure medium (**SI Table A1.1**) is a modified MGP growth medium with no trace elements, reduced [Mg^{2+}] (20 µM) and reduced [glycerol] (5 mM). Discriminating between As(III) and As(V) is possible using MIP (MOPS Inorganic Phosphate) exposure medium, which is an MGP exposure medium supplemented with 10 mM inorganic phosphate (Pi) (speciation defined in **SI Table A1.1**). In order to test for the role of different carbon sources on As(III) uptake, the MGP exposure medium required the following substitutions: 1 mM BGP with 1 mM Pi, and 5 mM glycerol with 5 mM glucose.

Biosensor As standards consisted of sodium (meta)arsenite ($NaAsO_2$; Cat#S7400-100G) and sodium arsenate dibasic heptahydrate ($Na_2HAsO_4 \cdot 7H_2O$; Cat#A6756-100G), purchased from Sigma-Aldrich. Arsenic salts were dissolved in

ultrapure water and acidified with HNO_3 to a final concentration of 10 mM As and 0.1% HNO_3. Arsenic standards were kept up to 4 weeks in 15 mL polypropylene tubes at 4ºC in the absence of light. Arsenic species in our standard solutions were periodically verified using HPLC-ICP-MS and deemed stable for one month. Working standards of 10 µM were prepared daily before exposure to sensor cells.

Concentration of As species was measured using HPLC (1200 HPLC; Agilent Technologies) with ICP-MS (7700x; Agilent Technologies) in accordance with the Food and Drug Administration standards, Elemental Analysis Manual Section 4.11. Reagents used in HPLC-ICP-MS quantification and speciation were of analytical grades and used without further purification. Arsenic standards and other reagents were purchased from Sigma-Aldrich and SpexCertiprep. Stock solutions of 1000 mg/L of arsenite (Spex Certiprep, Cat#SPEC AS3M), arsenate (Spex Certiprep, Cat#SPEC-AS5M) with a certified value of As traceable to a NIST Standard Reference materials were purchased from SpexCertiprep. A 10 mM solution of ammonium phosphate dibasic was prepared by dissolving ammonium phosphate dibasic (Sigma, cat#379980-100G) in ultrapure water and pH adjusted to 8.25 with 28% Ammonium hydroxide solution (Sigma, Cat#: 338818-100ML). Mobile phase was filtered through 0.45 µm filter before use.

2.3.4 Arsenic exposure and quantification by biosensor.

Growth was initiated by transferring a single colony into MGP growth medium supplemented with 1% LB and 100 µg/mL ampicillin in round-bottom culture tubes with a 1 cm path length. Cultures were incubated aerobically overnight at 200 RPM and 37ºC until they reached an OD_{600} (optical density at 600 nm) range of 1.1 to 1.2. Before exposure to As, cells were statically incubated at room temperature for 3 hours and diluted to an OD_{600} of 1.050 using MGP growth medium. This culture was used as the inoculum in subsequent assays.

Unless otherwise noted, all As exposure assays include adding the following components in the following order: 1) exposure medium, 2) reagents, 3) water and 4) cells. Medium to inoculum ratio was consistent in all treatments by concentrating exposure media 2-fold. Step 1 involved the transfer of 800 µL of 2X concentrated MGP or MIP to a 7 mL borosilicate scintillation vial. Step 2 involved the addition of reagents such as arsenic and/or salts were added to the vials. Reagent working solutions were adjusted to allow a final dilution that does not exceed a total of 1 mL. During step 3, ultrapure water was used to adjust the final volume of reagents to 1 mL. Here, reagents and media constituents were incubated in the vials for 15 minutes at room temperature with periodical orbital shaking by hand. Finally, 200 µL of unwashed biosensor cell cultures were added to all treatments. Vials were incubated at 37ºC for 20 minutes at 200 RPM. In all assays, plating consisted of technical triplicates by adding 200 µL of each treatment in three separate wells of a Corning 96 well black plate with a non-binding surface and a clear bottom. Using a Tecan Infinite F200 Pro plate reader, fluorescence and OD_{600} of a 0.6 cm path length was measured from the top of the plate on kinetic cycles of 10 minutes for 22 hours at 37ºC and 25 flashes per read. We used an optically clear lid to minimize evaporation throughout the incubation. Fluorescence intensity was analyzed using 560/20x nm excitation and 620/10x nm emission bandpass filters with gain manually set to 100.

2.3.5 Speciation analysis of cell and supernatant fractions.

Using the previously described exposure protocol, 5 mL cultures of both wild-type and Δ*arsC* mutant strains were incubated at 37ºC with 32 µM As(V) for 3 hours in MGP exposure media. To determine the fraction and speciation of As inside the cells, cultures pre- and post-incubation were centrifuged at 15 000 RPM for 3 minutes. Pelleted cells were washed twice using MGP exposure media rather than ultrapure water to avoid cell lysis during washes. The use of preservation agents such as acids were also avoided for this same reason. Rather, pellets were separated from the supernatant, placed on ice and analyzed on the same day in biological triplicates

using HPLC-ICP-MS. No-cell controls underwent identical methodology including centrifugation and icing steps. As(III) was not detected in the controls, indicating that As(V) was not reduced by constituents in the growth medium nor from the steps used to fractionate cells from supernatant. Our mass balance for all biological replicates indicated that we retrieved ca. 100% of the As(V) added.

2.3.6 Analysis of glucose concentrations in culture supernatant.

Methods involving the monitoring of glucose consumption over time required an increase of the final volume to 12 mL. For each treatment, 200 µL was subsampled and plated for kinetic RFU and OD_{600} quantification. The remaining volume was incubated at 37ºC and used for glucose consumption monitoring, where a 1 mL subsample was extracted/filter sterilized (0.2 µm) every 1.5 hour for 10.5 hours. Samples were frozen and stored for 1 week before analysis by Evaporative Light Scattering Detector (ELSD) coupled to HPLC. Glucose concentration could only be accurately quantified from the initial 5 mM concentration until it reached a concentration of 2 mM. We found that one of the constituents common to both glucose and glycerol media led to an increase in the baseline at the 13.5-minute retention time making quantification of glucose not possible beyond this point.

2.3.7 Collection and chemical analysis of environmental lake samples.

In September 2017, water samples were collected by helicopter from the middle of 17 lakes near presumed to be affected by historical mining activity near the city of Yellowknife, in the Northwest Territories, Canada. At each site, two samples were collected where one was dedicated for water chemistry and the other for As analysis. Water chemistry data were provided by Taiga Environmental Laboratory, a full-service analytical laboratory located in Yellowknife, accredited by the Canadian Association for Laboratory Accreditation (CALA) to ISO/IEC 17025 standards. Unfortunately, we were not able to obtain Pi concentrations for these lakes because of major interferences between PO_4^{3-} and AsO_4^{3-} analyses. Samples dedicated for As

speciation analysis were collected using HDPE (high-density polyethylene) containers, kept in the dark and chilled before cross-analysis by the biosensor and HPLC-ICP-MS in Ottawa, ON Canada. Our study prioritized the preservation of natural matrix constituents (*e.g.*, organic matter, colloids) rather than the preservation of As species. Therefore, we refrained from filtering and acidifying these lake samples that may have affected the bioavailability of As or the viability of the cells once added to the assay. HPLC-ICP-MS speciation analysis revealed that although a small fraction of the As was in the form of arsenobetaine, over 99% of the As was in the oxidized inorganic form As(V), as expected from unpreserved samples. Cross-analysis between the biosensor and the HPLC-ICP-MS analyses were conducted on the same day.

Biosensor analysis of As concentration for 9 of 17 lakes was above the linear range of the calibration curve and required a 20x dilution before quantification (100 µL of lake water, 900 µL ultrapure water, 800 µL 2x MGP and 200 µL biosensor culture). A 2x dilution was used for the 8 remaining lakes (1000 µL lake water, 800 µL of 2x MGP and 200 µL biosensor culture). For the As standard addition protocol (**SI Fig. A2.5**), 10 µM As working solutions were prepared in 2x MGP exposure media rather than ultrapure water. This modification to the As exposure protocol ensured that lake water would not be diluted by the spiked As.

2.4 Results and discussion

2.4.1 Arsenic detection and speciation determination by a fluorescent biosensor.

The biosensor detected equally well As(III) and As(V) when each As species was provided independently as the sole source of As in the non-selective medium, MGP (**Figure 2.1**a; upper panels). The fluorescent signal output was linearly proportional to the concentration of both As species from 25 nM to 800 nM (**SI Fig. A2.3**). As predicted, the presence of inorganic phosphate (10 mM) in the selective medium

(MIP) prevented the detection of As(V) up to [As(V)] = 1500 nM, while minimally affecting As(III) detection (**Figure 2.1**a; lower panels). Under all conditions tested, growth was not affected (**Figure 2.1**b), indicating that substitution of inorganic phosphate for BGP did not limit the growth rate nor yield.

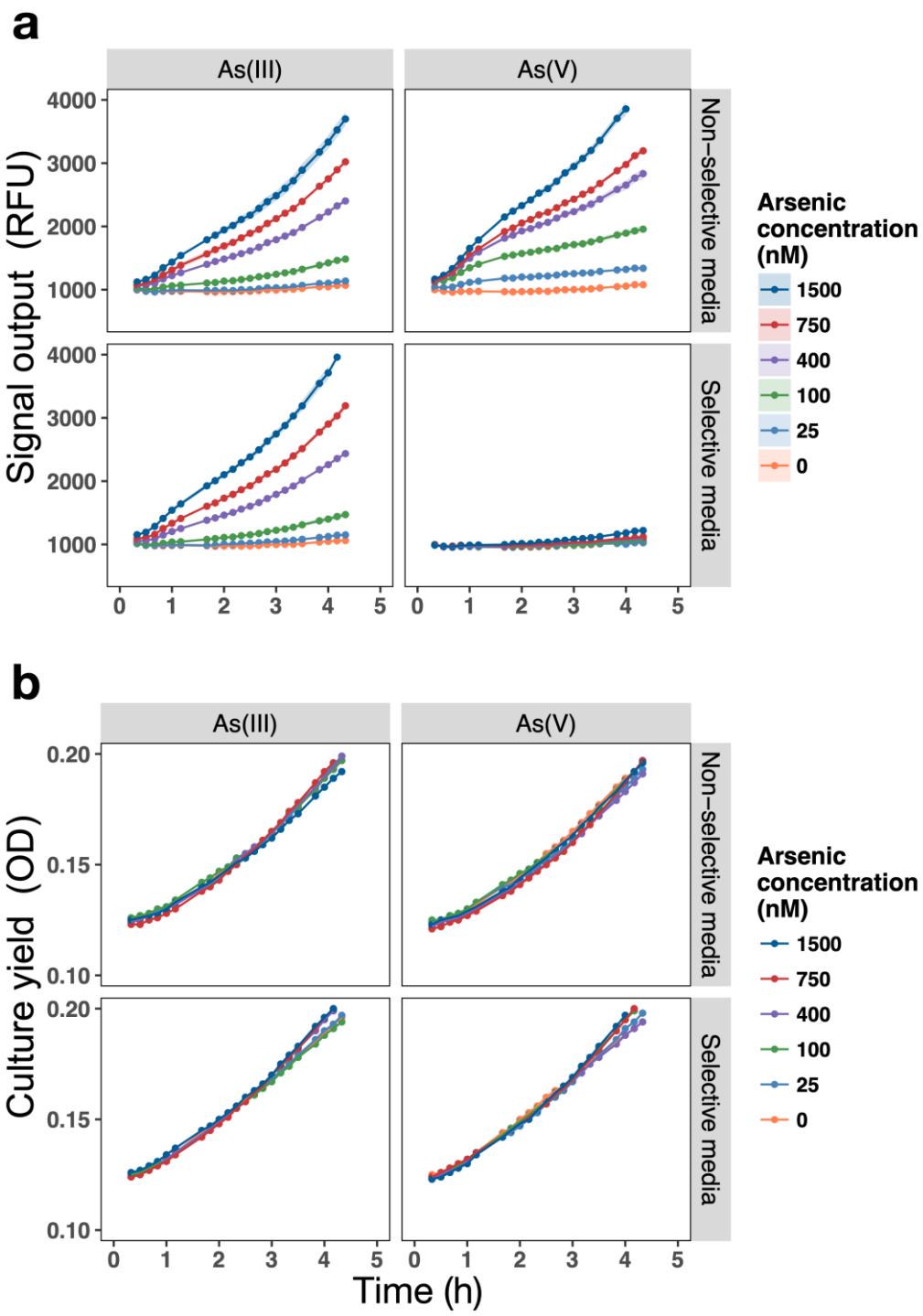

Figure 2.1 | Role of inorganic phosphate addition in detection of As(III) and As(V). **(a)** Biosensor was exposed to the indicated concentrations of As(III) or As(V) in MGP media lacking inorganic phosphate (Non-selective media) or MIP media containing 10 mM inorganic phosphate (Selective media). The output signal of the biosensor is presented in relative fluorescence units (RFU) during the first 6 hours of growth immediately following exposure to As. **(b)** The optical density of biosensor cultures at 600 nm (OD_{600}) is shown, indicating similar growth rates for the cultures in both exposure media.

These results showed that As(V) bioavailability, and thus detection, was dependent on Pi concentrations. Previous work in *E. coli* (*55*) and plants (*1, 27*) have established that Pi and As(V) compete for cellular uptake, but so far, this knowledge had not been fully exploited in biosensor applications. As previously suggested, the inhibition of As(V) uptake at high Pi concentrations could arise from i) competition between Pi and As(V) at Pi transporter sites, or ii) repression of the high-affinity phosphate transporter (Pst), which occurs at Pi concentrations exceeding 20 μM (*30*). We also show that inclusion of excess Pi (>100 μM) in the exposure media selectively blocked detection of As(V) with minimal effect on the detection of As(III) ($p=0.04$) (**Figure 2.2**).

We were also interested in investigating the effects of other major freshwater ions such as Ca^{2+}, Mg^{2+} and Na^{+} on the detection of As(III) and As(V) by the biosensor (**Figure 2.2**; center left and right panels). We altered the ionic strength of the medium by increasing sodium chloride (NaCl) concentrations to those found in seawater (600 mM) (**Figure 2.2**; center left panel). Interestingly, as NaCl concentrations increased, the fluorescent signal was equally reduced for both the As(III) and As(V) ($p=0.073$). Here, signal reduction was associated with the inhibitory effect of NaCl on growth rather than a change in As species bioavailability. Additions of calcium chloride ($CaCl_2$) and magnesium chloride ($MgCl_2$) in MGP exposure medium had little effect on the detection of As; a slight enhancement in bioavailability was observed for $[Ca^{2+}]$ = 100 μM (**Figure 2.2**).

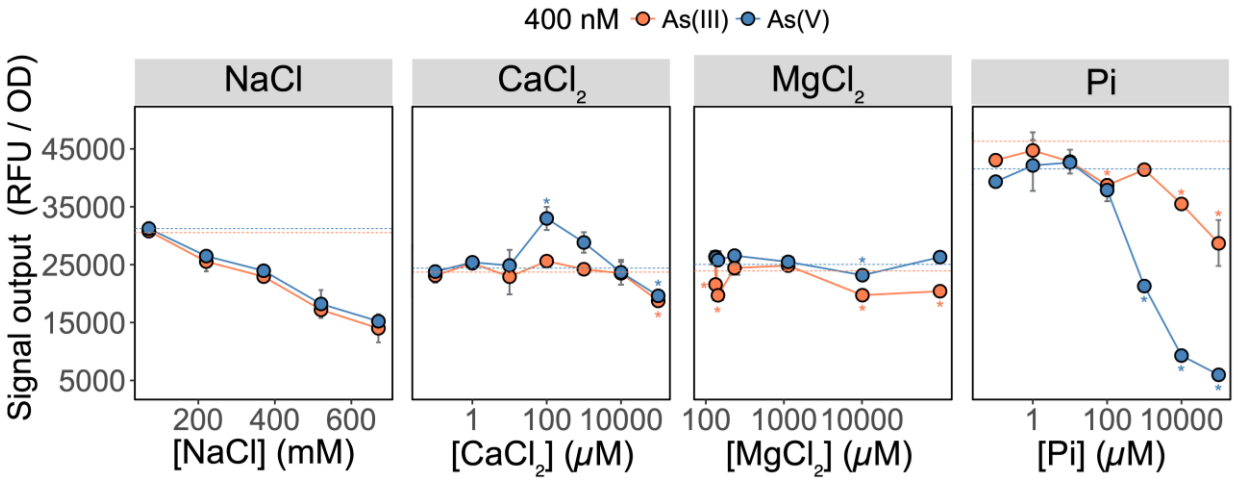

Figure 2.2 | Effect of major ions on As species detection. Detection of As(III) and As(V) in MGP exposure medium (pH=7.150) supplemented with NaCl, inorganic phosphate (Pi), $CaCl_2$, or $MgCl_2$. Pi was supplemented as a mixture of sodium/potassium phosphate salts (**SI Table A1.1**). The As concentration was 400 nM in each treatment. The mean and standard deviation of RFU per OD_{600} after 18 h of growth is presented for triplicate samples. Left panel, no significant differences were observed between linear regressions of As(III) and As(V) output signal over the NaCl concentration gradient (p=0.07). In conjunction with ANOVAs, TukeyHSD was used for calcium, magnesium and phosphate treatments. Stars indicate a statistically significant difference in output signals when compared to the control (dotted line; no added ions).

2.4.2 Quantifying arsenic species in samples containing both As(III) and As(V).

We tested the ability of our biosensor to selectively detect As(III) over a wide range of As(V) concentrations (**Figure 2.3**). We first set total As level at 400 nM while varying the relative concentrations of each species (**Figure 2.3**a; [As] indicated on the X-axes). We showed that MGP exposure media can accurately quantify total inorganic As concentration (orange circles: no Pi added) irrespective of the relative proportion of each As species. In contrast, fluorescence in the As(III)-selective exposure media (blue circles: 10 mM Pi) was proportional to the As(III) input concentration, indicating that [As(III)] was accurately quantified irrespective of background [As(V)].

Next, we tested the effect of adding a large excess of As(V) (2 µM) on the detection of As(III) using the As(III)-selective exposure medium (MIP). The output signal was proportional to the concentration of As(III) in both exposure conditions,

regardless of the presence of As(V) (**Figure 2.3**b). We noted, however, that the baseline output signal (intercept) for the detection of As(III) in the presence of 2 µM As(V) treatments was significantly higher. This increase in baseline output signal corresponds to an overestimation of ~100 nM across each [As(III)] tested. We attribute this baseline shift to the presence of a threshold, where 10 mM Pi is effective at excluding low background [As(V)]. However, once this threshold is exceeded, we estimate that 10 to 15% of background As(V) can enter the cell and increase signal output.

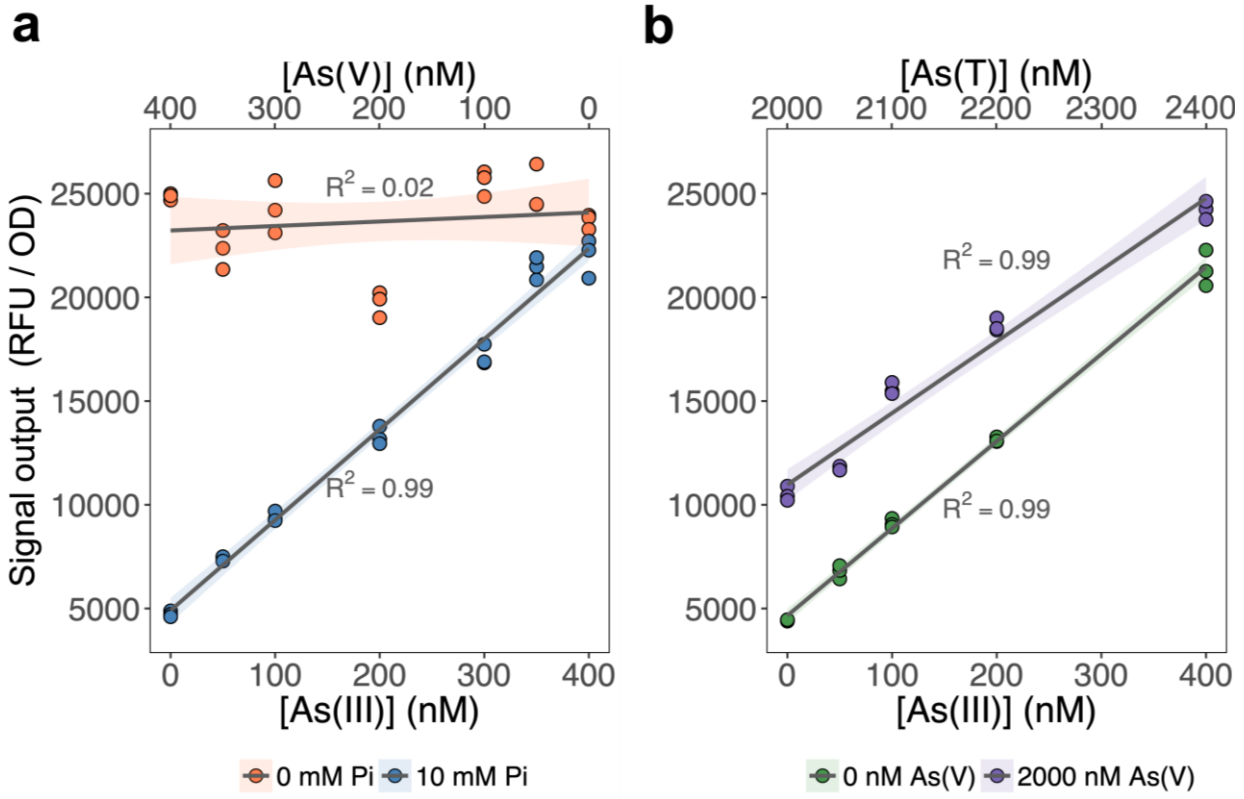

Figure 2.3 | As(III) can be detected independent of As(V) concentration. **(a)** The biosensor was exposed to samples that contained 400 nM total inorganic As and variable input concentrations of As(V) and As(III), indicated on the upper and lower x-axes. MGP (0 mM Pi) and MIP (10 mM Pi) exposure media were used for detection of total inorganic As and As(III), respectively. **(b)** As(III) was detected using MIP exposure media in samples containing 0 nM or 2000 nM As(V). Input concentrations of As(III) are presented on the x-axis. On both plots, triplicate RFU per OD_{600} treatment points are presented rather than means with error bars. The star indicates a statistically significant difference in output signals when compared to the regression analysis.

2.4.3 As(V) detection involves an ArsC-independent reduction to As(III).

To determine As speciation, our assay requires the addition of phosphates to block As(V) uptake and prevent its detection. This approach could be impractical in natural waters with elevated phosphate concentrations (>100 μM). Moreover, Pi addition increases ionic strength and may change the way As interacts with natural ligands, thus altering its bioavailability. In an effort to alleviate the need to amend the sample with inorganic phosphate, we explored the option of taking a genetic approach in preventing the detection of As(V). Previous studies have suggested that As(V) first requires enzymatic reduction to As(III) by ArsC before it can be detected by biosensors (*43, 47*). Indeed, affinity of As to ArsR has only been reported for As(III) (*44, 56*) and not As(V).

We first tested whether ArsC was solely required for As(V) detection and deleted *arsC* from the biosensor host genome. We predicted that As(V) detection would be limited by the inability of the mutant to reduce As(V) to As(III). We found that deletion of *arsC* had no significant effect on the output signal following exposure to either inorganic As species (As(III) and As(V)), indicating that ArsC is not required for As(V) detection.

We then tested the possibility that an ArsC-independent mechanism mediates As(V) reduction in the exposure medium (**Figure 2.4**b). We compared As(V) reduction efficiency of a wild-type strain harbouring the full *ars*-operon to that of an *arsC* mutant. Both the wild-type and Δ*arsC* strains reduced >94% of the As(V) initially provided, with most of the As located in the supernatant fractions. We suspect that the time elapsed between sample collection and speciation analysis by HPLC-ICP-MS is responsible for the reduction observed in the pre-incubation samples. However, the similar reduction rates between wild-type (NEB10-beta) and mutant (Δ*arsC*) treatments post-incubation, strongly support the existence of ArsC-independent As(V) reduction mechanism(s) in *E. coli*. We confirmed these findings

by transforming the Δ*arsC* mutant strain from the Keio collection (JW3470) with the biosensor construct (pMP01). The Δ*arsC* JW3470 biosensor responded to As(V) at a similar rate and signal intensity as the exposure to As(III) (**SI Fig. A2.4**). Furthermore, our mass balance and ICP-MS measurements showed that >94% of As(V) was reduced to As(III), while no As(V) was reduced in our abiotic controls. Although we did not specifically test for extracellular As(V) reduction, to the best of our knowledge the only As(V) reduction pathways in *E.coli* reported in the literature are intracellular. Therefore, our data suggest that >94% of As(V) was available to the *E. coli* cells under these conditions.

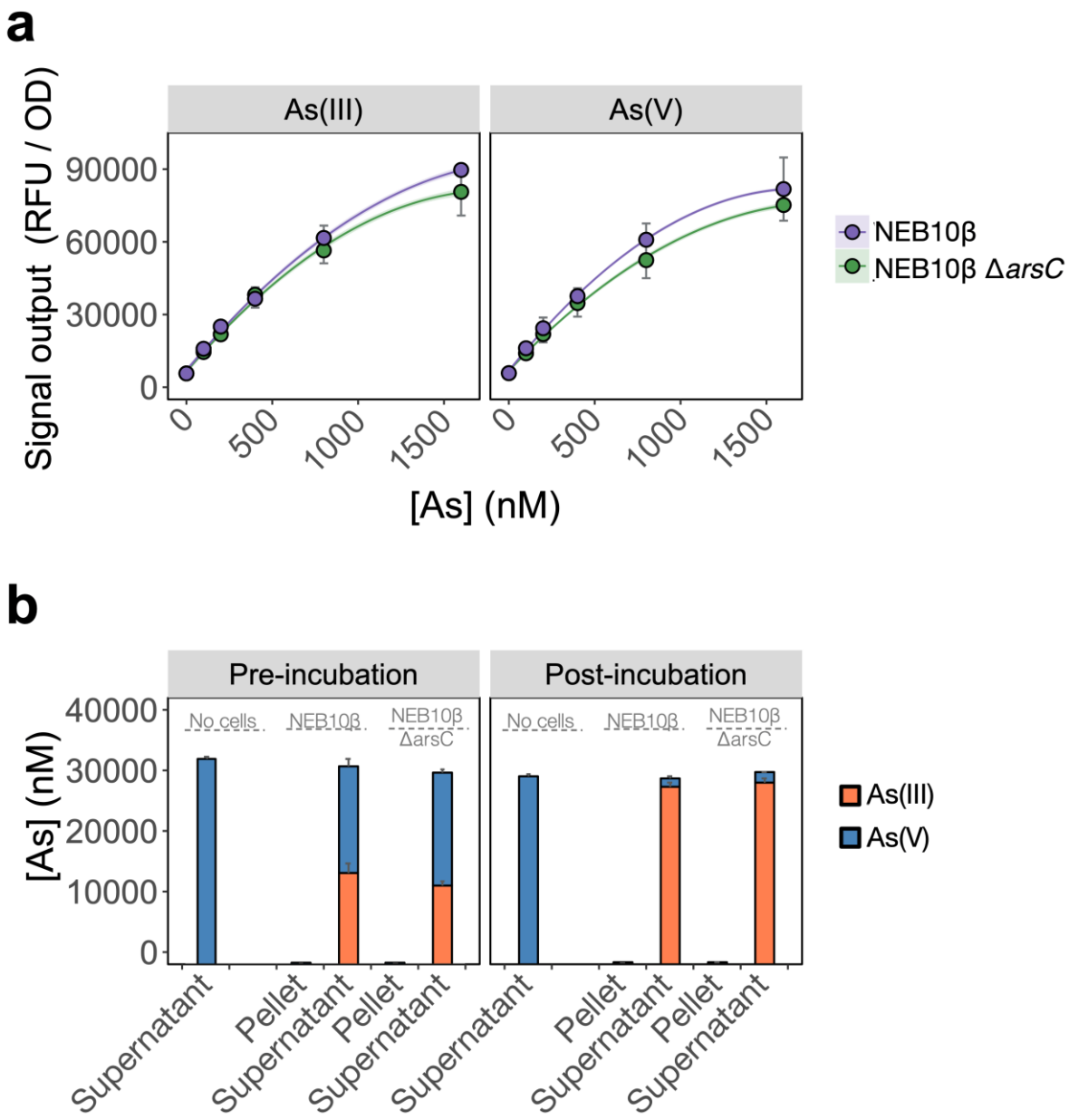

Figure 2.4 | As(V) detection involves an ArsC-independent reduction to As(III). **(a)** As(III) and As(V) detection by the pMP01 biosensor plasmid was compared for the E. coli host strain (NEB10-beta) and a deletion mutant lacking arsenate specific reductase (NEB10-beta Δ*arsC*). Data points represent the mean output signal after 18 h of As exposure in MGP of three independently grown cultures, quantified in triplicate. Error bars indicate standard deviations. We found no significant difference between wild-type and mutant strains (p=0.07). **(b)** Speciation analysis following addition of 32 µM As(V) to MGP exposure media (no cells), NEB10-beta cultures and NEB10-beta Δ*arsC* cultures. Treatments were subsampled, fractionated by centrifugation and analyzed before (left panel) and after (right panel) a 3-hour incubation. As(III) and As(V) concentrations in pellet and supernatant fractions were quantified using HPLC-ICP-MS. The mean and standard deviation of three independent treatments are presented.

Together, these findings suggest that As(V) detection by the *E. coli* biosensor involves a biologically mediated As(V) reduction step, independent of ArsC. Interestingly, a recent study (*12*) identified an ArsC-independent reduction pathway when screening an *E. coli* Δ*arsC* mutant for resistance to As(V). The authors found that overexpression of Glutathione-S-Transferase (GstB) increased As(V) resistance by reducing As(V) to As(III). Our data suggest that intracellular As(V) in *E. coli* is susceptible to non-specific reduction pathways (possibly via Glutathione-S-Transferase) in addition to the specific As-inducible pathway (*arsC*). Because GstB is likely essential to the cell central metabolism, a GstB deletion mutant does not currently represent a good candidate for future biosensor hosts.

2.4.4 As(III) uptake is affected by central carbon metabolism.

The apparent sensitivity of As(V) uptake to media constituents led us to also revisit how As(III) uptake is affected by such media constituents. Previous studies have suggested that 90% of As(III) enters *E. coli* cells via glycerol uptake facilitator channels (GlpF) (*34, 37*). These channels are responsible for the passive transport of water and small hydrophilic molecules including glycerol across the inner membrane (*21*). Transcriptional induction of *glpF* during growth on glycerol is mediated by the interaction between glycerol-3-phosphate and the GlpR repressor (*25, 53*). Expression of *glpF* is repressed by GlpR and sensitive to catabolite repression during growth on preferred carbon sources such as glucose (*53*). We hypothesized that uptake of As(III) is affected by conditions that alter the expression of the *glpF* transporter.

We compared As(III) detection during growth on a carbon source favouring *glpF* induction (glycerol) to one favouring *glpF* repression (glucose). We observed that fluorescence produced in response to As(III) exposure was 2-fold higher during growth on glycerol than on glucose, consistent with greater uptake of As(III) in cells growing on glycerol (**Figure 2.5**). Analysis of glucose consumption in the cultures indicated that the increased signal output occurred after most of the glucose (>60%)

was consumed. As a control, glycerol treated cells were also analyzed for glucose content and no glucose was found in any of the triplicate glycerol treatments at T=0 h (data not shown). This result is consistent with catabolite repression of the *glpF* transporter leading to reduce As(III) uptake during exponential growth on glucose, with increased detection occurring under conditions following relaxation of catabolite repression.

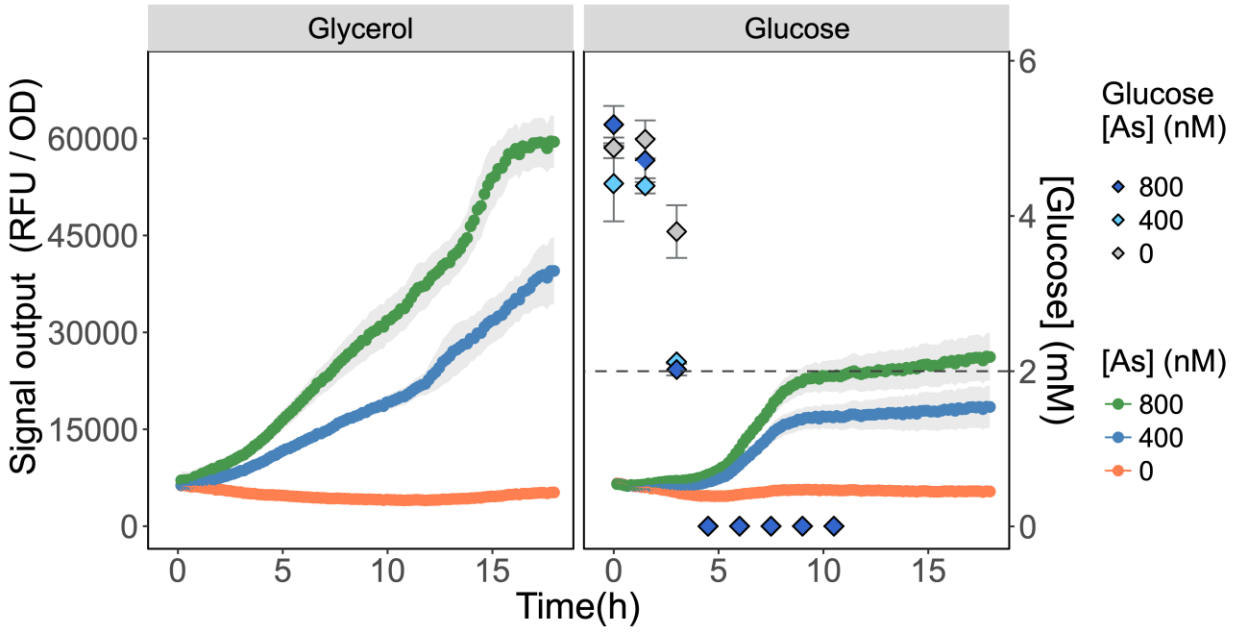

Figure 2.5 | Detection of As(III) is hampered in glucose grown biosensor cultures. As(III) was detected in biosensor cultures grown and exposed in media containing glycerol (**left panel**) or glucose (**right panel**) as primary carbon sources. The RFU per OD_{600} is given for the 18 h following As exposure. The concentration of glucose in culture supernatant fractions was quantified using HPLC-ELSD over time and is presented on the secondary y-axis. The mean and standard deviations of biological triplicate exposures are represented for both RFU and the glucose concentration estimates. HPLC-ELSD limit of detection is presented as the dotted line.

2.4.5 Application of the biosensor to arsenic quantification in lake samples.

We were interested in testing the performance of the biosensor in quantifying total inorganic As levels in environmental samples. We chose Yellowknife, Northwest Territories in subarctic Canada as our study area. Gold mine operations in this area have severely affected the surrounding lakes due to the atmospheric deposition of As

trioxide (As_2O_3) from Giant Mine roaster stack emissions (*18*). The heterogeneity of the underlying bedrock (*52, 57*) has resulted in lakes with diverse chemical profiles. Despite cessation of gold mining operations in 2004, legacy As contamination in many lakes still far exceeds Canadian guidelines for the protection of aquatic life (5 µg/L or 67 nM) and drinking water standards (10 µg/L or 133 nM).

We compared the detection of total inorganic arsenic (As_{total}) by the biosensor to that of HPLC-ICP-MS using water samples collected from 17 lakes in the area surrounding Yellowknife (**Figure 2.6**a). Speciation analysis by HPLC-ICP-MS indicated that >99% of the inorganic As in the lake surface water samples was in the form of As(V) and <1% was in the form of As(III), arsenobetaine or organoarsenic species. This result was expected as we did not chemically preserve the samples (see method section for details). The biosensor accurately quantified total inorganic As (R^2=0.96) over the entire range of As concentrations in the lake samples (**Figure 2.6**a). The high accuracy of As(V) quantification by the biosensor is likely due to the improved detection of As(V) in the non-selective exposure medium, which we have found likely permits uptake of greater than 94% of As(V) into the biosensor host (**Figure 2.6**b). Thus, our data suggest that most of the legacy inorganic As from anthropogenic sources in these environmental samples is available for microbial uptake.

In addition to quantifying legacy As contamination, we also assessed bioavailability of newly added As(III) and As(V) to natural water samples. We performed standard additions of both As(III) and As(V) in 17 surface lake water samples of contrasting water chemistry (**SI Fig. A2.5**). The fluorescence response of the biosensor to standard additions varied with lakes (slopes ranged from -0.46 to 146.16 for As(V) and 24.64 to 170.05 for As(III)) when compared to the calibration curve performed in exposure media, suggesting that water chemistry affected the ability of the biosensor to detect newly added As(III) and As(V) (*e.g.*, BC-17, YK67). Furthermore, and surprisingly, a subset of lakes exhibited a muted response to newly

added As(III) and As(V) when compared to the exposure media controls (*e.g.*, BC-17, YK-12, YK67, Vee). This muted response (standard addition slopes) could be indicative of a lower bioavailability of the newly added As species, compared to "older" legacy As already present in the system (standard addition intercept). This matrix effect is likely a consequence of direct or indirect interactions between As and chemical constituents of the water samples.

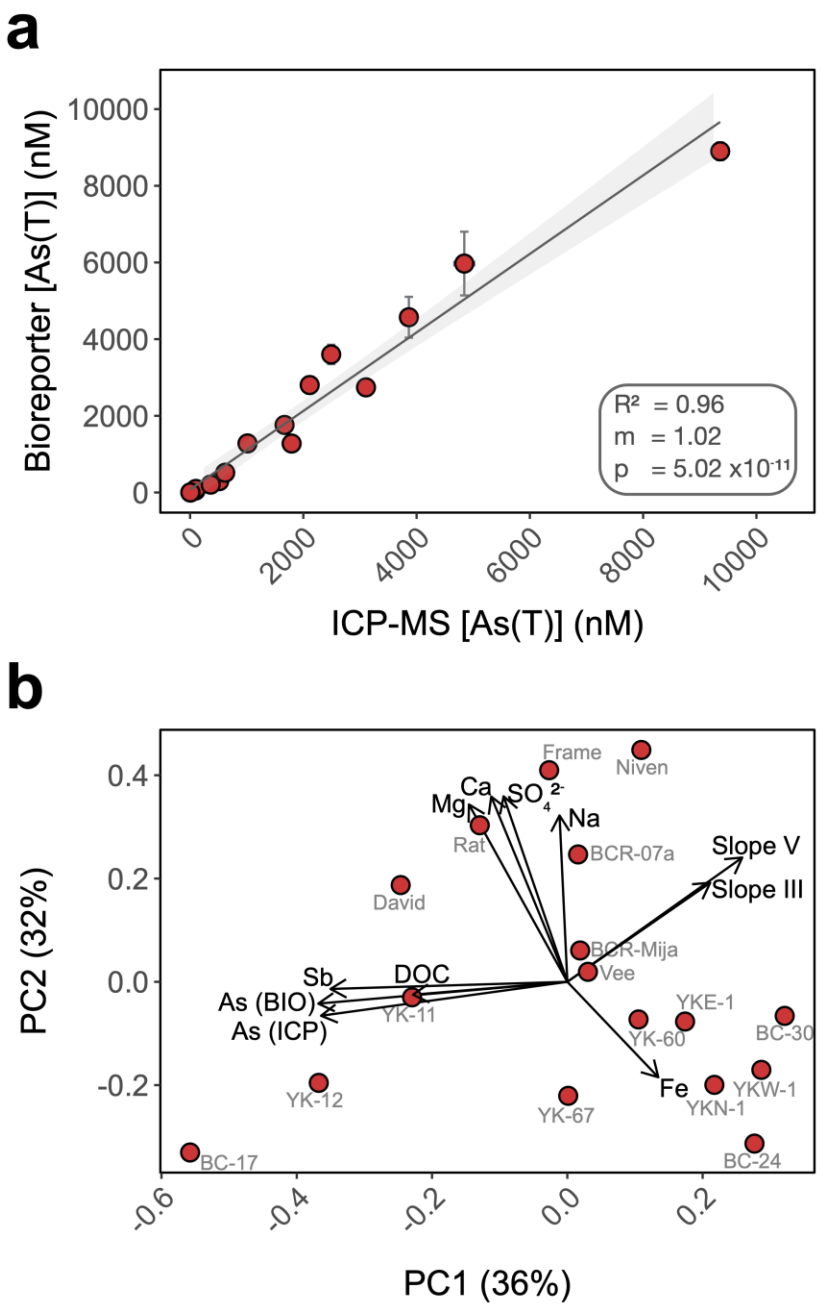

Figure 2.6 | Total inorganic As concentrations are accurately quantified using the biosensor assay through a wide range of water chemistry profiles. **(a)** Cross-analysis of As quantification in 17 surface water samples using the biosensor and HPLC-ICP-MS. **(b)** PCA of the surface water chemistry of 17 lakes in Yellowknife. Each PCA point represents an individual lake separated by Euclidian distances as a metric of variations in water chemistry profile. Overlaid are biplot vectors, pointing in the direction of most rapid change in a specified environmental variable. The strength of the gradient direction is presented by the length of the vector. Standard addition slopes for As(III) and As(V) are used as proxies for their respective bioavailability.

We ran a principal component analysis (PCA) to explore which chemical variables may contribute to explaining the variation observed in As bioavailability between lakes (**Figure 2.6**b) (*29*). Biplot vectors include standard addition slopes for As(III) and As(V) as proxies for their respective bioavailability along with lake chemical variables. Principal components 1 and 2 explained a total of 68% of the variance. The absence of clustering between lakes is indicative of heterogeneity in water chemistry profiles. The vectors corresponding to As bioavailability (slopes) were orthogonal to vectors for the following chemical constituents (Fe, Na, Ca, Mg) suggesting that these matrix components have little control on the bioavailability of added As in these samples, supporting our experimental data (**Figure 2.2**). In contrast, the slope vectors had closer alignment, in opposite directions, with DOC (dissolved organic carbon), antimony (Sb) and legacy As concentration (As (ICP) and As (BIO)) vectors. We found a significant negative correlation between As(III) bioavailability and [DOC] (R^2=0.212; p=0.04) but not for As(V) (R^2=0.09; p=0.13) (**SI Fig. A2.6**). Together these data suggest differential bioavailability of new vs. old (legacy) As that might be explained by interactions with matrix constituents such as DOC. DOC has been shown to form ternary complexes with As(III) and As(V) (*24*) and to control As distribution in the sediments of lakes in this region (*18*). The role of DOC on As bioavailability remains to be tested.

2.5 Conclusion

Whereas biosensors have routinely detected As(III) at environmentally relevant concentrations, detection of As(V) has been less reliable. We found that elimination of inorganic phosphate from the exposure medium, led to an improved detection of As(V). The selective inclusion of phosphates in the exposure media proved to be a useful tool for estimating As speciation under controlled laboratory conditions (**Figure 2.1** and **Figure 2.3**a) even when the cells are faced with a high background of As(V) (**Figure 2.3**b). The mechanism responsible for the inhibition of As(V) uptake

at high Pi concentrations likely involves competition between Pi and As(V) at the Pit transport site, or to the reduced expression of the high-affinity phosphate transporter system (Pst). Contrary to previous suggestions, we were surprised to find the existence of an ArsC-independent mechanism of As(V) reduction relevant for As biosensor applications (**Figure 2.4**). We also saw that As(III) detection (**Figure 2.5**) is affected by the carbon source used in the bioassay. These findings have implications for environments where available carbon sources might alter As(III) bioavailability and thus its biotransformation by microbial communities. Moreover, the pervasiveness of non-specific As(V) reduction in the environment has never been investigated, and, as previously described for mercury (*20*), could act as a major route for environmental As redox cycling.

Our field work tested the impacts of heterogeneous environments on the detection of legacy As contamination (**Figure 2.6**a). Our biosensor assay positively compared to HPLC-ICP-MS data. Despite the accurate quantification of legacy As contamination, we observed a muted response to newly added As species in several water samples (**SI Fig. A2.5**). We identified naturally occurring DOC as a potential contender in the environmental control of As bioavailability. We propose that DOM has the potential to kinetically control the bioavailability of As; further work is warranted to characterize the nature of the As-DOM interactions and better predict As mobility and availability in the environment.

2.6 Funding

An Early Researcher Award from the Province of Ontario, a Discovery Grant, an Accelerator Grant and a Northern Supplement from the Natural Sciences and Engineering Research Council of Canada to A.J.P. funded this study.

2.7 Acknowledgments

We would like to thank two reviewers for their comments as well as Dr. Emmanuel Yumvihoze for providing As speciation analysis using HPLC-ICP-MS as well as Jessica Gaudet and Dr. Ammar Saleem for assistance with HPLC-ELSD analyses. We would like to thank the Blais Laboratory, namely Dave Eickmeyer, at the University of Ottawa for helping with logistical details in Yellowknife, Canada.

2.8 Conflict of Interest

The authors declare that the research was conducted in the absence of any commercial or financial relationships that could be construed as a potential conflict of interest.

2.9 Bibliography – Chapter 2

1. M. J. Abedin, J. Feldmann, A. A. Meharg, Uptake kinetics of arsenic species in rice plants. *Plant physiology* **128**, 1120-1128 (2002).
2. C. M. Andy *et al.*, Assessing Models of Arsenic Occurrence in Drinking Water from Bedrock Aquifers in New Hampshire. *Journal of Contemporary Water Research & Education* **160**, 25-41 (2017).
3. T. Baba *et al.*, Construction of Escherichia coli K‐12 in‐frame, single‐gene knockout mutants: the Keio collection. *Molecular systems biology* **2**, (2006).
4. R. Bentley, T. G. Chasteen, Microbial methylation of metalloids: arsenic, antimony, and bismuth. *Microbiology and Molecular Biology Reviews* **66**, 250-271 (2002).
5. P. Bhattacharya *et al.* (Elsevier, 2007).
6. F. R. Blattner *et al.*, The complete genome sequence of Escherichia coli K-12. *science* **277**, 1453-1462 (1997).
7. L. Cai, C. Rensing, X. Li, G. Wang, Novel gene clusters involved in arsenite oxidation and resistance in two arsenite oxidizers: Achromobacter sp. SY8 and Pseudomonas sp. TS44. *Applied microbiology and biotechnology* **83**, 715-725 (2009).
8. P. C. Chan, J. Huff, Arsenic carcinogenesis in animals and in humans: Mechanistic, experimental, and epidemiological evidence. *Journal of Environmental Science and Health - Part C Environmental Carcinogenesis and Ecotoxicology Reviews* **15**, 83-122 (1997).
9. J. S. Chang, Y. H. Kim, K. W. Kim, The ars genotype characterization of arsenic-resistant bacteria from arsenic-contaminated gold-silver mines in the Republic of Korea. *Applied Microbiology and Biotechnology* **80**, 155-165 (2008).
10. C.-J. Chen, C.-J. Wang, Ecological correlation between arsenic level in well water and age-adjusted mortality from malignant neoplasms. *Cancer research* **50**, 5470-5474 (1990).
11. J. Chen, S. Sun, C.-Z. Li, Y.-G. Zhu, B. P. Rosen, Biosensor for organoarsenical herbicides and growth promoters. *Environmental science & technology* **48**, 1141-1147 (2014).
12. C. Chrysostomou, E. M. Quandt, N. M. Marshall, E. Stone, G. Georgiou, An Alternate Pathway of Arsenate Resistance in E. coli Mediated by the Glutathione S-Transferase GstB. *ACS chemical biology* **10**, 875-882 (2015).
13. P. Corbisier, G. Ji, G. Nuyts, M. Mergeay, S. Silver, luxAB gene fusions with the arsenic and cadmium resistance operons of Staphylococcus aureus plasmid pI258. *FEMS microbiology letters* **110**, 231-238 (1993).
14. F. Cortés-Salazar, S. Beggah, J. R. van der Meer, H. H. Girault, Electrochemical As(III) whole-cell based biochip sensor. *Biosensors and Bioelectronics* **47**, 237-242 (2013).
15. A. Date, P. Pasini, S. Daunert, Construction of spores for portable bacterial whole-cell biosensing systems. *Analytical Chemistry* **79**, 9391-9397 (2007).
16. K. A. Datsenko, B. L. Wanner, One-step inactivation of chromosomal genes in Escherichia coli K-12 using PCR products. *Proceedings of the National Academy of Sciences* **97**, 6640-6645 (2000).
17. S. V. Flanagan *et al.*, Arsenic in private well water part 3 of 3: Socioeconomic vulnerability to exposure in Maine and New Jersey. *Science of the Total Environment* **562**, 1019-1030 (2016).
18. J. M. Galloway *et al.*, Organic matter control on the distribution of arsenic in lake sediments impacted by~ 65 years of gold ore processing in subarctic Canada. *Science of The Total Environment*, (2017).
19. C. M. George *et al.*, Arsenic exposure in drinking water: an unrecognized health threat in Peru. *Bulletin of the World Health Organization* **92**, 565-572 (2014).
20. D. Grégoire, A. Poulain, A physiological role for Hg II during phototrophic growth. *Nature Geoscience* **9**, 121 (2016).

21. J. Hénin, E. Tajkhorshid, K. Schulten, C. Chipot, Diffusion of glycerol through Escherichia coli aquaglyceroporin GlpF. *Biophysical journal* **94**, 832-839 (2008).
22. IARC, Arsenic and Arsenic Compounds. *IARC Monographs*, 52 (2013).
23. K. T. Kitchin, Recent advances in arsenic carcinogenesis: Modes of action, animal model systems, and methylated arsenic metabolites. *Toxicology and Applied Pharmacology* **172**, 249-261 (2001).
24. V. Lenoble *et al.*, Evaluation and modelling of dissolved organic matter reactivity toward AsIII and AsV - Implication in environmental arsenic speciation. *Talanta* **134**, 530-537 (2015).
25. E. Lin, Glycerol dissimilation and its regulation in bacteria. *Annual Reviews in Microbiology* **30**, 535-578 (1976).
26. P. Lu, C. Zhu, Arsenic Eh-pH diagrams at 25°C and 1 bar. *Environmental Earth Sciences* **62**, 1673-1683 (2011).
27. A. A. Meharg, J. Hartley - Whitaker, Arsenic uptake and metabolism in arsenic resistant and nonresistant plant species. *New Phytologist* **154**, 29-43 (2002).
28. D. Melamed, Monitoring arsenic in the environment: A review of science and technologies with the potential for field measurements. *Analytica Chimica Acta* **532**, 1-13 (2005).
29. J. Oksanen *et al.*, The vegan package. *Community ecology package* **10**, 631-637 (2007).
30. N. N. Rao, A. Torriani, Molecular aspects of phosphate transport in Escherichia coli. *Molecular Microbiology* **4**, 1083-1090 (1990).
31. R. J. Reeder, M. A. A. Schoonen, A. Lanzirotti, in *Reviews in Mineralogy and Geochemistry*. (2006), vol. 64, pp. 59-113.
32. P. A. Riveros, J. E. Dutrizac, P. Spencer, Arsenic disposal practices in the metallurgical industry. *Canadian Metallurgical Quarterly* **40**, 395-420 (2001).
33. C. Roggo, J. R. van der Meer, Miniaturized and integrated whole cell living bacterial sensors in field applicable autonomous devices. *Current opinion in biotechnology* **45**, 24-33 (2017).
34. B. P. Rosen, M. J. Tamás, Arsenic transport in prokaryotes and eukaryotic microbes. *Adv. Exp. Med. Biol* **679**, 47-55 (2010).
35. H. Rosenberg, R. Gerdes, K. Chegwidden, Two systems for the uptake of phosphate in Escherichia coli. *Journal of bacteriology* **131**, 505-511 (1977).
36. C. W. Saltikov, D. K. Newman, Genetic identification of a respiratory arsenate reductase. *Proceedings of the National Academy of Sciences* **100**, 10983-10988 (2003).
37. O. I. Sanders, C. Rensing, M. Kuroda, B. Mitra, B. P. Rosen, Antimonite is accumulated by the glycerol facilitator GlpF in Escherichia coli. *Journal of bacteriology* **179**, 3365-3367 (1997).
38. J. M. Santini, R. N. vanden Hoven, Molybdenum-containing arsenite oxidase of the chemolithoautotrophic arsenite oxidizer NT-26. *Journal of Bacteriology* **186**, 1614-1619 (2004).
39. H. P. Schweizer, Escherichia-Pseudomonas shuttle vectors derived from pUC18/19. *Gene* **97**, 109-112 (1991).
40. M. C. Sforna *et al.*, Evidence for arsenic metabolism and cycling by microorganisms 2.7 billion years ago. *Nature Geoscience* **7**, 811 (2014).
41. N. C. Shaner *et al.*, Improved monomeric red, orange and yellow fluorescent proteins derived from Discosoma sp. red fluorescent protein. *Nature Biotechnology* **22**, 1567-1572 (2004).
42. N. C. Shaner, P. A. Steinbach, R. Y. Tsien, A guide to choosing fluorescent proteins. *Nature Methods* **2**, 905-909 (2005).
43. P. Sharma, S. Asad, A. Ali, Bioluminescent bioreporter for assessment of arsenic contamination in water samples of India. *Journal of Biosciences* **38**, 251-258 (2013).

44. S. Shen, X.-F. Li, W. R. Cullen, M. Weinfeld, X. C. Le, Arsenic binding to proteins. *Chemical reviews* **113**, 7769-7792 (2013).
45. K. Siegfried *et al.*, Field testing of arsenic in groundwater samples of Bangladesh using a test kit based on lyophilized bioreporter bacteria. *Environmental Science and Technology* **46**, 3281-3287 (2012).
46. S. Silver, L. T. Phung, Genes and enzymes involved in bacterial oxidation and reduction of inorganic arsenic. *Applied and Environmental Microbiology* **71**, 599-608 (2005).
47. J. Stocker *et al.*, Development of a set of simple bacterial biosensors for quantitative and rapid measurements of arsenite and arsenate in potable water. *Environmental Science and Technology* **37**, 4743-4750 (2003).
48. S. Tauriainen, M. Karp, W. Chang, M. Virta, Recombinant luminescent bacteria for measuring bioavailable arsenite and antimonite. *Applied and environmental microbiology* **63**, 4456-4461 (1997).
49. P. T. K. Trang, M. Berg, P. H. Viet, N. Van Mui, J. R. Van Der Meer, Bacterial bioassay for rapid and accurate analysis of arsenic in highly variable groundwater samples. *Environmental Science and Technology* **39**, 7625-7630 (2005).
50. F. Truffer *et al.*, Compact portable biosensor for arsenic detection in aqueous samples with Escherichia coli bioreporter cells. *Review of Scientific Instruments* **85**, (2014).
51. A. Valenzuela, Université Laval, (2000).
52. M. Villeneuve, C. Relf, Tectonic setting of 2.6 Ga carbonatites in the Slave Province, NW Canada. *Journal of Petrology* **39**, 1975-1986 (1998).
53. D. L. Weissenborn, N. Wittekindt, T. J. Larson, Structure and regulation of the glpFK operon encoding glycerol diffusion facilitator and glycerol kinase of Escherichia coli K-12. *Journal of Biological Chemistry* **267**, 6122-6131 (1992).
54. *Guidelines for drinking-water quality: recommendations* (9241546387, 2004).
55. G. R. Willsky, M. H. Malamy, Effect of arsenate on inorganic phosphate transport in Escherichia coli. *Journal of Bacteriology* **144**, 366-374 (1980).
56. J. Wu, B. Rosen, Metalloregulated expression of the ars operon. *Journal of Biological Chemistry* **268**, 52-58 (1993).
57. K. Yamashita, R. A. Creaser, Geochemical and Nd isotopic constraints for the origin of Late Archean turbidites from the Yellowknife area, Northwest Territories, Canada. *Geochimica et Cosmochimica Acta* **63**, 2579-2598 (1999).
58. J. Ye, C. Rensing, B. P. Rosen, Y.-G. Zhu, Arsenic biomethylation by photosynthetic organisms. *Trends in plant science* **17**, 155-162 (2012).
59. Y. B. Zhang *et al.*, ArsR arsenic-resistance regulatory protein from Cupriavidus metallidurans CH34. *Antonie van Leeuwenhoek, International Journal of General and Molecular Microbiology* **96**, 161-170 (2009).

Annex A – Chapter 2 SI

SUPPLEMENTARY MATERIALS

Insights into arsenite and arsenate uptake pathways using a whole cell biosensor

Martin P. Pothier[1]*, Aaron J. Hinz*[1]*, Alexandre J. Poulain*[1]

[1] *Biology Department, University of Ottawa, 30 Marie Curie, Ottawa, ON, K1N 6N5, Canada*

List of supplementary materials:

A modified version of the supplementary materials can be found online at:
***Frontiers in Microbiology* |**
https://www.frontiersin.org/articles/10.3389/fmicb.2018.02310/full#supplementary-material

Annex A1 Supplementary table

SI Table A1.1 | MGP media recipes and constituents' concentrations.

Reagents	Constituents	[Constituents] in stock solution (M)	[Constituents] in MGP growth media (M)	[Constituents] in MGP exp media (M)	[Constituents] in MIP exp media (M)
MGP buffer (pH=7.150)	$C_7H_{14}NO_4S$	0.40	0.020	0.020	0.020
	NaCl	0.40	0.020	0.020	0.020
	KCl	0.40	0.020	0.020	0.020
	$(NH_4)_2SO_4$	0.64	0.032	0.032	0.032
β-glycerophosphate	$(HOCH_2)_2CHOP(O)(ONa)_2 \cdot xH_2O$	0.40	0.001	0.001	0.001
Magnesium sulphate	$MgSO_4$	2.0	$1.25x10^{-3}$	$2.00x10^{-5}$	$2.00x10^{-5}$
Glycerol	$C_3H_8O_3$	4.0	0.030	0.005	0.005
Amino acids	L-Leucine	0.075	$2.28x10^{-4}$	$2.28x10^{-4}$	$2.28x10^{-4}$
	L-Isoleucine	0.075	$2.28x10^{-4}$	$2.28x10^{-4}$	$2.28x10^{-4}$
	Valine	0.075	$2.28x10^{-4}$	$2.28x10^{-4}$	$2.28x10^{-4}$
Trace elements #1 (0.1M H_2SO_4)	$NiCl_2 \cdot 6H_2O$	$8.41x10^{-5}$	$8.41x10^{-8}$	—	—
	$CoCl_2 \cdot 6H_2O$	$4.20x10^{-5}$	$4.20x10^{-8}$	—	—
	$ZnSO_4$	$3.48x10^{-4}$	$3.48x10^{-7}$	—	—
	$MnSO_4$	$9.41x10^{-3}$	$9.41x10^{-6}$	—	—
Trace elements #2 (0.1M NaOH)	H_3BO_3	$4.85x10^{-3}$	$4.85x10^{-6}$	—	—
	$Na_2MoO_4 \cdot 2H_2O$	$1.24x10^{-4}$	$1.24x10^{-7}$	—	—
Pi buffer (pH=7.150)	$NaH_2PO_4 \cdot H_2O$	0.43	—	—	0.01
	K_2PO_4	0.57			

Annex A2 Supplementary figures

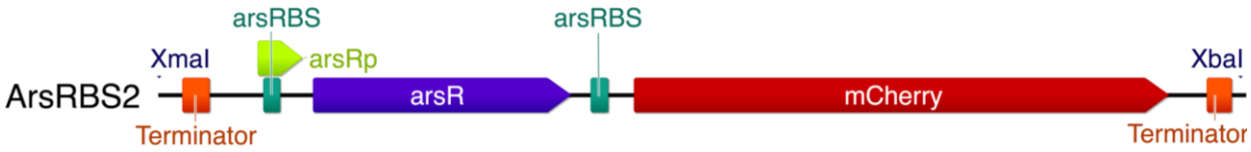

SI Fig. A2.1 | Map representing the pMP01 construct inspired by Stocker et al. 2003.

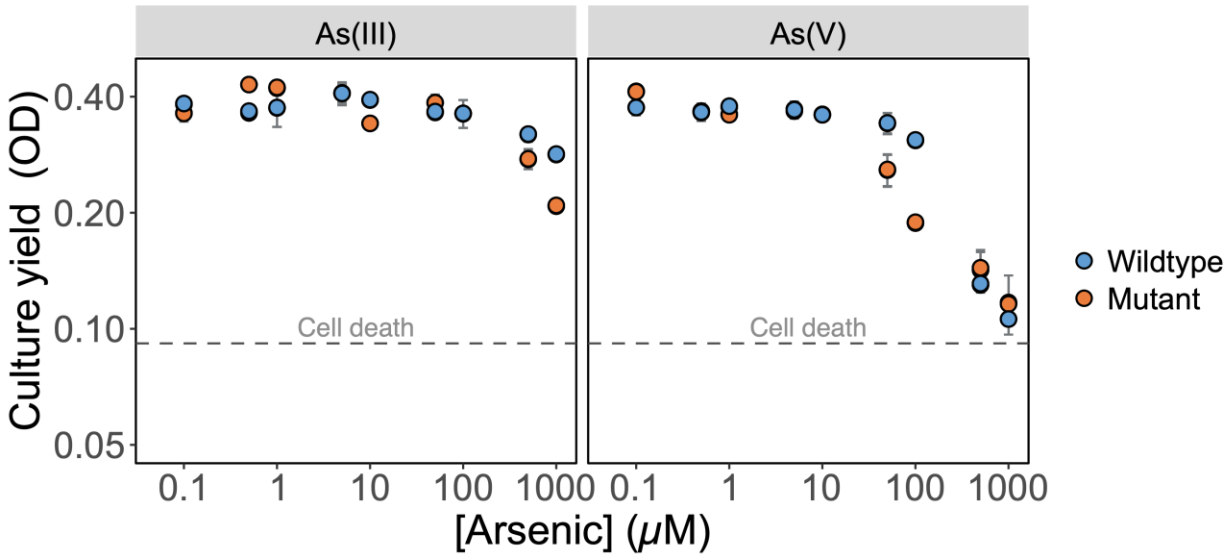

SI Fig. A2.2 | Δ*arsC* deletion mutants are more sensitive to As(V) than wild-type *E. coli* NEB10-beta. Minimal inhibitory concentrations of As(III) (left panel) and As(V) (right panel) were determined for both wild-type and mutant strains using standard As exposure protocol in MGP exposure medium. Cell culture yields at 18 hours are presented on the Y-axis. Error bars represent the standard deviation of biological triplicates. For As(III), toxicity was not observed below 500 µM for both strains. For As(V), a decrease in yield was observed at 100 µM for wild-type, but 50 µM for Δ*arsC* deletion mutant. The dashed lines represent complete inhibition of cell growth.

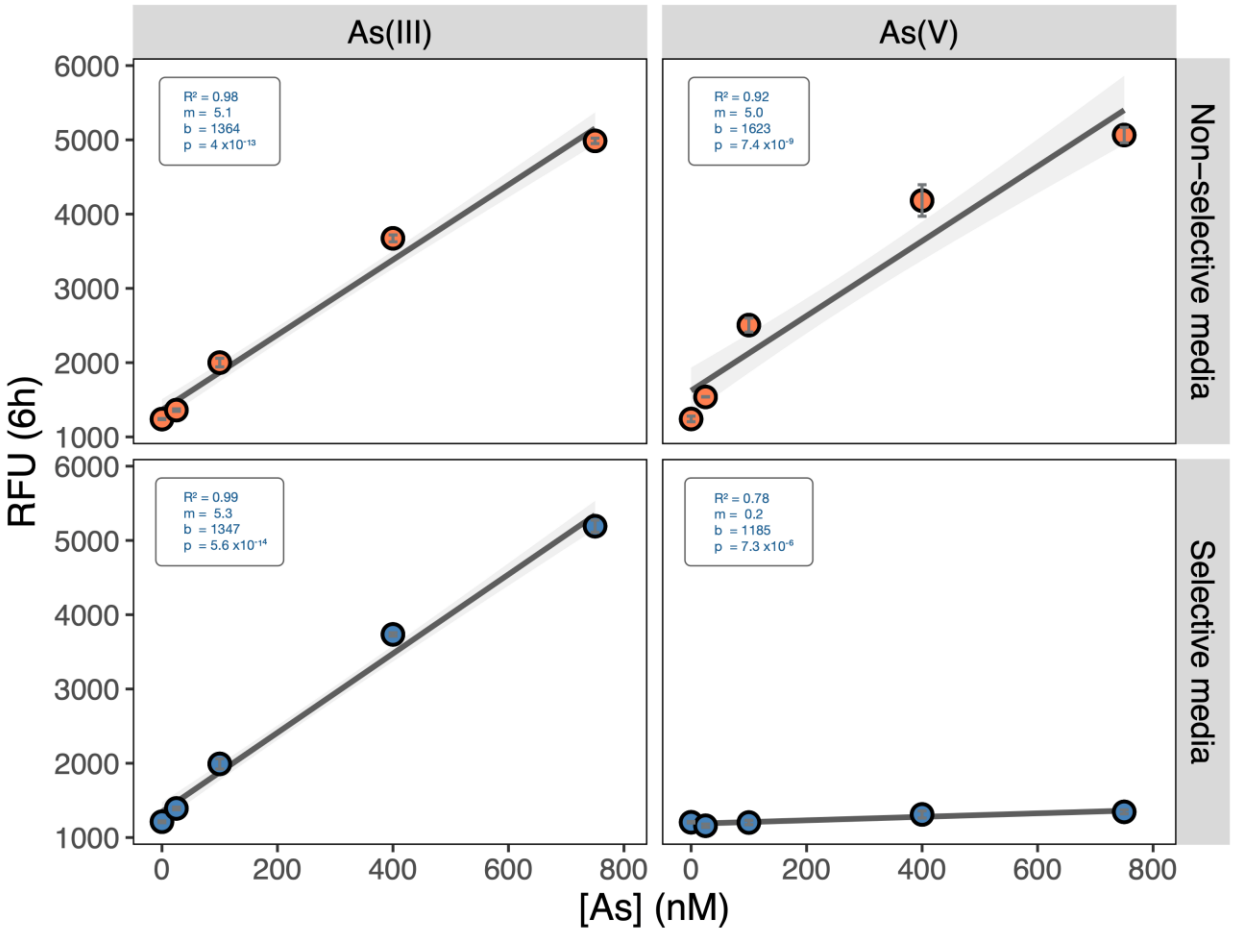

SI Fig. A2.3 | Numeric conversion of biosensor signal to arsenic concentration involves capturing endpoint fluorescence at a specified time point. Presented is the 6-hour fluorescent output (RFU) plotted over spiked As concentrations (X-axis). Raw RFU values were captured every 10 minutes and presented in **Figure 2.1**. The mean and standard deviation of triplicate exposures are presented. Linear regressions (y~x) are presented by the lines and 95% confidence intervals by the shadings.

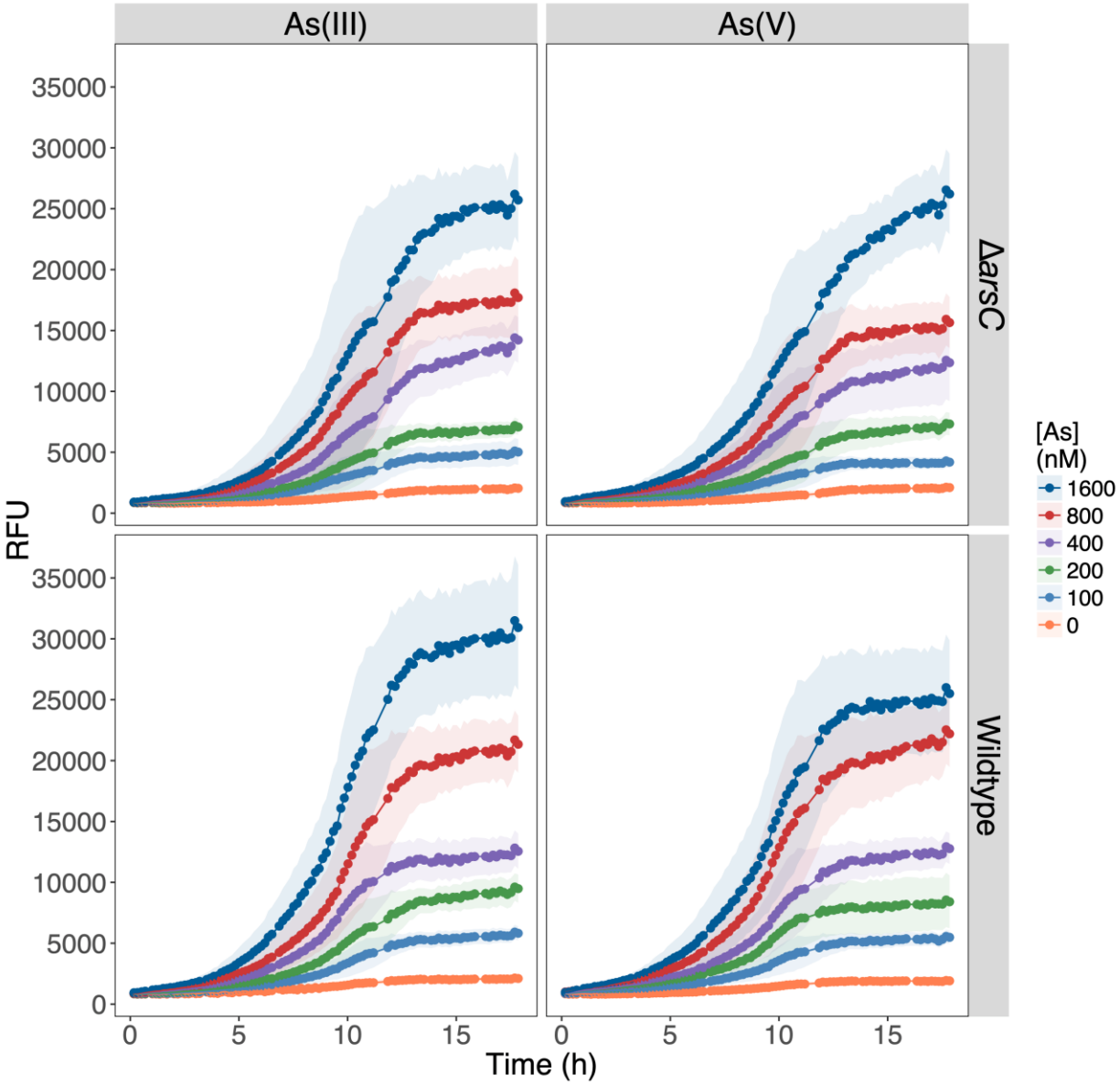

SI Fig. A2.4 | deletion of Δ*arsC* from the biosensor chassis minimally affects biosensor response to As(III) and As(V). The pMP01 reporter plasmid was cloned into the wild-type NEB10β biosensor chassis (**lower panels**), and into an NEB10β mutant chassis absent genomic *arsC* (**upper panels**). These biosensors were exposed to the indicated concentrations of As(III) or As(V) in MGP media lacking inorganic phosphate (Non-selective media). The output signal of the biosensor is presented in relative fluorescence units (RFU) during the first 6 hours of growth immediately following exposure to As. The mean and standard deviation of three independent treatments are presented by the shaded area surrounding the data points.

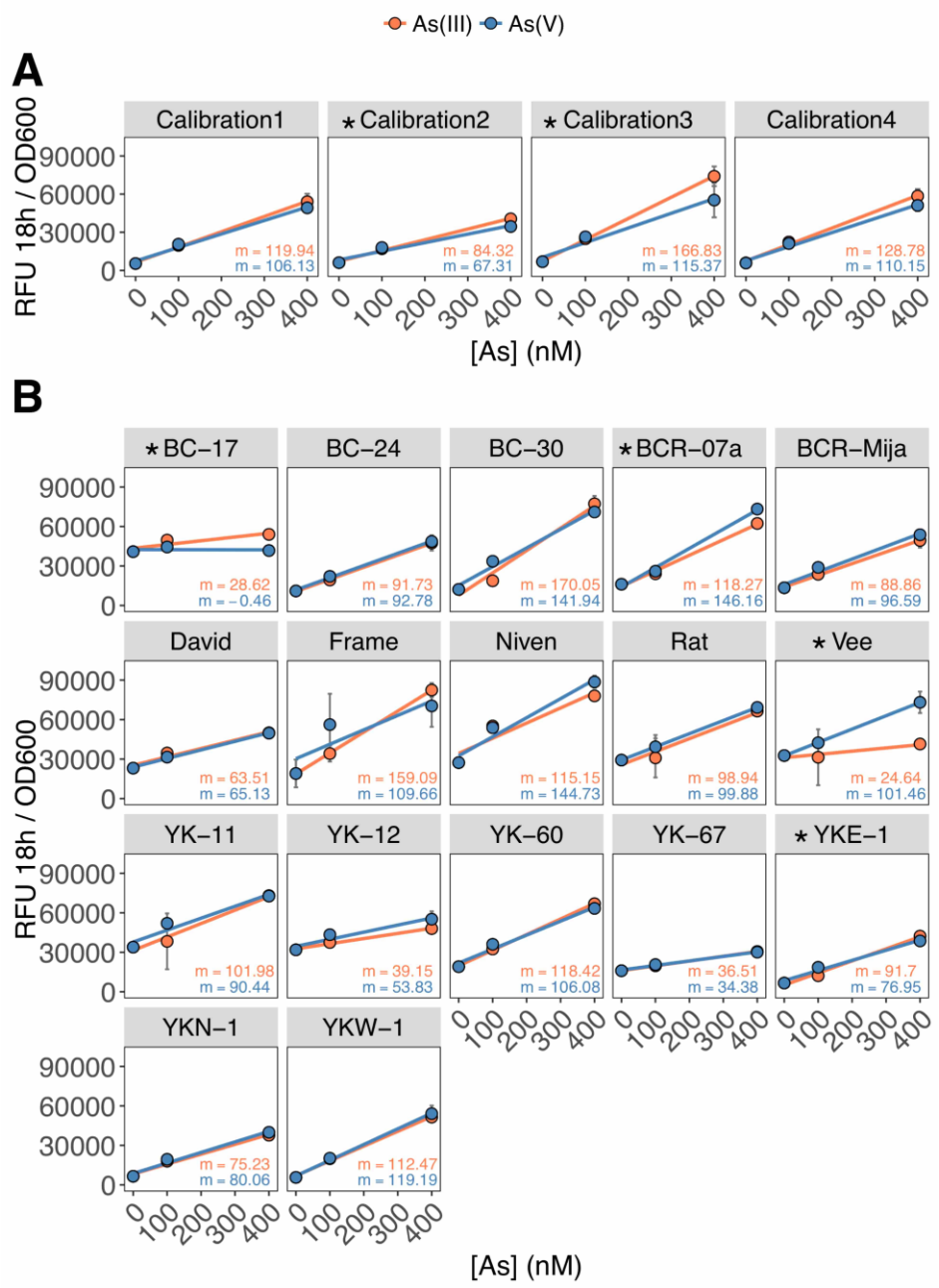

SI Fig. A2.5 | Bioavailability of As is sensitive to sample matrix. Selected lakes were located in close proximity to Yellowknife, Northwest Territories in subarctic Canada. Regression lines were fitted to standard additions of As(III) (**orange**) and As(V) (**blue**) using **(A)** ultrapure water (calibration, performed daily), and **(B)** natural surface waters from 17 lakes of varying water chemistry profiles. Input As concentration is denoted on the X-axis in nanomolar. Output signal (RFU) on the Y-axis is normalized to culture yield (OD_{600}) after 18 hours of growth. Lake names are found in the panel title. Regression line slopes for As(III) is indicated in orange coloured text and As(V) in blue coloured text at the bottom right of each panel. Regression intercepts vary among lakes due to the naturally occurring As concentrations in each lake. Differences in slopes between lakes is used as a proxy for a change in bioavailability of newly added As species.

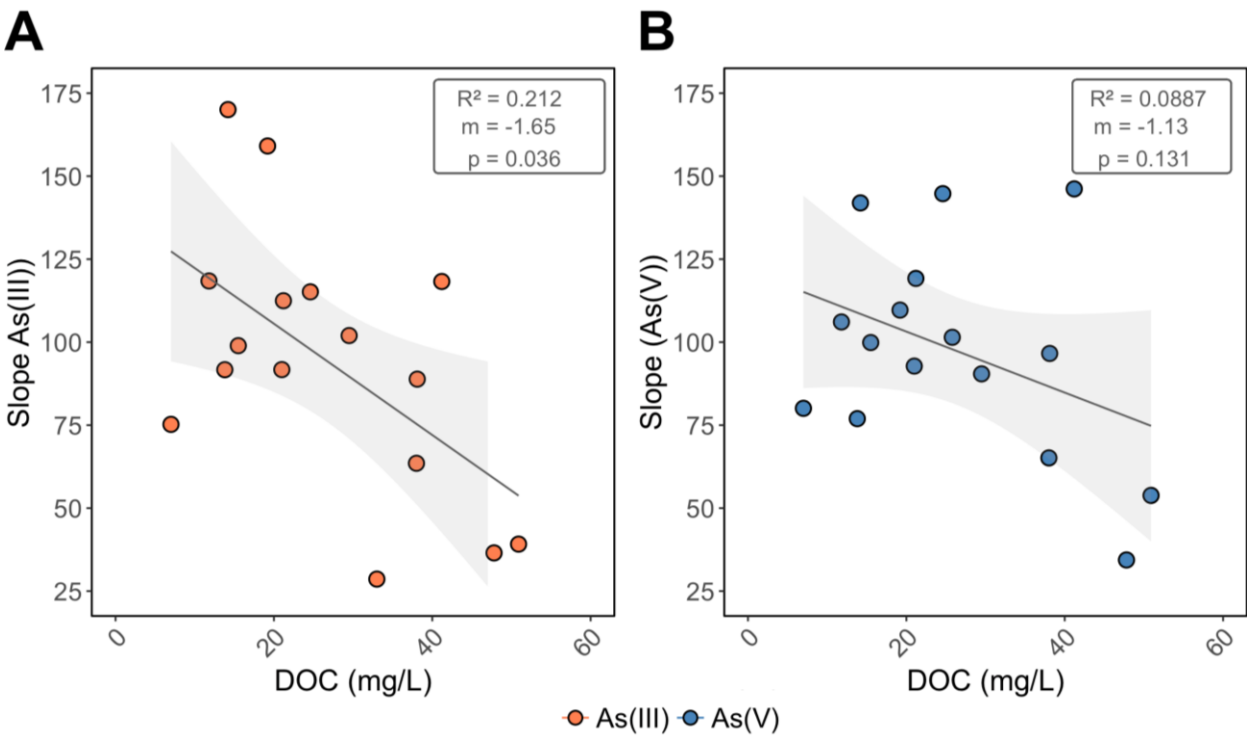

SI Fig. A2.6 | Relationship between [DOC] on As(III) and As(V) bioavailability. Dissolved organic carbon (DOC) concentrations in each lake are plotted on the X-axis. As a proxy for As bioavailability, slope data gathered from As standard additions of **SI Fig. A2.5** is presented on the Y-axis. Significant negative correlation is observed between As(III) bioavailability and [DOC], but not between As(V) bioavailability and [DOC].

ORIGINAL RESEARCH

Dissolved organic matter controls arsenic bioavailability to bacteria

Martin P. Pothier[1]*, Véronique Lenoble*[2]*, Cédric Garnier*[2*]*, Benjamin Misson*[2]*, Charlotte Rentmeister*[1]*, Alexandre J. Poulain*[1]

[1] *Biology Department, University of Ottawa, 30 Marie Curie, Ottawa, ON, K1N 6N5, Canada*

[2] *Univ Toulon, Aix Marseille Univ., CNRS/INSU, IRD, MIO UM 110, Mediterranean Institute of Oceanography, La Garde, France*

[*] *Deceased*

Highlights:

i) Bioavailable arsenic is both unbound As and As weakly complexed to DOM.
ii) Time and [As]/[DOM] ratio governs As-DOM bond strength, thus As bioavailability.
iii) DOM affects the magnitude of As(III) photooxidation in solution.
iv) Phosphate affects As(III) binding to DOM and enhance As photooxidation rates.

Contributions to the field:

i) First study to directly test the control DOM exerts on As(III) and As(V) bioavailability and under environmentally relevant conditions.
ii) Identified conditions that dictate the As-DOM bond strength.
iii) Found the notion of DOM-bound metal(oid)s being inaccessible to microbes to be inaccurate in the case of As.
iv) Found aging of As(III)-DOM complex can increase As(III) bioavailability.
v) Insights into DOM's photoreactive nature and impact on As(III) redox in solution.

A modified version of this manuscript was published online: 04 February 2020
Science of the Total Environment **|** *doi.org/10.1016/j.scitotenv.2020.137118*

3.1 ABSTRACT

The presence of arsenic in irrigation and drinking waters is a threat to worldwide human health. Dissolved organic matter (DOM) is a ubiquitous and photoreactive sorbent of arsenic, capable of both suppressing and enhancing its mobility. Microbes can control the mobilization of mineral-bound arsenic, through redox processes thought to occur intracellularly. The role that DOM plays on the bioavailability of arsenic to microbes is often invoked but remains untested experimentally. Here, using a whole-cell biosensor, we tested the role of DOM on As(III) and As(V) bioavailability. Using cation amendments, we explored the nature of As-DOM interactions. We found As bioavailability to be dependent on [As]/[DOM] ratio and on the strength of As binding to DOM which varied as a function of time. We further tested the role of DOM on As(III) photooxidation and showed that As(III) photooxidation rate is limited by the strength of its interactions with DOM and sensitive to ionic competitive desorption. Our study demonstrates the dynamic control that photoreactive DOM poses on the bioavailability and reactivity of As in the environment and highlights the kinetic controls that DOM can possibly exert on As toxicity at various levels in food webs.

Keywords: biosensor; bioavailability; arsenic; water quality; photooxidation

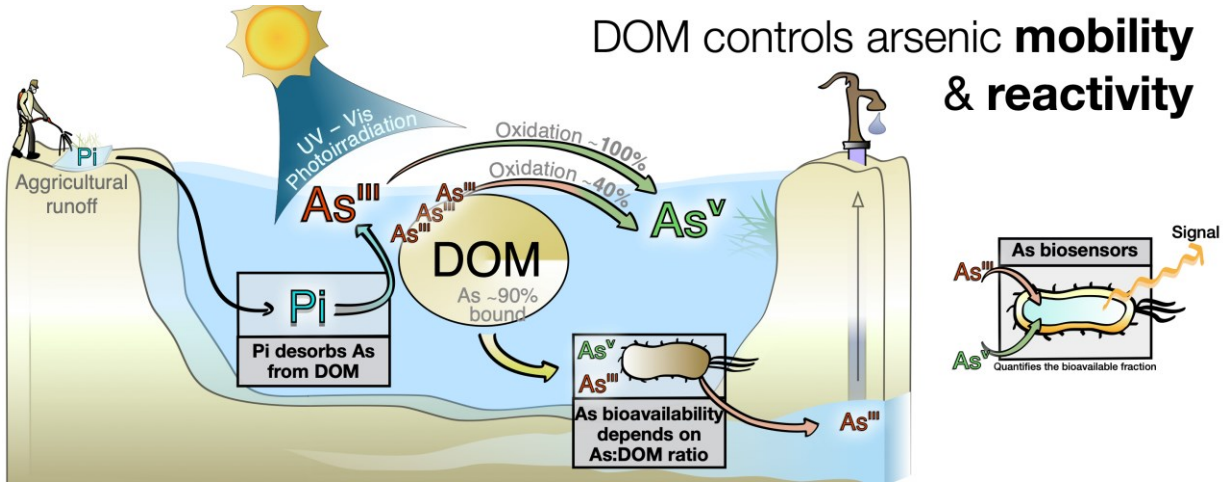

Figure 3.1 | Graphical abstract.

N.B. Supplementary Materials (**Annex B**) are appended at the end of this chapter.

3.2 Introduction

Arsenic (As), classified as a group 1 carcinogen (*20*), is estimated to affect the food and drinking waters of over 140 million people worldwide (*42*). The effects of human-mediated As release through mining, farming and manufacturing processes (*20, 48*) are observed at local, or even regional scales (*48*). Microbes, ubiquitous organisms operating at a global scale (*61*), are capable of affecting As mobility via catabolic (*e.g. aio, aso, aox, arr*…) or resistance (*e.g.*, *ars, arsM*…) pathways (*4, 60*). Therefore, conditions limiting As availability to microbes will reduce As remobilization.

Several environmental drivers of As bioavailability have been proposed (*18*) but very few have been directly tested. Such drivers include changes in redox (*44*), nutrients (*58*), cations (*47*) and solar radiation, known to profoundly affect organic material degradation, nutrient release and organic matter mineralization (*57*). Recently, Langner *et al.* (*30*) have presented spectroscopic evidence of covalent bonds between trivalent arsenic (As(III)) and natural organic matter (NOM), and therefore suggested that NOM strongly governs the bioavailability and thus the mobility of As in anoxic peat.

DOM acts as a ubiquitous environmental sorbent of As through the formation of covalent (*30*) and ternary complexes with As (*8, 31*), thereby preventing solid phase sorption (*18*) and maintaining high As levels in soils (*26*) and in water (*7, 14, 29*). With the rise of terrestrially derived DOM concentration of surface waters over the past few decades (*56*), we can expect that the role that DOM plays on As cycling will be increasing. The current mechanistic understanding of the interactions between As species and DOM includes: i) specific binding of As(III) to sulphur (*30*), and to amino (*52*) functional groups within DOM; ii) indirect cationic bridging of As(V) with calcium (*31*) and of As(III) with iron (*9*), and iii) weak electrostatic complex formation of As(III) and As(V) with phenolate or carboxylic functional groups (*8, 9*). Furthermore, previous experiments during which we evaluated As bioavailability in 17 lakes sampled around Giant Mine (YK, Canada) and exhibiting a wide range of As and DOC

concentrations, identified a role for DOC on As bioavailability (*40*). Surprisingly, we found that newly added As to lake water samples was less bioavailable than older, "legacy" arsenic, already present in the system. This led us to hypothesize that As-DOM complex aging is important in controlling its bioavailability.

In this study, we hypothesized that DOM acts as a strong predictor of As bioavailability to microbes and predicted that strong As binding to DOM would reduce the pool of As available for microbial uptake. Using an As-specific biosensor (*40*), we monitored for changes in As(III) and As(V) bioavailability by altering [As]/[DOM], equilibration time, DOM origin, and investigated the role of DOM photoirradiation on As redox state and bioavailability. We found As bioavailability to be dependent on [As]/[DOM] ratio and on the strength of As binding to DOM which varied as a function of time.

3.3 Materials and methods

3.3.1 Reagents.

All media and reagents were made and kept in pre-sterilized, acid- washed containers. Purification of ultrapure water (Milli-Q), preparation/preservation of the 10 mM As standards, and constituents of growth (LB & MGP) and exposure media (MGP & MIP) have been previously described (*40*). Dissolved organic matter (DOM) standards were sourced from the International Humic Substance Society (IHSS): i) Suwannee River Natural Organic Matter 2R101N (NOM), ii) Suwannee River Humic Acid 3S101H (SRHA), iii) Suwannee River Fulvic Acid 3S101F (SRFA), and iv) Elliott Soil Fulvic Acid 5S102F (ESFA). These represented a wide range in sulphur (0.41 to 1.78% (w/w)), carboxyl (9.13 to 13.24 mg/g C) and phenolic (2.27 to 3.72 mg/g C) functional groups (*15, 21, 46*). Properties of the DOM origins used to produce this RDA can be found in Supplementary Materials (**SI Table A1.1**). DOM standards were prepared in acid-washed volumetric flasks at 100 mg/L by dissolving 0.0050 g in 50 mL of ultra-pure (Milli-Q) water and incubated at 37°C and 200 RPM for 24 h. Orbital

shaking/incubation ensured complete dissolution of the standards in Milli-Q water without adjustment of ionic strength or pH. Filtropur 0.2 µm PES membrane filters (Sarstedt 83.1826.001) were used to ensure sterility of the standards and prevent microbial degradation during storage. Refraining from using buffering and preservation agents drove the pH to approximately 4.5. All DOM standards were prepared following the above-noted method, and kept in dark containers at 4°C for no longer than 3 weeks.

3.3.2 Containers.

Containers used in this study include: i) Simport Scientific polypropylene 3 mL containers (Fisher Scientific 22-040-408) for all DOM incubation treatments that did not involve photoirradiation; ii) Globe Scientific Spectrophotometer polymethyl methacrylate 4.5 mL UV grade (280–800 nm) cuvettes (Fisher Scientific 111157) for all photoreactor assays; iii) Nalgene® High Density Polyethylene (HDPE) 500 mL bottles for all dialysis experiments, and Trace Metal Grade Corning® tubes for storage and analyses; and iv) Fisherbrand glass bottles (FB800100) for all media and reagent storage.

3.3.3 Biosensor culture and exposure protocol.

Biosensor construct, speciation protocol, and instrumentation used to incubate and quantify fluorescent output and culture yield of the biosensors are fully described elsewhere (*40*). Briefly, the biosensing construct was inspired by the design of J. Stocker (*49*), for which we used two ArsR binding sites shown to provide optimal detection while minimizing noise. The sensing-reporting sequence (ArsRBS2-mCherry) was constructed by custom gene synthesis (Integrated DNA Technologies) and cloned into the XmaI and XbaI restriction sites of the high copy pUCP19 shuttle vector upstream of the sequence encoding for mCherry. The reporter plasmid was transformed into *E. coli* NEB10-beta (New England BioLabs) – a level 1, non-pathogenic, non-regulated host. The MGP growth and exposure media, comprised of

glycerol and organic phosphate, were used in all biosensor exposure assays. Use of these media was found to allow for the uptake of over 94% of the added As(III) and As(V) additions (*40*).

For all assays, As concentration was set at 200 nM because this concentration falls at a mid-point in the linear range of the biosensor's calibration curve and has previously led to reproducible quantification (*40*). Furthermore, this concentration is environmentally relevant as the World Health Organization set a guideline of 133 nM (10 µg/L) for As in drinking water (*55*). Biosensor exposure protocol consists of two steps. First, all working solutions (DOM, ions, and As) were prepared at a final concentration of 2× and added to the containers in the following order: (i) Milli-Q water, (ii) DOM, (iii) cations (if required), and (iv) arsenic. Time of interaction prior to exposing the biosensor cells was assay dependent and conducted in the dark and at room temperature. Second, pre-incubated working solutions were then subsampled into three separate wells on the 96 well plate then analyzed by three individually grown biosensor cultures. Exposure occurred in the following order: (i) 100 µL subsample of the pre-incubated 2× concentrated working solution, (ii) 80 µL of 2× concentrated exposure medium (MGP or MIP), and (iii) 20 µL of MGP grown biosensor cells for a final biosensor cell concentration of 10%.

3.3.4 Data analysis.

The biosensor fluorescent output present in all figures has been corrected for autofluorescence, noise and culture health using R programming language. First, autofluorescence is a background interference that differs by DOM origins, bacteria cultures, reagents, and by well in the exposure plate. Standardization consists of subtracting endpoint output signal (20 h) of each well from the initial output (T0) of that same well (**Figure 3.2**a). Second, we refer to background noise as the signal produced by biosensor cells that are not exposed to As; even in the absence of the inducer (As) there is a basal expression of fluorescence that must be controlled for. Removal of background noise consists of the difference between signal output of the

treatment (*e.g.*, As + SRHA) and of the no-As control at the same time point (20 h) and of the same biosensor culture (**Figure 3.2**b). Third, differences in biosensor fitness or yield can arise when working with environmental samples (**SI Fig. B1.1**). Normalization consists of dividing the corrected output signal by the culture's optical density (OD_{600}) at the same time point (**Figure 3.2**c). Finally, assuming no-DOM controls represents 100% bioavailability, we can convert the biosensor's fluorescent output signal to percent biouptake. This correction involves dividing the normalized biosensor output of the treatments (*e.g.*, As + SRHA) by output signal of the As-only calibration point control and multiply by 100 (**Figure 3.2**d).

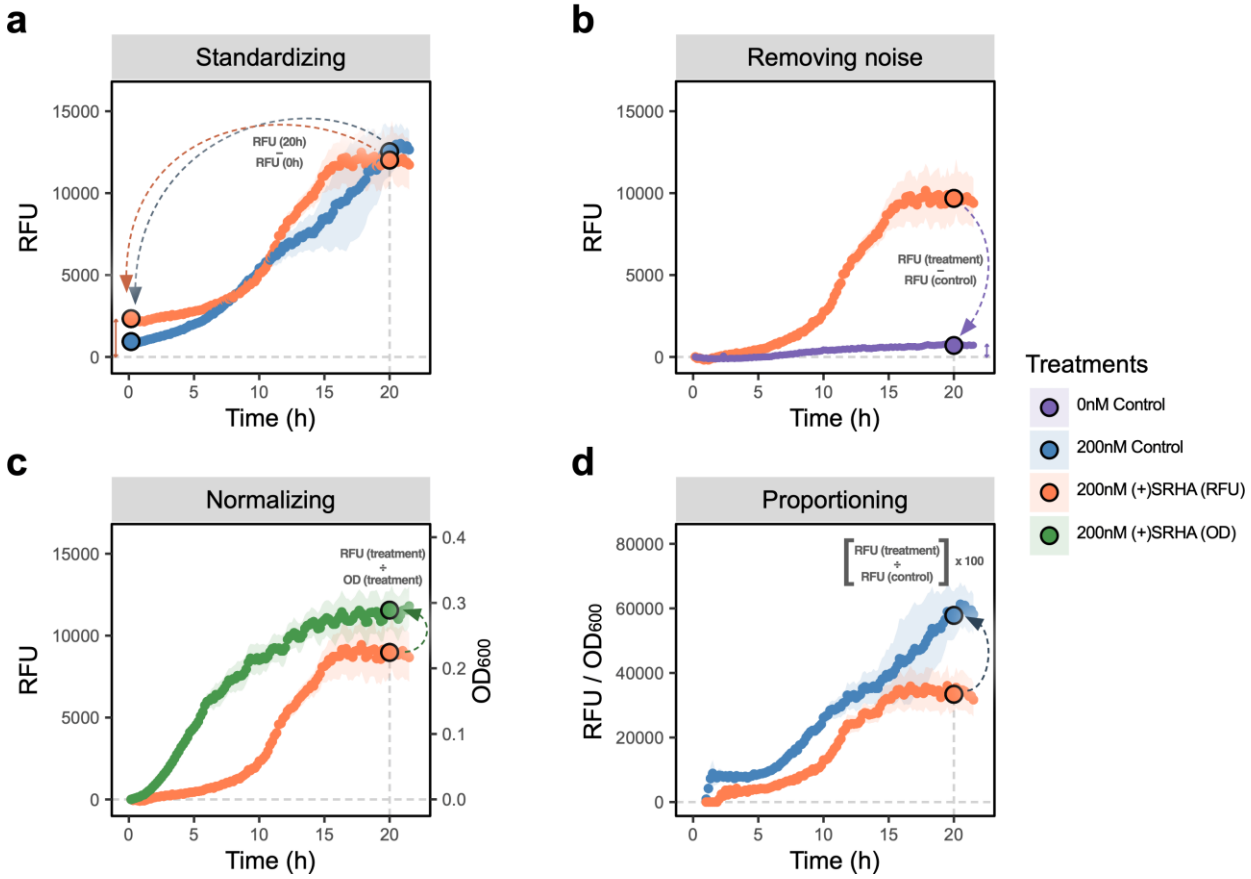

Figure 3.2 | Example of data analysis steps applied to raw data to generate figures. The optical density at 600 nm (OD_{600}) including the mean (points) and standard deviation (ribbon) of independently grown triplicate biosensor cultures are shown. The output signal of the biosensor is presented in relative fluorescence units (RFU) during the first 22 h of growth immediately following exposure to arsenic. Controls shown here are those used in correction and normalization steps that generate the 25 mg/L T0 As(V) box shown in **Figure 3.3**. Controls are figure dependent. Step details are further described in the methods section.

3.3.5 Photoirradiation.

A Luzchem Photoreactor was used for all photoirradiation assays. These consisted of a 22 h pre-incubation assay followed by a 4 h irradiation step subsampled at 0 h (T0), 2 h (T2) and 4 h (T4). Similarly to the exposure protocol previously described, samples were prepared, incubated, and irradiated at 2× their final concentration (400 nM As(III) & 20 mg/L DOM), then diluted to 1× upon exposure to the biosensors. The power per unit area (irradiance) for wide-band UV radiation was measured using GOLDILUX ultraviolet meters, UVA (315–400 nm), and UVB spectrum (280–315 nm). Irradiance intensity for UVA averaged 0.037 $J \cdot m^{-2} \cdot s^{-1}$ and for UVB averaged 0.129 $J \cdot m^{-2} \cdot s^{-1}$. Spectral components of light from 200 nm to 1000 nm were analyzed using a ThorLabs compact CCS200 (**Figure 3.8**).

3.3.6 Chemical analysis.

Cross-analysis of HPLC-ICP-MS and the biosensor speciation technique was performed on the same day and on the same samples. Sub-samples for As speciation analysis was preserved using HNO_3 at 0.3% (2 µL of 70% HNO_3 in 398 µL Milli-Q plus 100 µL of sample). Details regarding HPLC-ICP-MS speciation analysis are detailed elsewhere (*40*).

3.3.7 Dialysis experiments.

All dialysis experiments, used to quantify the fraction of As bound to DOM, were performed in triplicate and consisted of adding DOM (10 mg/L) and As (200 nM, either As(III) or As(V)) to the inside of a dialysis bag (pore size 500 Da). Similarly to the biosensor exposure assays, no buffering agents were used. For experiments involving major ions, 10 mM Na^+ or Ca^{2+} were added both inside the dialysis bag and in the external solution, at the same ionic strength to prevent crossing of As induced by osmotic gradient.

Quantification of As species levels (ICP-MS) for the external solution was performed at both 0 h (T0) and at 24 h (T24) whereas measurement for the internal

solution was only quantified after a 24 h contact time. Here, quantification of [As] inside the dialysis bag represents both bound and unbound As, whereas the amount of As found outside the dialysis bag represents unbound As. These categories are based on the assumption that As-DOM ternary complexes are larger than the "free" or unbound As, and therefore cannot cross the 500 Da dialysis bag membrane. To account for differences between the internal (3 mL) and external bag (300 mL) volumes, all µg/L concentrations were first converted to pmols before adding, subtracting or proportioning (eqn i).

$$\text{(eqn i)} \qquad \text{As (pmol)} = \text{V (mL)} * \left(\frac{[\text{As}]\ (\mu \frac{g}{L})}{\text{MM As } (\frac{\text{g}}{\text{mol}})} \right) * 10^9$$

Where, V is the volume of water in mL of the inside or the outside of the dialysis bag, [As] is the ICP-quantified As concentration in µg/L, MM is the molar mass of As (74.92 g/mol), and 10^9 is the unit conversion factor. The result is As quantity in pmols rather than As concentration. We then used the pmol quantities to proportion the amount of As bound to DOM (eqn ii).

$$\text{(eqn ii)} \qquad \%\ \text{bound} = 100 * \left(\frac{\text{As bag } (pmol)}{\text{As added } (pmol)} \right)$$

Because unbound As is osmotically driven across the membrane, the amount of As measured inside the bag should therefore contain both bound and unbound As. Thus, in eqn (ii), As_{bag} represents the amount of As measured inside minus the amount measured outside the dialysis bag. Use of these equations results in a As unit that is proportioned as percent (**SI Fig. B1.2**).

3.3.8 FEEM analysis.

Measurement of Fluorescence Excitation/Emission Matrices (FEEM), was performed in triplicate by mixing DOM (10 mg/L) and As (200 nM, either As(III) or As(V)) to a 3 mL quartz Suprasil cells, at room temperature, in the dark. No buffering or acidifying agents were used. Fluorescence Excitation/Emission Matrices were

regularly measured on a HITACHI F4500 spectrofluorometer. The excitation wavelength ranged from 320 to 460 nm, with 10 nm step and an excitation slit of 1 nm. The corresponding emission spectra were acquired from 350 to 550 nm with a scan speed of 2400 nm/min and a slit of 1 nm. The photomultiplier tension was fixed at 950 V and the integration time set at 0.1 s. The extraction of the 5 nm stepped emission was obtained by FL-Solution software. Each experiment was performed in triplicate.

3.4 Results and discussion

3.4.1 DOM kinetically controls As bioavailability to bacteria.

In a first series of experiments, we tested the role of i) DOM concentrations and ii) the duration of As-DOM pre-incubation, prior to exposure to the biosensor, on the bioavailability of As(III) and As(V). Here, DOM was provided as Suwannee River Humic Acid from IHSS over a range of concentrations representative of what can typically be found in natural surface waters (streams, lakes, wetlands) and porewaters (*25*).

First, we observed that without a pre-incubation step, addition of 25 mg/L SRHA decreased As(III) and As(V) bioavailability by 25% and 16%, respectively (significant decrease of 25% for As(III), $p<0.0001$) (**Figure 3.3**e), supporting our previous observation with natural lake water samples (*40*). Second, in the presence of [SRHA] ≥ 10 mg/L, As(III) and As(V) bioavailability increased with increasing pre-incubation time (**Figure 3.3**e), to values comparable to the no-DOM control (**Figure 3.3**c-f). Here, the pre-incubation time required to reach control values ranged from 1 ([SRHA] = 10 mg/L) to 3 days ([SRHA] = 25 mg/L). After a 6-day pre-incubation time in the presence of [SRHA] = 25 mg/L, As(III) bioavailability was greater than in the no-DOM control. This corresponded to a significant increase of 45% of As bioavailability over a 6-day period ($p<0.001$). Note that increasing DOM concentration also stimulated biosensor cells yield (**SI Fig. B1.1**c-f), probably due to the presence of

nutrients within the DOM pool but this stimulation was not time dependent and did not affect accuracy of the As-specific biosensor signal (**Figure 3.3**c-f).

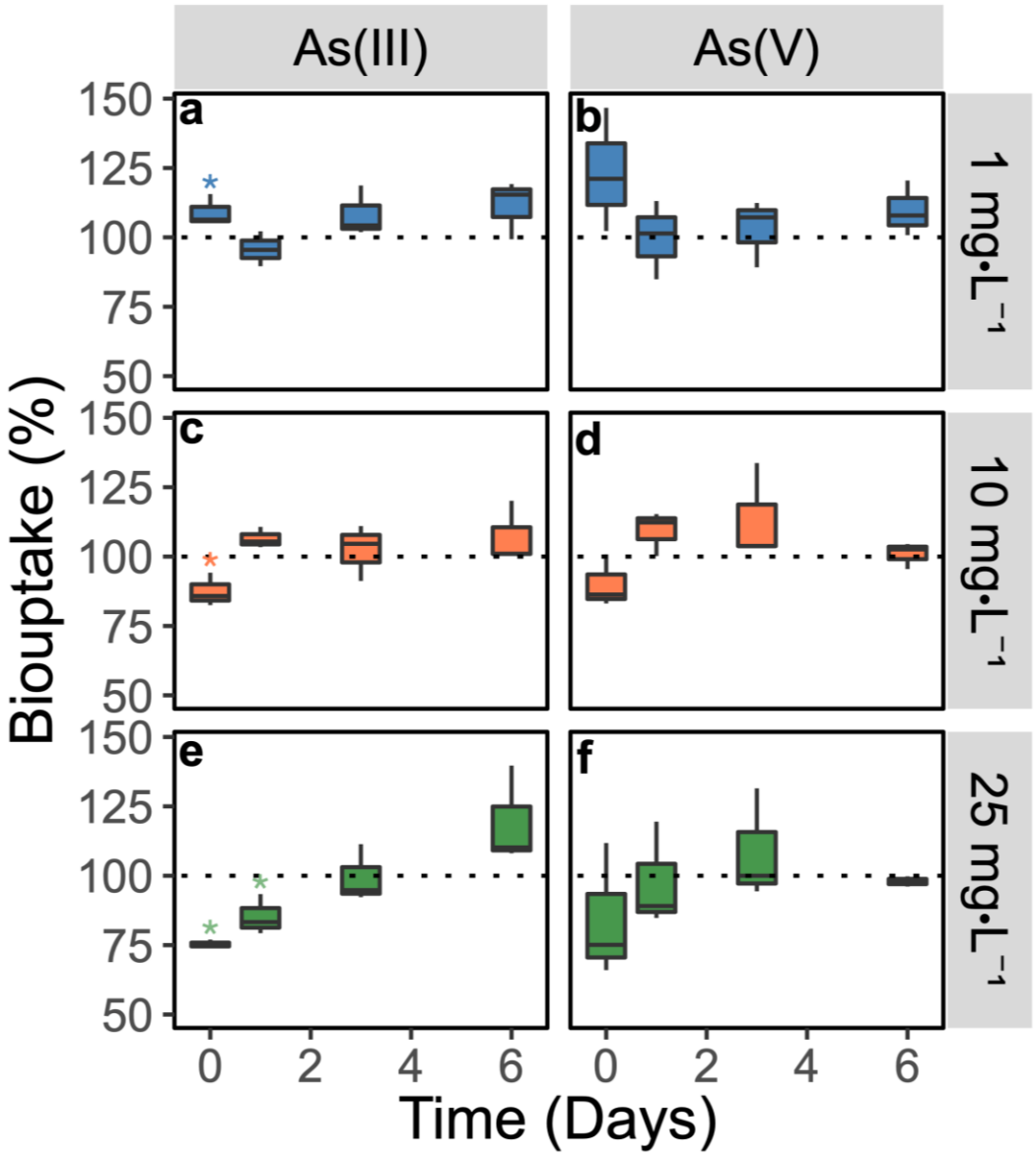

Figure 3.3 | DOM control on As(III) and As(V) bioavailability over time. DOM control on As(III) and As(V) bioavailability over time. Boxplots represent biological replicates (n=3) containing either 200 nM of As(III) (**a, c, e**) or 200 nM As(V) (**b, d, f**) in the presence of a DOM (SRHA) gradient (**vertical facets**). Axes include room-temperature pre-incubation time (X-axis) and output signals of treatments are indicated as percent deviation from our no-DOM controls (Y-axis). Dotted line represents biosensor output signal of the no-DOM controls. Stars represent a significant decrease from the 200 nM (no-DOM) control incubated for the same period of time determined using raw fluorescent signals and TukeyHSD post-hoc analysis on a one-way ANOVA.

Our data showed that DOM hampered As bioavailability at low As(III) to DOM ratio (8 nmol As(III)·mg^{-1} DOM) and during a short time period after As and DOM were placed together (t<30 min). This observation is in line with what was predicted in the literature, indeed, both higher stability constants (*32*) and stronger binding (*9*) have been reported when working at pH and [As]/[DOM] ratios similar to the values used in this study. Using a two-site ligand binding model, Liu and Cai (2010) have shown that humic acids have a limited number of strong As binding sites that are sensitive to increases in [DOM] (*32*). Furthermore, Buschmann *et al.* (*9*) proposed that the limited number of strong As binding sites on DOM is sensitive to competition and/or conformational changes of humic macromolecules, which may explain the time-dependent nature of our results.

To document a possible change in DOM conformational properties over time and in the presence of As, we used FEEM (Fluorescence Excitation/Emission Matrices). Though widely used to quantify DOM, contour maps of the 3D FEEM can also be used to characterize changes in DOM's fluorescent components (*54*). Using FEEM, we predicted that time-dependent changes in fluorescence would correspond to changes in the nature of the interactions between As and DOM. Using colour distance matrix and k-mean cluster analyses, we confirmed a change in fluorescence spectrum intensity and profile over time, both peaking in intensity after a 2-day incubation and shifting in profile following a 6-day incubation (**Figure 3.4**).

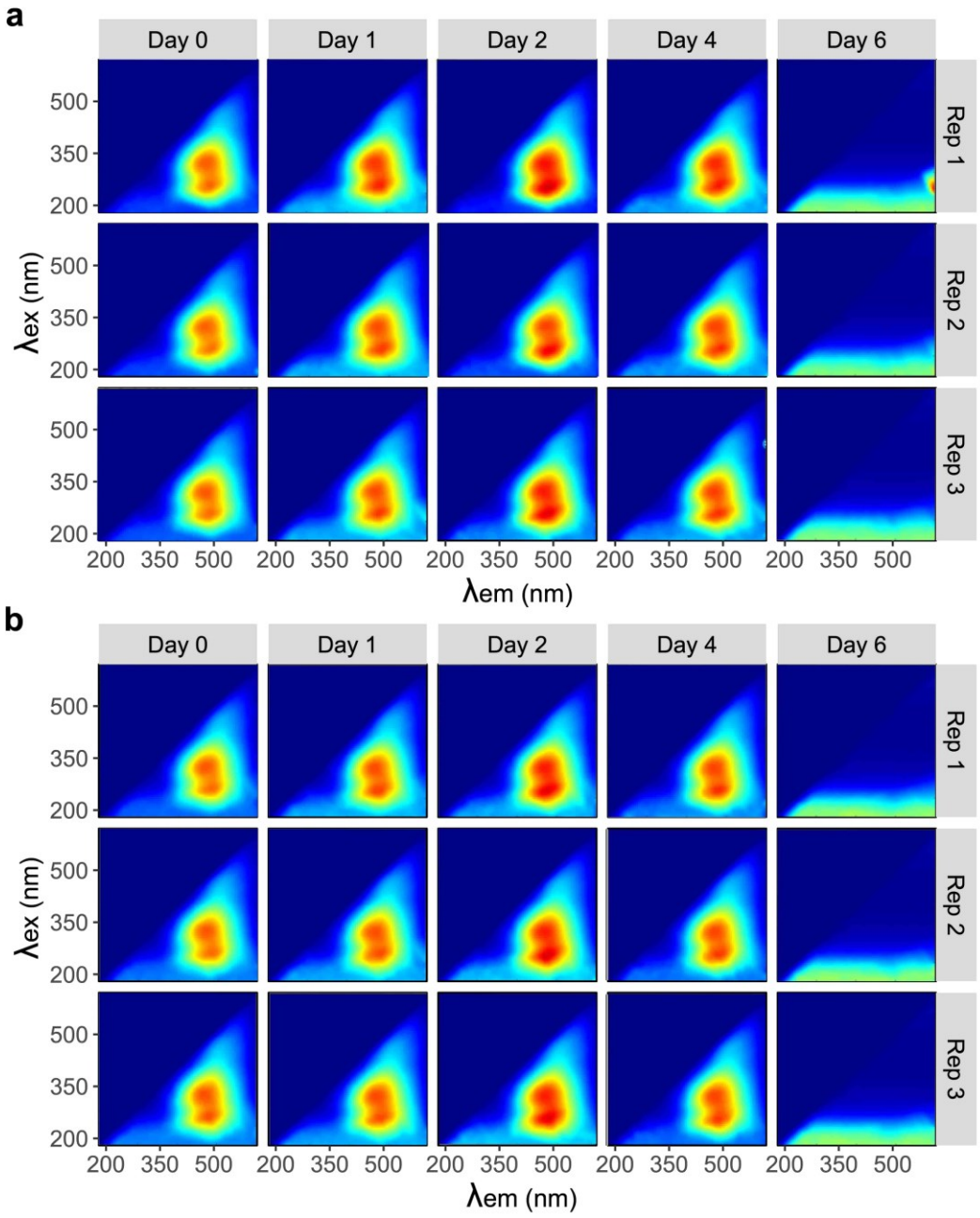

Figure 3.4 | Shift in the fluorescence spectrum/intensity of As-SRHA solutions over time. Triplicate samples are shown by the vertical facets, and pre-incubation time (in days) by the horizontal facets for **a)** As(III) + SRHA and for **b)** As(V) + SRHA.

Changes in the molecular conformation of DOM over time can result from modifications of the surface charge (*38*), and from the intramolecular cationic bridging (*45*). We recognize that fluorescence data presented here offer little mechanistic insight into the underlying interactions between As and DOM. That being said, quantification of changes in fluorophore intensity (or quenching) through time

does present evidence of the dynamic nature of As-DOM interactions (**Figure 3.4**), which is also reflected in the response of the biosensor (**Figure 3.3**).

It is generally recognized that cationic metal-DOM interactions strengthen over time. Arsenic, an oxyanion under most environmentally relevant conditions, would predictably offer different binding dynamics. We propose that increasing As(III) bioavailability over time resulted from a series of ligand exchange within the DOM pool, induced by DOM conformational changes; this transfer of As(III) from the few sites at which it formed strong bonds, towards sites that are more abundant but exhibiting weaker electrostatic affinity, made it more accessible to the biosensor and hence bioavailable. Contrary to what appears to be currently accepted in the literature for bacteria (*41*) and derived from DGT experiments (*2*), our data suggest that inorganic As species do remain bioavailable in the presence of DOM, through time, even when abiotic conditions favour As complexation.

In addition to free As species, As weakly bound to DOM also represents a pool of labile As that is bioavailable to microbes. Furthermore, microbial cells themselves may play a role in actively releasing weakly bound As from DOM. Possible mechanisms include: i) internalization of co-transported As during microbial consumption of DOM (*3*); ii) release of weakly bound As induced by extracellular electron transfer (*34*) and shuttled by quinone moieties within the DOM pool (*19, 39*); and iii) uptake of As through siderophores channels (*e.g.*, ABC-type exporters (*35*)) that are possibly upregulated by phosphate/iron starvation during biosensor growth. Determining the mechanisms involved will require further work.

3.4.2 The nature of As binding to DOM controls its bioavailability.

Our interest in identifying the mechanism involved in DOM's control on As bioavailability required more targeted experiments. Carboxylic groups are one of the main contributors to DOM's negative charge (*22*) and thus promote strong surface and inner-sphere complexes with cationic metals (*9, 23, 43*). Moreover, cations are

known to affect the sorption of As to DOM by changing its affinity to functional moieties such as carboxylic, phenolic, amino and sulphydryl groups (*9, 30, 32*). These associations can induce aggregation and structural reorientation of the organic matter by increasing the compression and rigidity of the structure while favouring a hydrophobic core (*37*).

We first tested the effect of cations on As bioavailability in the presence of DOM (20 nmol As·mg^{-1} DOM), by adding 10 mM Na^+, 10 mM Ca^{2+}, or 5 µM Cu^{2+}. Mono- and divalent cations (Na^+ and Ca^{2+}) were selected for their ubiquity in the environment and pronounced effects on DOM charge (*12*) and structure (*5*), respectively. Cu^{2+} is a trace metal with high affinity for DOM (*11*), and is expected to form strong covalent bonds at complexation sites (*13, 17*). The concentration of cations was limited by their toxicity and chosen to maintain relevance to concentrations commonly found in freshwaters. We found that across all tested commercially available DOM treatments, As(III) and As(V) bioavailability variably increased in the presence of Cu^{2+}, was unaffected in the presence of Na^+, and consistently decreased in the presence of Ca^{2+} (**Figure 3.5**). These data suggest that the mechanisms involved in controlling As bioavailability are conserved across DOM samples.

Experiments performed in the presence of copper support our finding that strong binding of As to DOM limits its bioavailability. In this case, we suspect that the presence of Cu^{2+} prevented As binding, maintaining its accessibility and bioavailability to the biosensor. Although the mechanism remains unclear, we speculate that it relates to the nature of the DOM conformational changes differentially induced by calcium and copper. Copper, like calcium, electrostatically interacts with deprotonated carboxylic groups of DOM (*11, 53*). Copper (*53*), like calcium, electrostatically interacts with deprotonated carboxylic groups of DOM (*11*). However, Ca^{2+} interactions with DOM differ from that of copper in the strength and specificity of the bonds it forms with DOM (*11, 53*). Indeed, calcium is thought to

better penetrate DOM structure (*51*), thereby forming strong inner-sphere ionic bridges (*23, 31, 51*), creating more space for water molecules (*1*), and changes in DOM conformation (*27, 37*).

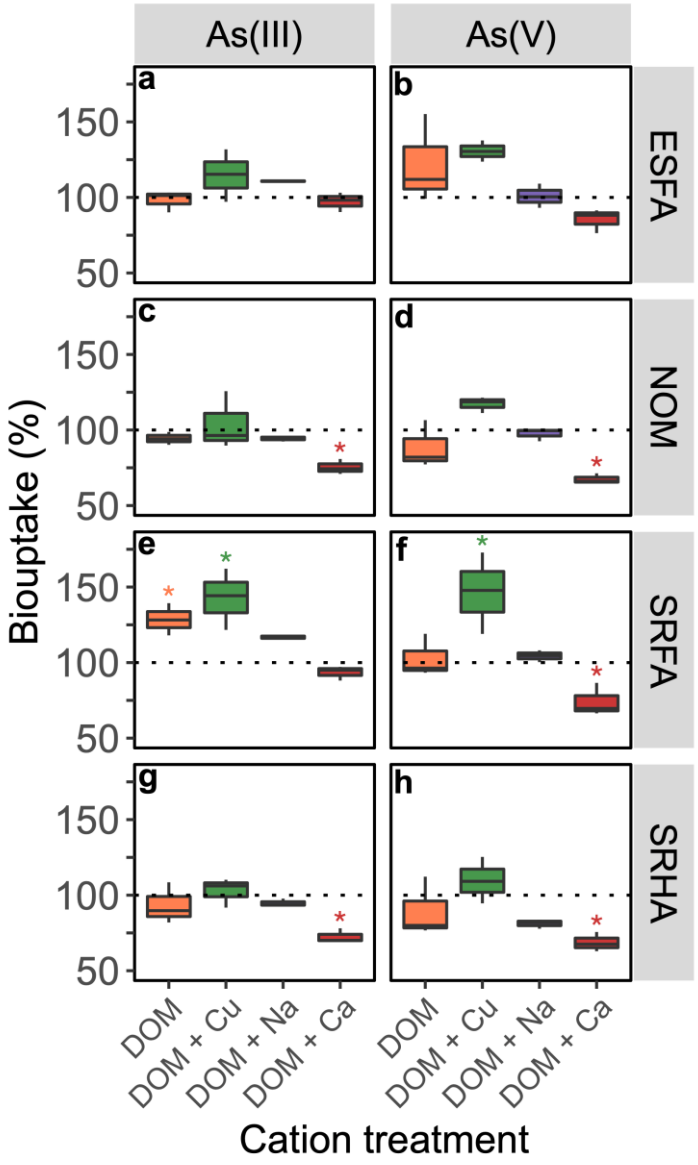

Figure 3.5 | As bioavailability in the presence of DOM of varying origins. Changes in As bioavailability (Y-axis) were plotted over various cation treatments (X-axis). Environmentally relevant concentrations of Na^{+} (10 mM), Ca^{2+} (10 mM), Cu^{2+} (5 µM), and DOM (10 mg/L) were used. The origin of the DOM used is identified by the vertical facet labels. Each box represents the mean and standard deviation of biological triplicate samples containing 200 nM of As(III) (**a, c, e, g**) or 200 nM As(V) (**b, d, f, h**). Percent conversions were based on presence vs absence of organic matter. Dotted line represents biosensor output signal of the no-DOM controls at the same ionic strength. Significant decrease from the no-DOM controls were determined using TukeyHSD post-hoc analysis on a one-way ANOVA.

Second, to test the extent to which As(V) binding to DOM affected its bioavailability, we subjected the exposure solution to a 500 Da dialysis membrane bag in the presence and absence of SRHA, Ca^{2+} or Na^{+}. In the absence of cations, >95% of As(V) was bound to SRHA, yet remained bioavailable (**SI Fig. B1.2**). Although the addition of Na^{+} and Ca^{2+} decreased the extent to which As(V) was bound to DOM (**SI Fig. B1.2**), only in the presence of Ca^{2+} did we observe a 25% decrease in the bioavailability of As bound to DOM (**Figure 3.5**). These results confirm that microbes are not limited to the unbound fraction of As but are also capable of accessing weak electrostatically held As.

We used FEEM to test the effects of Na^{+} and Ca^{2+} amendments on As(V)-SRHA treatments (**SI Fig. B1.3**). Both colour distance matrix and k-mean cluster analysis (*6, 28*) confirmed that all three Ca^{2+} treatments increased fluorescence intensity beyond that of the Na^{+} treatments and of the no-cation controls, suggesting an important role of Ca^{2+} in changing the structural properties of DOM. These findings are in line with reports indicating that Ca^{2+} affects DOM structure, namely its compression and rigidity (*27, 37*). Following the two-site ligand binding model proposed by Buschmann et al. (2006) and further characterized by Liu and Cai (2010), it is conceivable that changes to the molecular structure and arrangement of DOM evoked by 10 mM Ca^{2+}, led to the release of weakly but electrostatically bound As towards newly available/accessible, high affinity sites. The consistent yet modest (ca. 25%) decrease in As(III) and As(V) bioavailability in the presence of Ca^{2+} (**Figure 3.5**), supports the low number of strong As sites proposed by other studies (*9, 32*). Unfortunately, we do not yet have spectroscopic evidence supporting a change in bioavailability induced by conformational changes of DOM under our experimental conditions.

Finally, we performed a redundancy analysis (RDA) that assigns predictor variables to bioavailability measurements to explore the broad relationships existing between As species bioavailability and the various experiments performed in this

study (**Figure 3.6**). This analysis highlights that the drivers of As(III) and As(V) bioavailability in the presence of DOM are likely different, underscoring the relevance of our approach of performing speciation using a biosensor. Here, most variability was driven by predictor variables that align with RDA1 axis (N, S and aliphatic content of DOM) and with As(III) bioavailability vector. The magnitude of As(III) bioavailability in the presence of DOM appears to be less dependent on the presence of cations than As(V). Indeed, and despite low coverage of the RDA2 axis (6.7%), alignment of As(V) bioavailability vectors with cationic treatment groupings and predictor variables suggest a stronger cationic interference on As(V) bioavailability, best characterized by Q1 (carboxylic) and Q2 (phenolic) pools of binding sites.

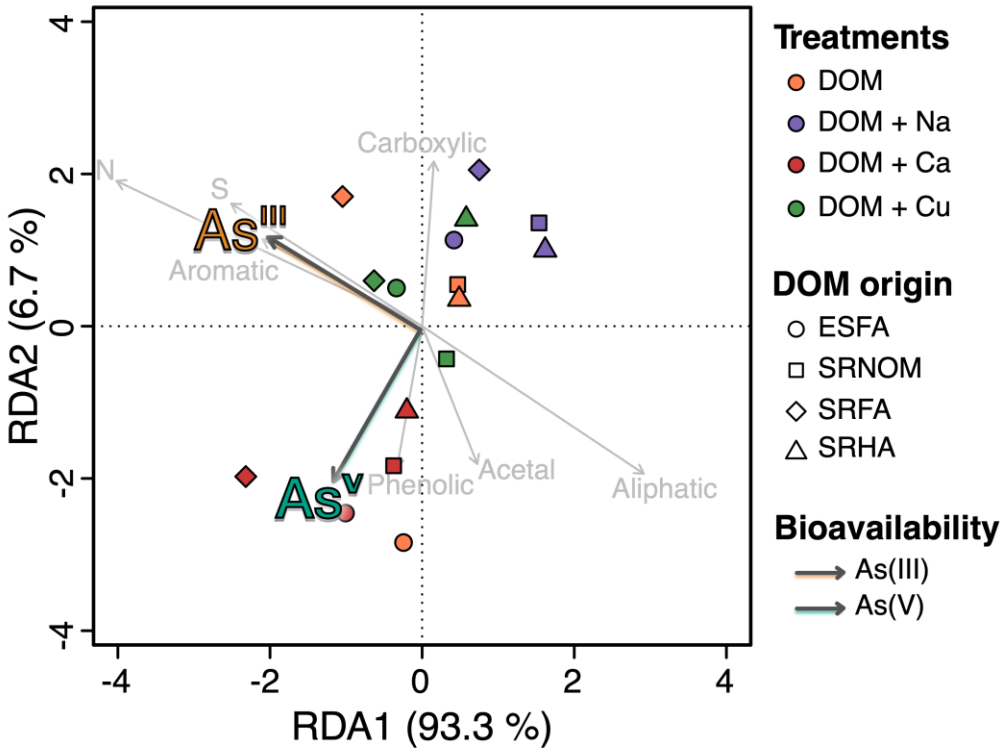

Figure 3.6 | RDA triplot assigning predictor variables to drivers of bioavailability. Each RDA point represents ordination of biosensor outputs (**Figure 3.5**) separated by Euclidian distances as a metric of variation. Overlaid are both bioavailability drivers (coloured vectors) and explanatory variables (grey vectors), pointing in the direction of most rapid change. The angle between vectors of explanatory variables and bioavailability drivers reflect their linear correlation. Properties of the DOM origins used to produce this RDA can be found in Supplementary Materials (**SI Table B3.1**). (For interpretation of the references to colour in this figure legend, the reader is referred to the web version of this article.)

3.4.3 Arsenic photoreactivity and bioavailability in the presence of DOM.

DOM can profoundly affect As(III) behaviour in the environment. Here, DOM can compete with mineral adsorption sites, and enhance mobility of this contaminant by maintaining As in dissolved or colloidal forms (*33*). One important variable controlling the fate of DOM in natural surface waters is its photochemical reactivity which has also been involved in As redox transformations (*8, 59*). Moreover, the effects of As-DOM photoirradiation on As bioavailability have yet to be characterized. Such information is relevant for situations when: i) groundwater reaches surface waters, ii) ice cover melts, iii) summer anoxia in DOM-rich wetlands/bogs, or iv) episodic draining and flooding of rice paddy soils. In this last series of experiments, we tested the role of As(III)-DOM photoreactivity on the bioavailability of As species (**Figure 3.7**).

Our 2-step experimental treatment required the pre-incubation of an As(III) solution under UV–vis radiation (with or without DOM), prior to exposure to the biosensor assay. Upon exposure, only As(III) can be detected because, as per our protocol, 10 mM PO_3^- is added to the bioassay medium to prevent As(V) uptake (*40*). We observed that virtually none of the As(III) remained bioavailable after 4 h of irradiation in the absence of DOM (**Figure 3.7**bd). In this case, a decrease of As(III) bioavailability could be attributed to i) conditions that directly prevent the biouptake of As(III) or ii) its oxidation to As(V). Our same-day control experiments analyzed using ICP-MS, confirmed the virtually complete As(III) oxidation to As(V) (**Figure 3.7**c).

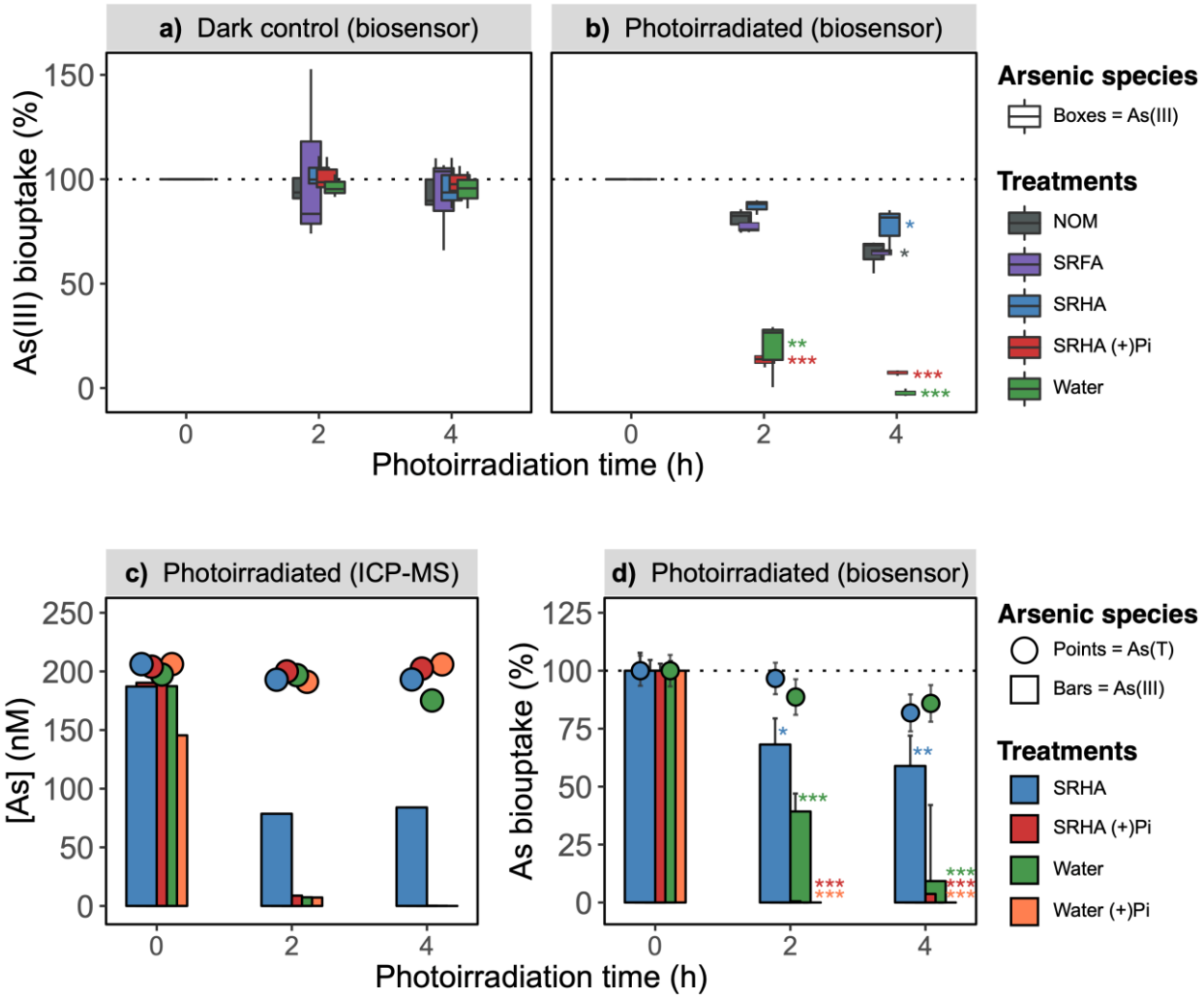

Figure 3.7 | DOM affects the extent of As(III) photooxidation. HPLC-ICP-MS mass balance **c)** was used for validation of biosensor speciation technique **a)**, **b)** and **d)** where a decrease in As(III) uptake over time suggests As(III) oxidation. Biosensor fluorescence was converted to percent biouptake (Y-axis) by comparing the output signal of the irradiated treatments to the pre-irradiated (T0) controls. Biosensor endpoints present the mean and standard deviation of three independent biological triplicates. Panels **b)** and **c)** present an independent same-day mass balance using ICP-MS and biosensor outputs respectively. Dotted line represents biosensor output signal at T0. A significance code of (*) represents a p-value between 0.01 and 0.05 and of (***) for a p-value > 0.001. Analysis of photoreactor light spectrum (**Figure 4.4**) including supplemental controls for this figure, can be found in Supplementary Materials (**Annex B**) (**SI Fig. B1.4**).

To maintain environmental relevance, no UVC bulbs were installed in our photoreactor. Yet in the absence of DOM and in the presence of light, oxidation of As(III) to As(V) in water alone was consistently observed in over two dozen separate replicated experiments. We performed a series of control experiments, to reasonably

rule out the role of atmospheric gases (*e.g.*, N_2, O_2, CO_2), the acid from the As stock solution preservative (HNO3), and the nature of the cuvette container as sources and/or acceptors of electrons in the As(III) photooxidation process (**SI Fig. B1.4**, **Annex B2.1**). We sought to investigate whether water could be a source of HO• and H• radicals likely involved in As(III) photooxidation. Our spectroradiometer measurements confirmed that mostly visible spectral components (**Figure 3.8**a) were emitted in the reactor with little spectral irradiance (0.166 J·m-2·s-1) in the UV regions (**Figure 4.4**b). The photooxidation of As(III) at environmentally relevant levels (nM) requires only a relatively small number of photons emitted at water's ionization energy threshold (~6.5 eV) (*16*). In our incubation experiments, what appears as inconsequential spectral peaks (Figure S5e) in the UV range (~6.1 eV), may provide the energy required to produce hydroxyl radicals needed to catalyze this reaction at the low As levels used. We unfortunately cannot properly report quantum efficiency yields considering CCD spectrometers sensors provide inaccurate absolute intensity measurements due to the nature of their integrated analogue (photons) to digital (volts) conversion process.

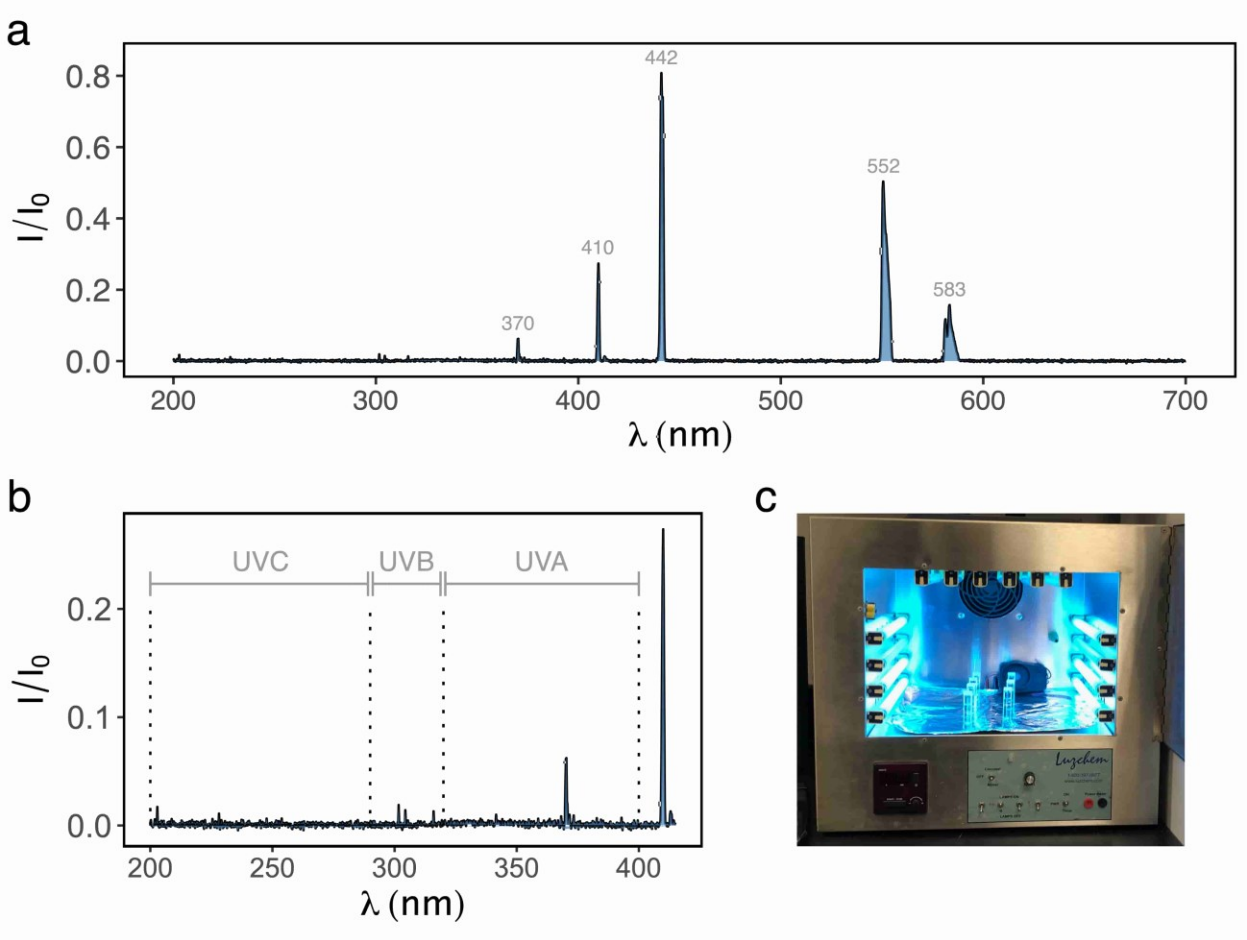

Figure 3.8 | Photoreactor light spectrum extends to visible components. Spectral components of light are presented from **a)** 200 nm to 700 nm and from **b)** 200 nm to 415 nm. Wavelengths of the peaks and UV ranges are present. **c)** A photo of the Luzchem photoreactor showing the placement of the cuvettes inside.

Surprisingly, the presence of DOM, amended as NOM, SRFA or SRHA greatly limited the extent to which As(III) was photooxidized to As(V) (**Figure 3.7**). Hydroxyl radicals, regardless of their origins (water or DOM), can affect C-H and S-H bonds (*10*). This photochemical-induced conformational change of DOM could enhance binding of As-DOM. In either case, we suspected that the presence of DOM both attenuated photon flux via shading and limited As(III) photoreactivity via As-DOM binding.

Finally, we tested the role of a possible association between As(III) and DOM on As(III) photooxidation by adding phosphate to an As(III)-DOM solution prior to its photoirradiation. Our prediction was that addition of PO_4^{3-}, which is known to limit

As(III) binding to DOM (*24*), would favour As(III) photooxidation by increasing the pool of unbound As(III) in solution. Indeed, in the presence of DOM + PO_4^{3-}, ICP-MS measurements indicated rates of As(III) photooxidation, similar to those observed in water alone. Our finding only partially supports previous literature claiming that As(III) oxidation is mediated by the transfer of electrons from DOM (*8*). We cautiously conclude that differences among published results on the role of DOM on As photooxidation likely result from variable As-DOM binding conditions due to variation in Pi content (*e.g.*, buffer), pH, and ionic strength of the exposure solutions. Overall, further experiments are required to determine the nature of the interaction between As and DOM in the presence of PO_4^{3-}. That being said, our data support our hypothesis that the nature and strength of As binding to DOM controls As bioavailability and reactivity.

3.5 Conclusion

It is generally accepted and often implied that the bioavailable fraction of As is the "free" or unbound one (*36, 50*). The work presented here showed that the bioavailable fraction of As is comprised of both labile and weakly complexed to DOM fractions. Though we found that 20 nmol As·mg^{-1} DOM ratio appears sufficient to saturate the low number of strong As binding sites in several types of commercially available DOM, further work is warranted to characterize the nature of weak vs strong As binding sites. Characterizing the strength and specificity of As-DOM interaction is fundamental in improving our understanding of microbially driven mobilization of As. This is an important gap of knowledge, which once addressed, will improve effective management of As contamination. Indeed, environmental changes brought by climate change such as variations in temperatures and precipitations already affect the physicochemical properties of natural waters making large-scale predictions on the fate of As-DOM complexes difficult (*57*). In the context of global water quality assessment, our work emphasizes the importance of considering the effects of

climate change and of agricultural practices as they affect the levels of nutrients and their remobilization. Changes in DOM concentrations and nutrient levels may affect the fraction of As bound to DOM, which also controls the bioavailability of As to the microbes responsible for its transformation and mobilization. Most importantly, this work calls for additional investigations on the kinetic controls that DOM exerts on As toxicity at various levels in food webs.

3.6 Acknowledgements

We would like to thank Dr. Emmanuel Yumvihoze for providing arsenic speciation analysis using HPLC-ICP-MS and Eric Kitchen for providing the spectroradiometer. This work was funded by an NSERC discovery grant, an Early Researcher Award from the Province of Ontario, and an NSERC Accelerator Grant funding to AJP, as well as Mitacs Globalink Research Award funding to MPP, AJP, VL and BM.

3.7 Author contributions

MPP, AJP, VL, BM initiated and designed the experiments; MPP, VL, and CR carried out the experiments; MPP wrote the R scripts for data analyses; MPP wrote the manuscript with support from AJP, VL, BM, and CR; AJP, VL, and BM supervised the project. All authors have given approval to the final version of the manuscript.

3.8 Appendix A. Supplementary data

Biosensor culture yield, fluorescence spectrum/intensity, bound vs bioavailable arsenic, photoreactor light spectrum, additional control experiments, and chemical properties of DOM extracts.

3.9 Abbreviations

As(III), arsenite; **As(V)**, arsenate; **DOM**, dissolved organic matter; **ESFA**, Elliot soil fulvic acid; **HPLC**, high-performance liquid chromatography; **ICP-MS**, inductively coupled mass plasma spectroscopy; **MGP**, mops glycerophosphate; **MIP**, mops inorganic phosphate; **NOM**, natural organic matter; **pMP01**, arsenic biosensor; **RDA**, redundancy analysis; **SRFA**, suwannee river fulvic acid; **SRHA**, suwannee river humic acid.

3.10 Declaration of interest statement

Authors declare no competing financial interest.

3.11 Bibliography – Chapter 3

1. W.-Y. Ahn, A. G. Kalinichev, M. M. Clark, Effects of background cations on the fouling of polyethersulfone membranes by natural organic matter: Experimental and molecular modeling study. *Journal of membrane science* **309**, 128-140 (2008).
2. E. D. Amato *et al.*, Assessing the effects of bioturbation on metal bioavailability in contaminated sediments by diffusive gradients in thin films (DGT). *Environmental science & technology* **50**, 3055-3064 (2016).
3. R. M. Amon, R. Benner, Bacterial utilization of different size classes of dissolved organic matter. *Limnology and Oceanography* **41**, 41-51 (1996).
4. P. N. Bertin *et al.*, Metabolic diversity among main microorganisms inside an arsenic-rich ecosystem revealed by meta-and proteo-genomics. *The ISME journal* **5**, 1735 (2011).
5. A. A. Bonapasta, F. Buda, P. Colombet, G. Guerrini, Cross-linking of poly (vinyl alcohol) chains by Ca ions in macro-defect-free cements. *Chemistry of materials* **14**, 1016-1022 (2002).
6. S. A. Burney, H. Tariq, K-means cluster analysis for image segmentation. *International Journal of Computer Applications* **96**, (2014).
7. J. Buschmann *et al.*, Contamination of drinking water resources in the Mekong delta floodplains: Arsenic and other trace metals pose serious health risks to population. *Environment International* **34**, 756-764 (2008).
8. J. Buschmann, S. Canonica, U. Lindauer, S. J. Hug, L. Sigg, Photoirradiation of dissolved humic acid induces arsenic(III) oxidation. *Environmental Science & Technology* **39**, 9541-9546 (2005).
9. J. Buschmann *et al.*, Arsenite and arsenate binding to dissolved humic acids: Influence of pH, type of humic acid, and aluminum. *Environmental science & technology* **40**, 6015-6020 (2006).
10. G. V. Buxton, C. L. Greenstock, W. P. Helman, A. B. Ross, Critical review of rate constants for reactions of hydrated electrons, hydrogen atoms and hydroxyl radicals (· OH/· O− in aqueous solution. *Journal of physical and chemical reference data* **17**, 513-886 (1988).
11. I. Christl, Ionic strength-and pH-dependence of calcium binding by terrestrial humic acids. *Environmental chemistry* **9**, 89-96 (2012).
12. I. Christl, Magnesium binding by terrestrial humic acids. *Environmental Chemistry* **15**, 317-324 (2018).
13. J.-P. Croué, M. Benedetti, D. Violleau, J. Leenheer, Characterization and copper binding of humic and nonhumic organic matter isolated from the South Platte River: evidence for the presence of nitrogenous binding site. *Environmental Science & Technology* **37**, 328-336 (2003).
14. S. Dobran, G. J. Zagury, Arsenic speciation and mobilization in CCA-contaminated soils: Influence of organic matter content. *Science of the total environment* **364**, 239-250 (2006).
15. S. J. Driver, E. M. Perdue, *Advances in the Physicochemical Characterization of Dissolved Organic Matter: Impact on Natural and Engineered Systems*. F. Rosario-Ortiz, Ed., (2014), vol. Volume 1160.
16. C. G. Elles, I. A. Shkrob, R. A. Crowell, S. E. Bradforth, Excited state dynamics of liquid water: Insight from the dissociation reaction following two-photon excitation. *The Journal of chemical physics* **126**, 164503 (2007).
17. D. Gondar *et al.*, Copper binding by peat fulvic and humic acids extracted from two horizons of an ombrotrophic peat bog. *Chemosphere* **63**, 82-88 (2006).
18. M. Grafe, M. Eick, P. Grossl, Adsorption of arsenate (V) and arsenite (III) on goethite in the presence and absence of dissolved organic carbon. *Soil Science Society of America Journal* **65**, 1680-1687 (2001).

19. D.-Y. Huang *et al.*, Comparison of dissolved organic matter from sewage sludge and sludge compost as electron shuttles for enhancing Fe (III) bioreduction. *Journal of soils and sediments* **10**, 722-729 (2010).
20. I. W. G. o. t. E. o. C. R. t. Humans, W. H. Organization, I. A. f. R. o. Cancer, *Some drinking-water disinfectants and contaminants, including arsenic*. (IARC, 2004), vol. 84.
21. IHSS. (International Humic Substances Society).
22. E. Illés, E. Tombácz, The role of variable surface charge and surface complexation in the adsorption of humic acid on magnetite. *Colloids and Surfaces A: Physicochemical and Engineering Aspects* **230**, 99-109 (2003).
23. E. Iskrenova-Tchoukova, A. G. Kalinichev, R. J. Kirkpatrick, Metal cation complexation with natural organic matter in aqueous solutions: molecular dynamics simulations and potentials of mean force. *Langmuir* **26**, 15909-15919 (2010).
24. S. E. Johnston, W. M. Barnard, Comparative Effectiveness of Fourteen Solutions for Extracting Arsenic from Four Western New York Soils 1. *Soil Science Society of America Journal* **43**, 304-308 (1979).
25. K. Kalbitz, S. Solinger, J.-H. Park, B. Michalzik, E. Matzner, Controls on the dynamics of dissolved organic matter in soils: a review. *Soil science* **165**, 277-304 (2000).
26. K. Kalbitz, R. Wennrich, Mobilization of heavy metals and arsenic in polluted wetland soils and its dependence on dissolved organic matter. *Science of the Total Environment* **209**, 27-39 (1998).
27. A. Kalinichev, R. Kirkpatrick, Molecular dynamics simulation of cationic complexation with natural organic matter. *European Journal of Soil Science* **58**, 909-917 (2007).
28. T. Kanungo *et al.*, An efficient k-means clustering algorithm: Analysis and implementation. *IEEE transactions on pattern analysis and machine intelligence* **24**, 881-892 (2002).
29. S. H. Lamm, M. B. Kruse, Arsenic ingestion and bladder cancer mortality—what do the dose-response relationships suggest about mechanism? *Human and Ecological Risk Assessment* **11**, 433-450 (2005).
30. P. Langner, C. Mikutta, R. Kretzschmar, Arsenic sequestration by organic sulphur in peat. *Nature Geoscience* **5**, 66-73 (2012).
31. V. Lenoble *et al.*, Evaluation and modelling of dissolved organic matter reactivity toward AsIII and AsV - Implication in environmental arsenic speciation. *Talanta* **134**, 530-537 (2015).
32. G. Liu, Y. Cai, Complexation of arsenite with dissolved organic matter: conditional distribution coefficients and apparent stability constants. *Chemosphere* **81**, 890-896 (2010).
33. G. Liu, A. Fernandez, Y. Cai, Complexation of arsenite with humic acid in the presence of ferric iron. *Environmental science & technology* **45**, 3210-3216 (2011).
34. J. B. McKinlay, J. G. Zeikus, Extracellular iron reduction is mediated in part by neutral red and hydrogenase in Escherichia coli. *Appl. Environ. Microbiol.* **70**, 3467-3474 (2004).
35. M. Miethke, M. A. Marahiel, Siderophore-based iron acquisition and pathogen control. *Microbiol. Mol. Biol. Rev.* **71**, 413-451 (2007).
36. F. M. Morel, J. G. Hering, *Principles and applications of aquatic chemistry*. (John Wiley & Sons, 1993).
37. Y. K. Mouvenchery, J. Kučerík, D. Diehl, G. E. Schaumann, Cation-mediated cross-linking in natural organic matter: a review. *Reviews in Environmental Science and Bio/technology* **11**, 41-54 (2012).
38. E. M. Murphy, J. M. Zachara, S. C. Smith, J. L. Phillips, T. W. Wietsma, Interaction of hydrophobic organic compounds with mineral-bound humic substances. *Environmental science & technology* **28**, 1291-1299 (1994).

39. J. T. Nurmi, P. G. Tratnyek, Electrochemical properties of natural organic matter (NOM), fractions of NOM, and model biogeochemical electron shuttles. *Environmental science & technology* **36**, 617-624 (2002).
40. M. P. Pothier, A. J. Hinz, A. J. Poulain, Insights Into Arsenite and Arsenate Uptake Pathways Using a Whole Cell Biosensor. *Frontiers in Microbiology* **9**, (2018).
41. I. Rathnayake, M. Megharaj, G. Krishnamurti, N. S. Bolan, R. Naidu, Heavy metal toxicity to bacteria–Are the existing growth media accurate enough to determine heavy metal toxicity? *Chemosphere* **90**, 1195-1200 (2013).
42. P. Ravenscroft, H. Brammer, K. Richards, *Arsenic pollution: a global synthesis*. (John Wiley & Sons, 2009), vol. 28.
43. A. D. Redman, D. L. Macalady, D. Ahmann, Natural organic matter affects arsenic speciation and sorption onto hematite. *Environmental science & technology* **36**, 2889-2896 (2002).
44. E. Revesz, D. Fortin, D. Paktunc, Reductive dissolution of arsenical ferrihydrite by bacteria. *Applied Geochemistry* **66**, 129-139 (2016).
45. D. Reynolds, S. Ahmad, The effect of metal ions on the fluorescence of sewage wastewater. *Water Research* **29**, 2214-2216 (1995).
46. J. D. Ritchie, E. M. Perdue, Proton-binding study of standard and reference fulvic acids, humic acids, and natural organic matter. *Geochimica et Cosmochimica Acta* **67**, 85-96 (2003).
47. P. A. Riveros, J. E. Dutrizac, P. Spencer, Arsenic disposal practices in the metallurgical industry. *Canadian Metallurgical Quarterly* **40**, 395-420 (2001).
48. C. E. Schuh, H. E. Jamieson, M. J. Palmer, A. J. Martin, J. M. Blais, Controls governing the spatial distribution of sediment arsenic concentrations and solid-phase speciation in a lake impacted by legacy mining pollution. *Science of the Total Environment* **654**, 563-575 (2018).
49. J. Stocker *et al.*, Development of a set of simple bacterial biosensors for quantitative and rapid measurements of arsenite and arsenate in potable water. *Environmental Science and Technology* **37**, 4743-4750 (2003).
50. W. Sunda, Massachusetts Institute of Technology and Woods Hole Oceanographic Institution, (1975).
51. R. Sutton, G. Sposito, M. S. Diallo, H. R. Schulten, Molecular simulation of a model of dissolved organic matter. *Environmental Toxicology and Chemistry: An International Journal* **24**, 1902-1911 (2005).
52. P. Thanabalasingam, W. Pickering, Arsenic sorption by humic acids. *Environmental Pollution Series B, Chemical and Physical* **12**, 233-246 (1986).
53. E. Tipping, *Cation binding by humic substances*. (Cambridge University Press, 2002), vol. 12.
54. M. Vera *et al.*, Fluorescence spectroscopy and parallel factor analysis as a dissolved organic monitoring tool to assess treatment performance in drinking water trains. *Science of the total environment* **584**, 1212-1220 (2017).
55. *Guidelines for drinking-water quality: recommendations* (9241546387, 2004).
56. C. E. Williamson *et al.*, Ecological consequences of long-term browning in lakes. *Scientific reports* **5**, 18666 (2015).
57. C. E. Williamson *et al.*, Solar ultraviolet radiation in a changing climate. *Nature Climate Change* **4**, 434 (2014).
58. G. R. Willsky, M. H. Malamy, Effect of arsenate on inorganic phosphate transport in Escherichia coli. *Journal of Bacteriology* **144**, 366-374 (1980).
59. S.-H. Yoon, J. H. Lee, S. Oh, J. E. Yang, Photochemical oxidation of As (III) by vacuum-UV lamp irradiation. *Water research* **42**, 3455-3463 (2008).
60. J. Zhao *et al.*, Diversity change of microbial communities responding to zinc and arsenic pollution in a river of northeastern China. *Journal of Zhejiang University-SCIENCE B* **15**, 670-680 (2014).

61. Y.-G. Zhu, X.-M. Xue, A. Kappler, B. P. Rosen, A. A. Meharg, Linking genes to microbial biogeochemical cycling: lessons from arsenic. *Environmental Science & Technology*, (2017).

Annex B – Chapter 3 SI

SUPPLEMENTARY MATERIALS

Dissolved organic matter controls arsenic bioavailability to bacteria

Martin P. Pothier[1]*, Véronique Lenoble*[2]*, Cédric Garnier*[2*]*, Benjamin Misson*[2]*, Charlotte Rentmeister*[1]*, Alexandre J. Poulain*[1]

[1] *Biology Department, University of Ottawa, 30 Marie Curie, Ottawa, ON, K1N 6N5, Canada*

[2] *Univ Toulon, Aix Marseille Univ., CNRS/INSU, IRD, MIO UM 110, Mediterranean Institute of Oceanography, La Garde, France*

[*] *Deceased*

List of supplementary materials:

A modified version of the supplementary materials can be found online at:
Science of the Total Environment **|** *https://ars.els-cdn.com/content/image/1-s2.0-S0048969720306288-mmc1.pdf*

Annex B1 Supplementary figures

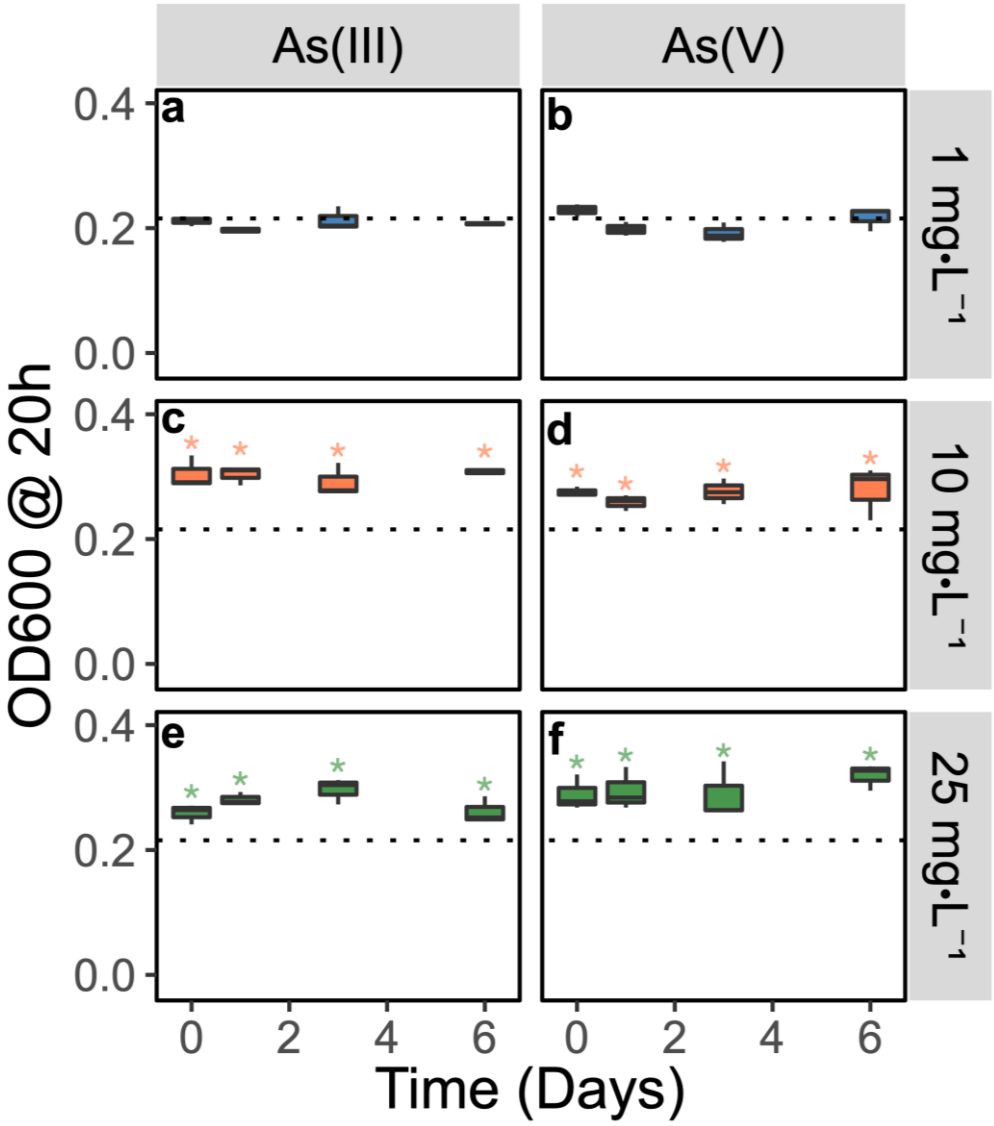

SI Fig. B1.1 | High DOM concentrations increase in the yield of biosensor cultures for **Figure 3.3**. Boxplots represent triplicate cultures containing either 200 nM of As(III) (**a, c, e**) or 200 nM As(V) (**b, d, f**) in the presence of a DOM (SRHA) gradient (**vertical facets**). Axes include room-temperature pre-incubation time (X-axis) and output signals of treatments are indicated as percent deviation from our no-DOM controls (Y-axis). Dotted line represents biosensor yield in the no-DOM controls. Stars represent a significant decrease from the no-DOM control incubated for the same period of time determined using raw OD_{600} measurements and TukeyHSD post-hoc analysis on a one-way anova.

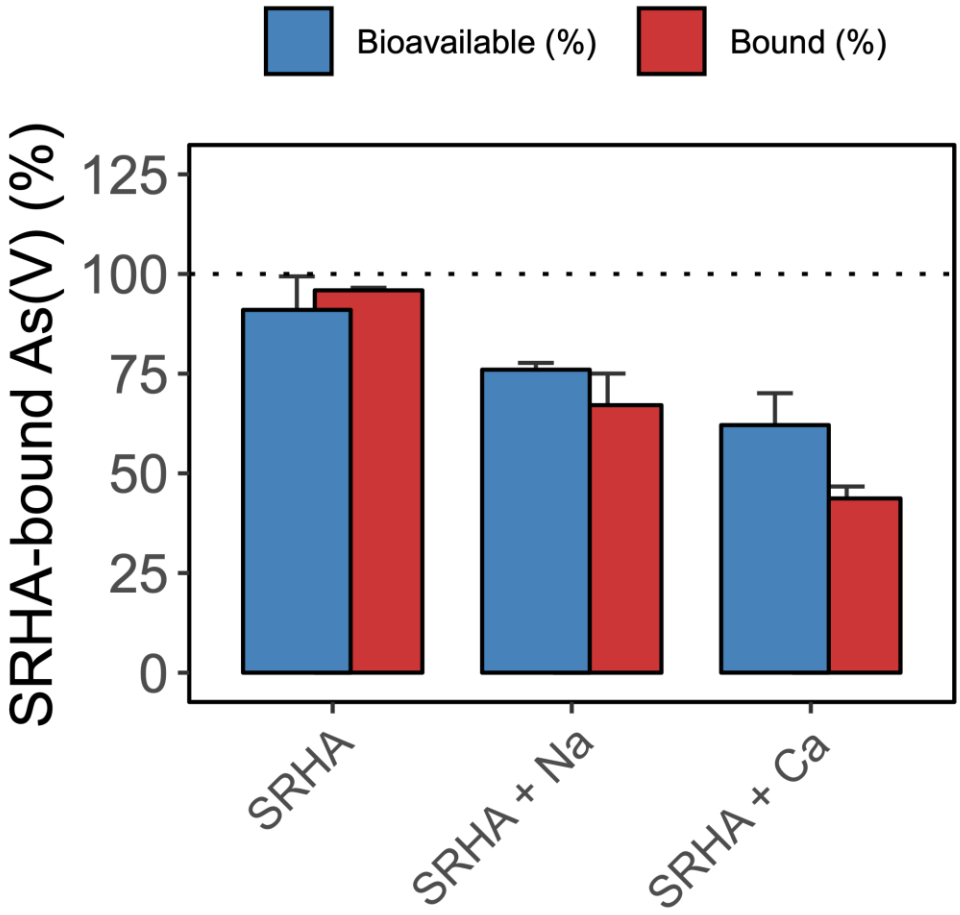

SI Fig. B1.2 | Cation influence on As(V) binding to SRHA and As(V) bioavailability. Total As(V) and SRHA concentrations were adjusted to 200 nM and 10 mg/L respectively. 10 mM Na^{+} or Ca^{2+} were added both inside of a 500 Da dialysis cut-off membrane and in the external solution, at the same ionic strength. Error bars represent standard deviation of triplicate biological samples. Dotted line represents biosensor output signal of the no-DOM controls at the same ionic strength.

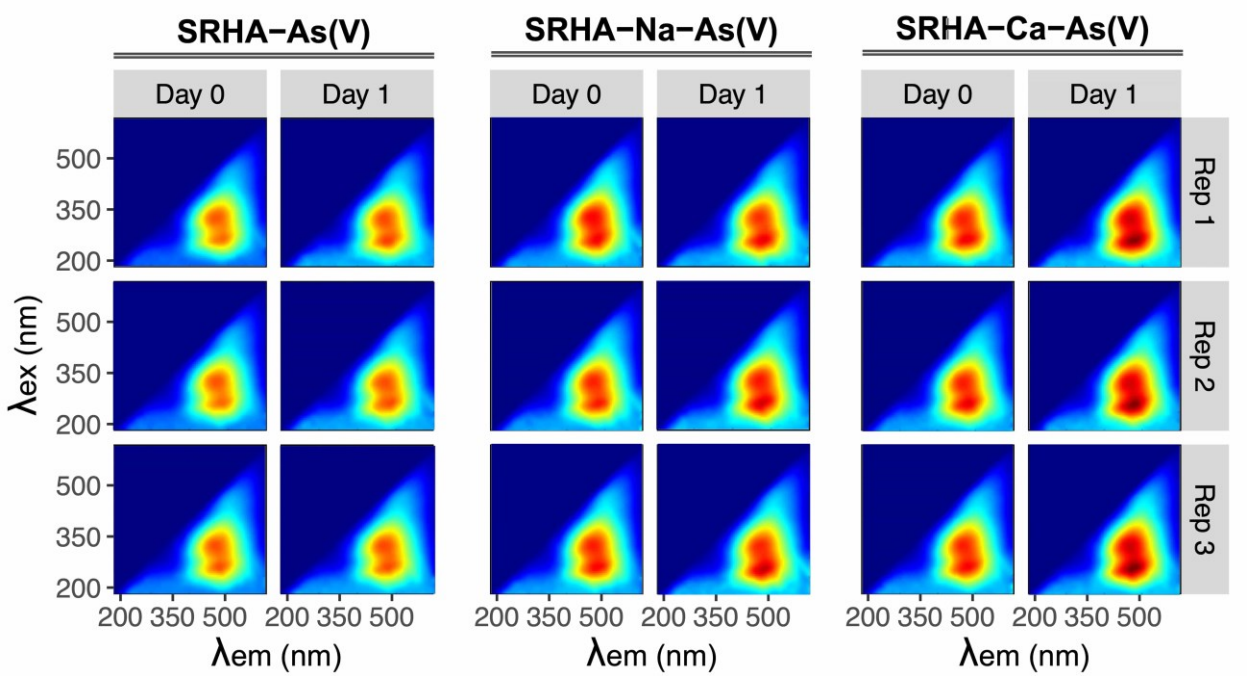

SI Fig. B1.3 | Cation increase As(V)-SRHA fluorescence intensity. Triplicate samples are shown by the vertical facets. 10 mM Na^{+} or Ca^{2+} was added to 200 nM As(V) and 10 mM SRHA concentrations.

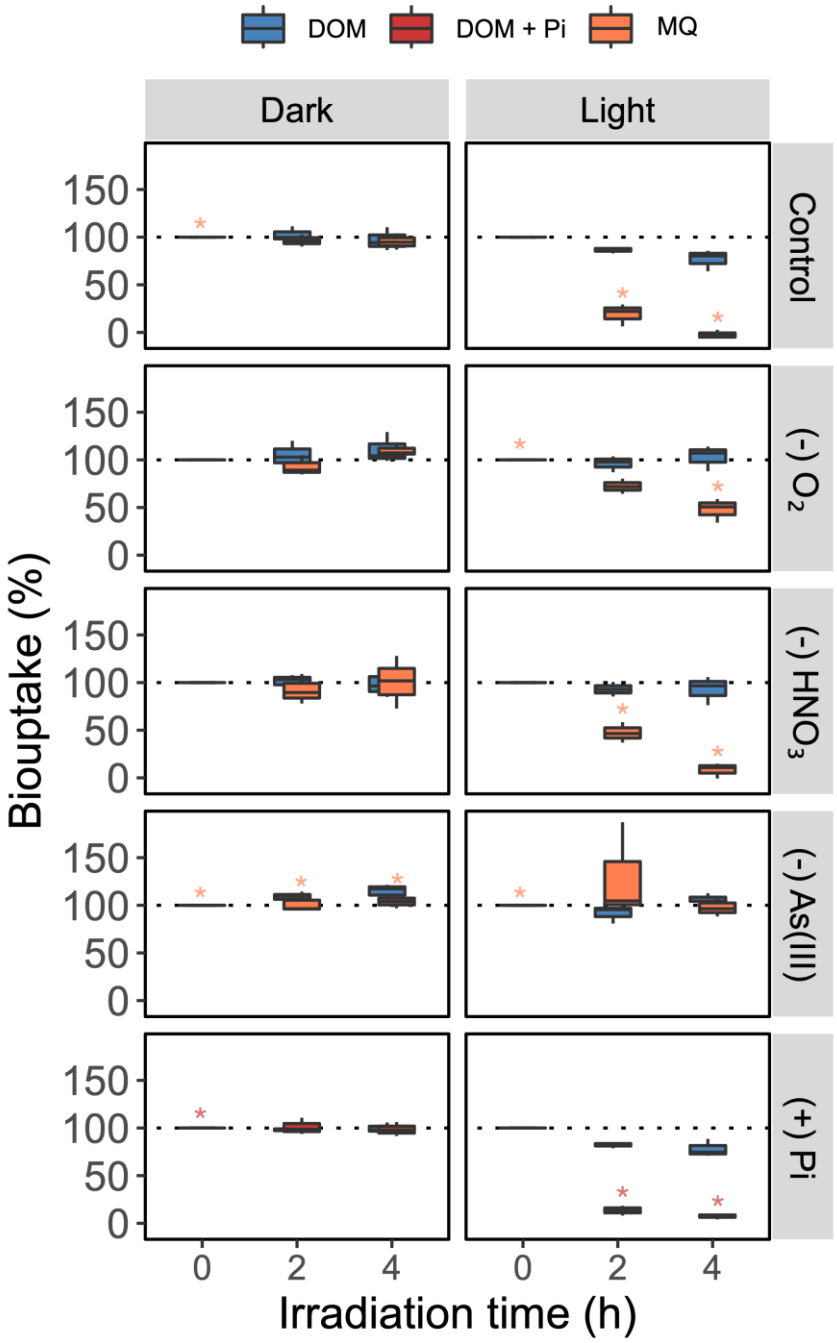

SI Fig. B1.4 | Supplemental controls for **Figure 3.7**. Each horizontal facet represents an independent assay reproduced on separate days. Here, a decrease in As(III) uptake over time suggests As(III) oxidation. Biosensor fluorescence was converted to percent biouptake (Y-axis) by comparing output signal of the irradiated treatments to the pre-irradiated (T0) controls. Biosensor endpoints present the mean and standard deviation of three independent biological triplicates. **Figure 3.7** findings **(Control)** were replicated absent oxygen **(-O_2)**, absent nitric acid in As(III) stock **(-HNO_3)**, and when PO_3^{2-} was added to the reaction vessel **(+Pi)**. Addition of As(III) after photoirradiation DOM did not induce As(III) oxidation **(-As(III))**.

Annex B2 Supplementary Protocol

Annex B2.1 | Anaerobic assay controls

To test whether these findings were an artifact of our experimental design, we performed the assay under anoxic conditions in one treatment and removed HNO_3^- from our As(III) stock solution in a separate treatment. In both cases, only in water treatments did we notice significant As(III) photooxidation (**SI Fig. B1.4**). We also tested whether As(III) oxidation in water alone was an artifact of the cuvette or of the water used in our laboratory by only introducing As(III) to the cuvettes after irradiation, 0.5h prior to exposing the microbes. As expected, we found no oxidation of As(III) for any of the biological triplicates (**SI Fig. B1.4**).

Annex B3 Supplementary table

SI Table B3.1 | Properties of DOM origins used to produce RDA **Figure 3.6**.

Condition	Cation	S	N	Acetal	Aromatic	Aliphatic	Carboxyl	Phenolic	Q1	Q2	pKa
ESFA	No	1.43	1.43	1	30	22	13.24	2.27	14.12	0.74	3.67
ESFA	Na	1.43	1.43	1	30	22	13.24	2.27	14.12	0.74	3.67
ESFA	Ca	1.43	1.43	1	30	22	13.24	2.27	14.12	0.74	3.67
ESFA	Cu	1.43	1.43	1	30	22	13.24	2.27	14.12	0.74	3.67
SRNOM	No	1.78	1.78	7	23	27	11.21	2.47	11.2	1.6	4.16
SRNOM	Na	1.78	1.78	7	23	27	11.21	2.47	11.2	1.6	4.16
SRNOM	Ca	1.78	1.78	7	23	27	11.21	2.47	11.2	1.6	4.16
SRNOM	Cu	1.78	1.78	7	23	27	11.21	2.47	11.2	1.6	4.16
SRFA	No	0.41	0.66	6	22	35	11.17	2.84	11.66	2.05	3.76
SRFA	Na	0.41	0.66	6	22	35	11.17	2.84	11.66	2.05	3.76
SRFA	Ca	0.41	0.66	6	22	35	11.17	2.84	11.66	2.05	3.76
SRFA	Cu	0.41	0.66	6	22	35	11.17	2.84	11.66	2.05	3.76
SRHA	No	0.55	1.5	7	31	29	9.13	3.72	9.74	4.48	4.35
SRHA	Na	0.55	1.5	7	31	29	9.13	3.72	9.74	4.48	4.35
SRHA	Ca	0.55	1.5	7	31	29	9.13	3.72	9.74	4.48	4.35
SRHA	Cu	0.55	1.5	7	31	29	9.13	3.72	9.74	4.48	4.35

Chapter 4 – Portability of the bioassay

ORIGINAL RESEARCH

Design and application of a portable spectrometer to detect As at nanomolar levels

Martin P. Pothier[1]*, Eric J. Kitchen*[1]*, Bill Sinclair*[2]*, Kongkea Phan*[3]*, Alexandre J. Poulain*[1]

[1] *Biology Department, University of Ottawa, 30 Marie Curie, Ottawa, ON, K1N 6N5, Canada*

[2] *Independent Consultant, Ottawa, ON, Canada*

[3] *Faculty of Science and Technology, International University, Phnom Penh, 12210, Cambodia*

Highlights:

i) Bacterial sensors, in combination with a portable spectrometer, enables highly accurate detection of arsenic in the field.

ii) Redesigned a dehydration protocol that facilitates transport of these cellular sensors to the field, with a single hydration upon arrival

iii) Integration of data normalization algorithms into the low-cost spectrometer improve usability and consistency of output.

iv) Standard additions of arsenic to the water sample could be used as a quality control measure by helping to quantify "matrix effects".

Contributions to the field:

i) New, single step hydration protocol to measure As content in water.

ii) Design and plans to a portable spectrometer.

iii) Complete arsenic testing solution capable of measuring both As(III) and As(V) at levels relevant to the World Health Organization drinking water guidelines.

The following manuscript contains confidential information that must be revised by uOttawa Innovation Support Services before submission for publication.

4.1 ABSTRACT

Arsenic is a naturally occurring carcinogen affecting the food and drinking waters of millions of people worldwide. Rapid and reliable detection of arsenic species directly in the field is critical to support evidence-based decision-making in choosing irrigation or drinking water sources. Current cost-effective colourimetric techniques are associated with poor accuracy, health risks and unacceptable levels of false negatives. Microbial biosensors offer a safe and affordable alternative but often require costly/fragile instruments to measure the signal produced by the biosensor. In this study, we report on the design and testing of a small, low-cost portable fluorometer/densitometer to measure As concentrations in water samples directly in the field. Using lyophilized biosensor cultures, we were able to accurately detect arsenic concentrations at nM levels, relevant to the World Health Organization guidelines. We hope this tool will contribute to education campaigns that encourage uptake by individuals who need it the most. For instance, farmers requiring the need to make rapid decisions about the quality of irrigation waters; thus, building local capacity and addressing a crippling, global problem of access to clean water.

Keywords: arsenic; field measurement; fluorometer; spectrometer; water quality

N.B. Supplementary Materials (**Annex C**) are appended at the end of this chapter.

4.2 Introduction

Arsenic (As) is classified as a group 1 carcinogen (*7*) and ranks among the World Health Organization's (WHO) ten chemicals of major public health concern (*14*). Regional distribution of As in groundwater is tightly associated to As content in bedrock (*1*). These tendencies, however, translate poorly to local scale predictions of As content in tube wells (*35*). This challenge stems from complex biogeochemical processes that change with seasons, land use (*e.g.*, groundwater pumping), groundwater flow/age, well depth, and availability of labile organic carbon fuelling microbial mediated As release (*6*). Despite these complex groundwater flow paths, high-As zones can be fairly restrained and near low-As zones. Mitigation strategies therefore involve choosing alternative nearby wells for water consumption (*26*). Yet, fundamental to effective water management is knowledge of its occurrence. Over the past two decades, a number of *in situ* detection solutions have been proposed, yet very little have reached the market due to a number of technical, collaborative, and socio-geopolitical barriers. These include:

i) Usability/reliability. Effective As monitoring is costly as it requires sample preservation care, and qualified staff for operation and maintenance of the instruments (*34*). In contrast, colourimetric field kits present cost-effective solutions yet are heavily criticized for their poor accuracy, health risks, and unacceptable levels of false negatives (*13*). Despite these limitations, the cost and convenience of "Gutzeit"-based colourimetric field kits make that it's often the most common method applied in the field (*13*).

ii) Engagement. Once developed, the sensing performance must meet real-world detection requirements. One option is to engage with the end user directly by way of citizen science (*3*). An important barrier preventing a community-based environmental monitoring is operational ease and cost of current field-ready solutions. This requires a major overhaul of currently accepted user interfaces, which is met with robust readouts, unlikely to fall victim of user error nor risk for the health of the user. Here, production of a field-ready instrument capable of numerically

quantifying As concentration in drinking water is essential for regulators, risk management, and citizen-based science.

Microbes, having lived alongside As for several billion years (*24*), has driven microbes to evolve a plethora of genetic machinery that grants them the abilities to access (*18, 19*), to remobilize (*6*) and to transform (*11*) As into a wide array of redox-sensitive chemical species (*41*). By utilizing the genes involved in these resistance pathways, a number of As-specific, whole-cell biosensors, have been developed and deployed through microfluidic chips (*20*), spores (*4*), lyophilization in vials (*26, 27*), immobilization in agar (*10*) and even attached to fibre-optic cables (*8*).

Whole cell As-specific biosensors offer cost-effective and scalable solutions. These microbes are specially designed to produce a quantifiable signal, proportional to the concentration of As in water (**Figure 4.1**). The use of biosensors in the field is a solution assessed over 15 years ago (*33*), yet faced technological and biological hurdles that encumbered advancement of field-ready bioanalytics. Over the past several years, advancements in the affordability of 3D printers, microcircuit printing, photodiodes, energy storage, drones for remote sensing, and the open sourcing of microcontrollers has stimulated a new area in environmental monitoring.

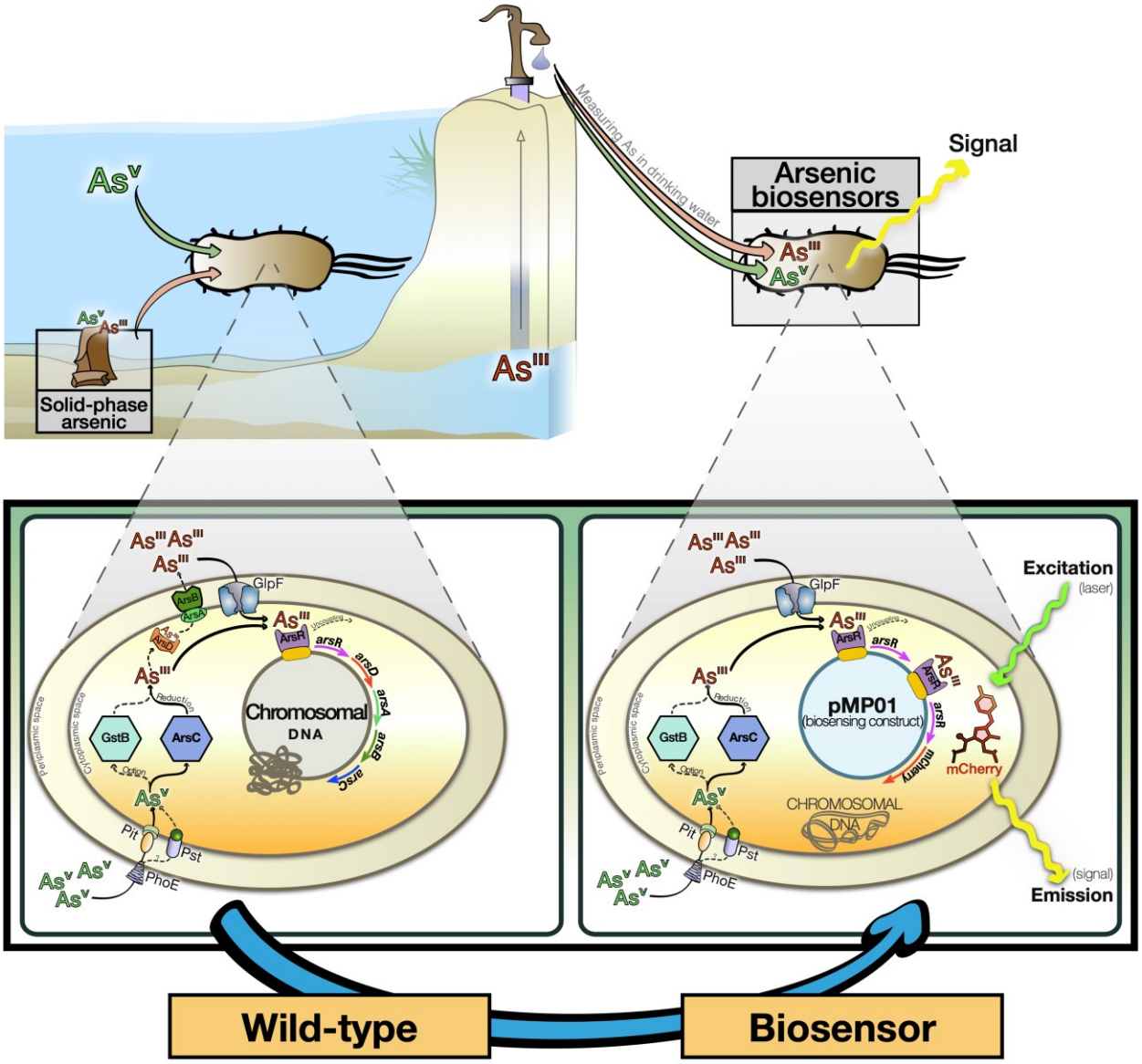

Figure 4.1 | Use of environmental genes in the design of As biosensors. The pMP01 high copy biosensor plasmid uses two wild-type As(III) sensory gene (*ars*R) (**left**), upstream from a reporter gene (mCherry) (**right**). Detection of As(V) requires cytoplasmic reduction to As(III) before binding and decoupling of the ArsR transcriptional repressor.

Logistics and regulations surrounding the culturing and storing of level-1 microbes such as derivatives of *E. coli* K12 have been well established through large-scale infrastructure involved in food processing, and in alcohol production. Despite these advantages, As-biosensors have been criticized for inconsistent signal outputs, lack of lower limit sensitivity, and for relying on short-lived bioluminescent signals (*e.g.*, *arsR-lux*) during As quantification. Moreover, most As-specific biosensors, even

those of recent studies (*2, 36*), produce little to no signal when exposed to As(V), the dominant inorganic As species found in oxygenated waters such as lakes, rivers and streams (*7*). In a previous study (*15*), we described a highly sensitive biosensor assays capable of identifying and quantifying the concentrations of both As(III) and of As(V), even within a mixture of both species. Regarding biosafety, the level 1, non-pathogenic, non-regulated bacterial host, was in part chosen for its auxotrophy [Δ(*ara-leu*)] to three essential amino acids (leucine, isoleucine and valine), making life outside of the provided medium, difficult. With a whole cell biosensor assay optimized to meet WHO guidelines, the challenge laid in designing a new interface, one capable of measuring the signal produced by these biosensors in the field at an affordable cost.

The first scalable solution at this redesign was recently made possible by the use of microfluidic chips with immobilized bacterial sensors (*36*). Despite previous efforts (*20*), this design does not require commercialization of a dedicated instrument to measure biosensor output since it enables the end user to visually assess the level of As toxicity using cellphone cameras. This promising technology presents a great leap as it adapts well known and globally distributed "smart devices" as new interfaces to determine As concentration in water. It, however, relies heavily on the user's manual adjustment of camera settings, mounting adapters, and on the user's visual interpretation of bacterial response. Overall, the technology involved in using of cellphone cameras to solve this problematic requires maturation before it can overcome usability and engagement issues when working at larger scale.

The focus of this study was to design a dedicated instrument that is affordable, buildable by the end users, and tailored for the measurement of biosensor signal in a numeric form. Once calibrated, a numeric readout would allow for precise quantification of As content in water so that it can be directly compared to established safety guidelines. Our goal throughout conception and design of this instrument was to simplify and minimize end-user interactions. Achieving a single step As monitoring

solution required breaking down fundamentals of As uptake pathways, electromagnetism, and stabilization of sensors a system in a state capable of supporting long-term storage. We found that the use of lyophilized fluorescent biosensor cells, in combination with the portable spectrometer capable of measuring fluorescence and absorbance, enabled accurate detection of inorganic As species in natural surface waters at nanomolar levels.

4.3 Materials and methods

4.3.1 Culturing.

All media and reagents used in this study were prepared and kept in sterilized, acid washed, Fisherbrand (FB800100) glass bottles. Water purification (Milli-Q), preparation of 10 mM As standards, Lysogeny Broth (LB) medium, and construction of the pMP01 biosensor have been previously described (*15*). The redesigned FBMS (field biosensor mixed salts) medium used in this study provides 30 mM pyruvate rather than 30 mM glycerol to improve drying/immobilization of the sensor cells during lyophilization. We also increased the buffering capacity (20 to 50 mM MOPS), amended with fumarate and iron, and modified the trace elements to facilitate the application of the biosensor in both oxic and anoxic conditions (*30*) should oxygen levels fluctuate in water samples or during the assay. Medium component concentrations are presented in **SI Table C1.1**.

Bacterial colonies were grown from cryostock (-80ºC) onto LB + 120 µg/mL ampicillin plates and kept for a maximum of one week. Fresh biosensor cultures were initiated by transferring a single colony into a culture tube with 5 mL of FBMS medium + 100 µg/mL ampicillin then incubated at 37ºC and 200 RPM overnight until they reached an OD_{600} (optical density at 600 nm) of 1.1 to 1.2. In this study, we enhanced doubling time of the pMP01 biosensor in the new FBMS medium through a series of 1-day acclimations. Further details regarding this culturing technique can be found in our previous study (*15*).

4.3.2 Lyophilization.

Previous successful field deployments of *ars*R-lux biosensors was shown possible through using a lyophilization process (*26, 27*). This dehydration process immobilizes the sensor cells and prolongs shelf life by removing water from the biosensor cultures through a solid to gas sublimation process. We used 150 mM (~5% $\frac{W}{V}$) sucrose as the lyoprotectant (*29*) to prevent damaging the sensor cells during flash freezing. Preparation of 50 mL cryoprotectant solution consists of: 15 mL of FBMS medium (2x concentrated), 7.5 mL of 1 M sucrose (Fisher Chemical S5-500), 15.8 mL of Milli-Q water, 400 µL of 10 mM Ethylenediaminetetraacetic acid (EDTA), and 9.5 mL of unwashed FBMS grown biosensor culture. Lyophilization involves addition of 3 mL of cyroprotectant solution to an 8 mL Kimble^{tm} glass scintillation vials (DWK K608101760) before flash freezing at -80ºC for 30 minutes. The flasks were then transferred to a Labconco FreeZone 2.5 L benchtop freeze dryer set to 0.470 mbar and -50ºC for 22 h. Vacuum intensity was then increased to 0.100 mbar for 2 h and cycled back to 0.470 mbar for another 22 h without change to the temperature. Finally, aluminum lined caps were used to seal the vials following replacement of headspace with nitrogen gas. Lyophilized cultures were stored at 4ºC. Stabilizers such as polyvinylpyrrolidone (PVP) were omitted from our recipe as these were found to prevent proper drying of the cultures. We used cultures that were lyophilized for up to two weeks and we are currently testing longer preservation times (i.e., months to years).

4.3.3 Cell exposure to As and signal quantification.

Detection of As by the biosensor is enabled once the lyophilized cells are rehydrated in the lab or in the field. Converting biosensor signal to an As concentration requires determining the slope and intercept of a calibration curve. We typically concentrate our exposure medium two-fold so that we can account for dilution factors when introducing reagents (*15, 16*). In this study, we minimized dilution bias of our protocol by concentrating the FBMS medium prior to dehydration. We estimate a 95%

loss in water content leaving 5% residual material in the vials once lyophilization is complete. Although minimal, upon rehydration, this residue does dilute the samples that are being analyzed. Because the cultures used for the calibration curves also contain this residue, any dilution is accounted for and therefore no further adjustments are necessary. Environmental samples that exceed [As]=600 nM, typically fall beyond the linear range of the calibration curve and should be diluted and reprocessed if accurate quantification is required.

4.3.4 Spectrometer design and construction.

Overall, the construction of the portable fluorometer/densitometer consisted of commercially available microelectronics, purpose-built circuits and 3D printed parts (**SI Fig. C2.1**, **SI Fig. C2.2**). An Arduino Uno R3 microcontroller was used as the interface and main controller of this instrument. Standard size 12V barrel adapters, 3S 18650 lithium ion 3.7V batteries, and commercially available battery management system (BMS) were used to power and charge the unit. We surface mounted a purpose-built power board to reduce instrument size and to separate the photo-detection circuits from power sources. This board included amplifiers, step up/down converters, and tunable pots to facilitate modularity of the instrument by controlling output current. Parts such as the circuit boards that required fine-tuned precision were designed using Fusion 360 by Autodesk. Most of the FB fluorometer parts, including the hinges, vial holder, battery compartment, and the main assembly were designed using Tinkercad, a free browser-based 3D modelling software by Autodesk. These parts were designed with an offset that matches the expansion profile of polylactic acid (PLA) plastic (approx. 0.8 mm) when extruded at 210ºC using a Cel Robox 3D printer.

4.3.5 Fluorescence detection.

Like most fluorophores, the red fluorescent proteins produced by the biosensor cells passively absorb and re-emit light in a specific emission spectrum (*25*). Crucial in the

detection of biofluorescence is to ensure that the signal output is free from photons belonging to other sources of electromagnetic radiation or of light (*e.g.*, excitation source). This is typically achieved using short bandpass filters that isolate emission spectra. Reaching high gain amplification of the biosensor's fluorescent signal required lowering the signal-to-noise ratio by shielding the circuits from local electromagnetic (EM) interferences. This was achieved by integrating an ultrasensitive photodetection unit onto miniaturized circuit boards with large grounding plates (**SI Fig. C2.1**).

We found high impedance amplification with minimal noise interference required a customized solution that could not be achieved using "off-the-shelf" components. We started by mounting a dual voltage LT 1792 transimpedance amplifier (TIA) onto a custom printed circuit board with grounding plane starting at input pin. Gain regulation could then be achieved by combining this a low bias, low signal TIA, with a 24-bit ARD LTC 2499 analogue to digital converter (ADC) with on-board voltage reference.

We used a Jolooyo 50 mW 532 nm 3.7 V laser diode, to excite the microbial fluorophores and isolated the emitted light using a 590 to 640 nm optical band-pass filter (**SI Fig. C2.3**). Going forward, a higher quality laser is recommended considering we could only achieve a power output of 7 mW before burning out the inexpensive laser. We then characterized spectral components of the light crossing the bandpass filter using a ThorLabs CCS200 compact charged-coupled device spectrometer with 200-1000 nm wavelength range. We found proper isolation of the bacterial signal was achieved and free from 532 nm (excitation sourced) photons (**SI Fig. C2.3**). Finally, a filter-based BioTek Synergy HTX multimode plate reader was used as a lab-based independent instrument to cross-calibrate fluorescent output and culture yield (OD_{600}) of the FB portable fluorometer/densitometer.

4.3.6 Preliminary field verification.

We first tested a prototype of the instrument using well water collected in the regions surrounding Phnom Penh, Cambodia in May 2017. Freeze-dried biosensor cells were shipped to Cambodia by express mail ahead of time and were kept in the dark in a fridge until they were used for the experiment. Our preliminary tests confirmed that cells could be revived after a period of a few weeks (**SI Fig. C2.4**). Water samples were collected using plastic containers by students at International University in Phnom Penh and were immediately analyzed by the biosensors in the laboratory at International University. Aliquots of the samples were acidified and shipped to Ottawa (Canada) for HPLC-ICP-MS speciation and analyses. We found the biosensor performed well when compared with ICP-MS measurements in measuring As(III) and total inorganic As in all but one of the collected samples (**SI Fig. C2.5**, sample 6). Indeed, for one of the samples, there was an overestimation of the As concentration which we attributed to excessive growth of the cells in the natural water sample. Upon visual inspection of the vials, it was clear that the cells had grown as evidenced by the turbidity of this anomalous sample. Because background fluorescence increases with the growth of the microbes, it is likely that the false positive generated by this sample was a result of the increased background fluorescence generated by the enhanced bacterial growth observed in this culture. Based on this first deployment of the instrument in the field, we deemed important to include the ability to measure absorbance for all samples, in addition to fluorescence.

4.3.7 Absorbance measurement.

A 350 mA 610~615 nm led diode (Cree Inc. XPEBRO-L1-R250-00B02CT-ND) was placed in the direct path of the photodiode diode, on the opposite side of the cuvette (**SI Fig. C2.2**e). Through a series of light burst, this instrument can accurately measure the optical density of a sample by quantifying the decrease in the transmittance of the sample when compared to its blank. The following formula used

to determine OD_{600} is based on the Beer-Lambert law to witch we applied a 1.4x instrument conversion factor to align with plate reader measurements (*12*) (eqn i):

$$(\text{eqn i}) \qquad \mathrm{OD}_{600} = -\log\left(\frac{\Phi\text{sample}}{\Phi\text{blank}}\right) * 1.4$$

Here, **Φsample** is the radiant flux transmitted by the sample following a 10 µs light burst. The **Φblank** readout is captured upon first boot up when the user is instructed to calibrate the instrument by inserting a blank vial filled with 1 mL of the water sample to be tested. It represents the maximum transmittance of that medium, absent of biosensors.

4.3.8 Onboard algorithms.

We needed a complete solution, one where the software and hardware are specially tuned to detect and normalize microbial signals. Regarding hardware, we reduced electromagnetic interferences by combining i) a low-fluctuation and purpose-built power supply, ii) gain control, iii) a shielded dual voltage TIA, and iv) a high-end photodiode.

Regarding software, first, we included a short delay between the laser's on/off time and the photodiode's response time to further reduce possible interferences. Improving accuracy and consistency of calculated output meant standardizing the output through a series of laser burst then calculating the average. Calculating the delays also involved timing the laser bursts with the fluorescent decay time of the biosensor's fluorophore (mCherry). Here, the number of burst and laser intensity were also important to consider as these could increase likelihood of photobleaching (*32*). Second, we remove autofluorescence of the sample after each measurement to decrease likelihood of false positives (Chapter 3, **Figure 3.2**). This step also reduces background signal and improves accuracy of the instrument. Finally, we normalize each fluorescent output to the optical density of the sample (Chapter 3, **Figure 3.2**).

Integration of (eqn i) into the onboard algorithms of this instrument provides us with the option of capturing and quantifying a change in the optical density of the sample at a wavelength representative of bacterial growth (*12*). Through a single click, these algorithms compute an analogue to digital conversion that captures signal output of the microbes into a normalized relative fluorescent unit (RFU) that is then displayed on the screen of the FB spectrometer.

4.3.9 Sample collection.

Samples presented in **Figure 4.4** were all collected in the summer of 2019 in southern Ontario, Canada. Coordinates of the environmental samples are presented in **SI Table C1.2**, while the precise coordinates of the tap water, groundwater and surface pond samples were omitted for privacy reasons. The data table instead presents the general location of the municipalities. We used 15 mL polypropylene conical centrifuge tubes (Corning 352196) to collect the water samples. Tubes were capped under water to ensure no air bubbles were present. Lyophilized biosensor cultures were then exposed in the laboratory to the raw water samples without any filtration steps. All further steps involved in incubation and collection of culture readouts are described above.

4.4 Results

4.4.1 Process.

The use of bacterial sensors in the field has been limited. One reason is the lack of suitable field-ready instruments capable of amplifying and quantifying the signals produced by biosensor cells. This study focused on developing a low-cost (ca. $150 USD) and lightweight (680 g) portable fluorometer/spectrometer that can be used to measure signal output of As-specific bacterial sensors in the field. Our approach involved: i) dehydration of the cells for field transport, ii) rehydration using natural

water samples, iii) incubation, and iv) measurement of biosensor signals using the portable spectrometer (**Figure 4.2**).

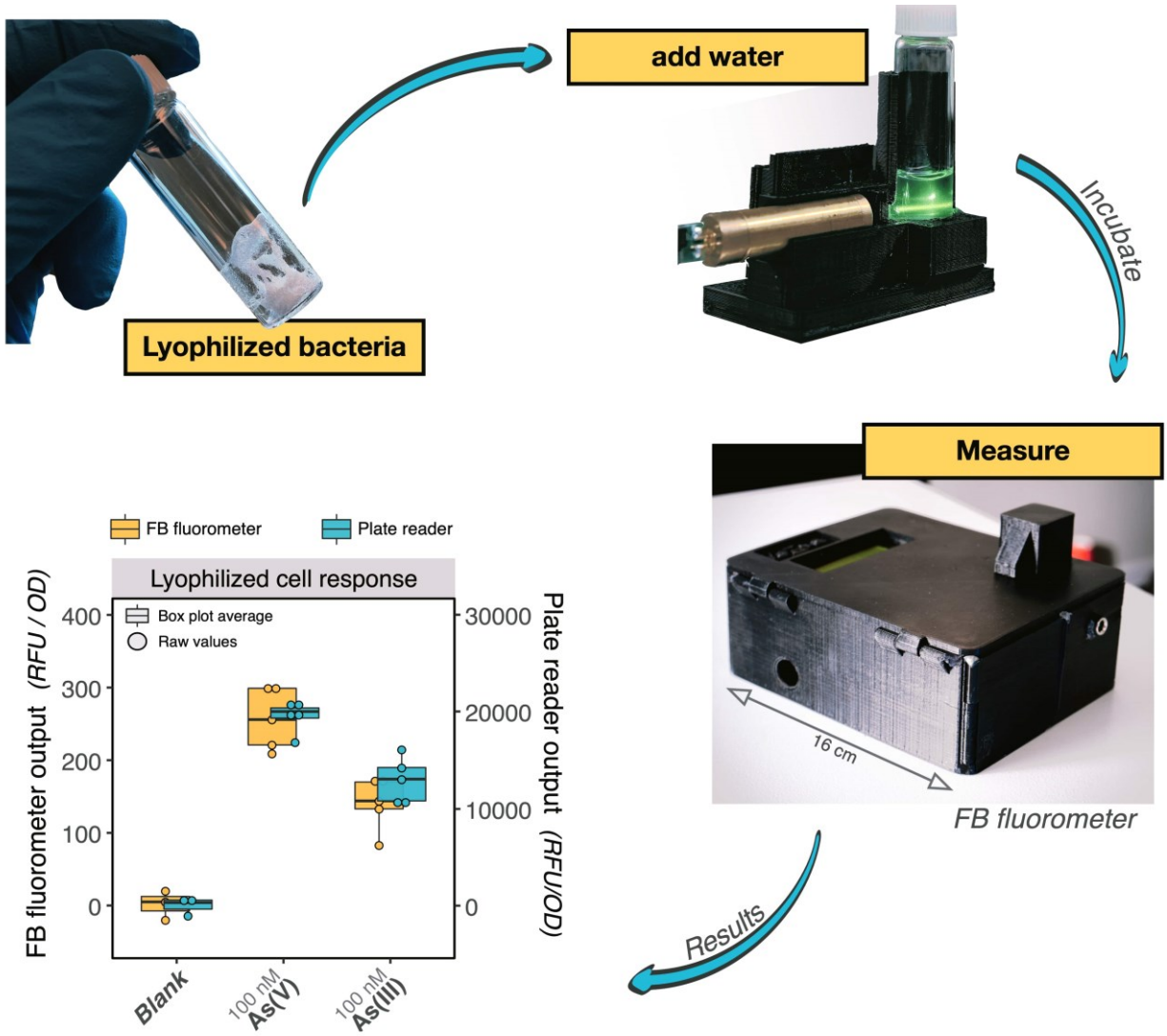

Figure 4.2 | Illustration of the single-step analysis of arsenic concentration in water using lyophilized biosensors and the Field Biosensor (FB) spectrometer. In a single measurement, the FB spectrometer removes the sample's baseline signal from the biosensor's fluorescent output (RFU) and displays a value that is normalized to the optical density (OD) of that culture. This digitization process (**orange boxes**) was compared to the analogue to digital conversion process of a BioTek microplate reader (**cyan boxes**). The resulting values of 5 individually lyophilized and rehydrated biosensor cultures (**points**), and the group's quartiles (**boxes**), are displayed.

4.4.2 Data analysis.

Current microplate readers, such as the one used in this study (BioTek Synergy HTX), are multimode instruments that produce excellent results and set the standards for measuring a sample's fluorescence and optical density. To enable detection of fluorescence at a cost and convenience applicable for large-scale deployment meant simplifying and specializing instrument design. By purpose building an instrument and integrating onboard algorithms (i.e., a computer connected to the instrument is not required), we managed to greatly reduce the steps involved in data collection and data analysis (**Figure 4.2**). We analyzed the same samples using the FB spectrometer and the multimode plate reader. Here, each box represents the response of 5 individually lyophilized pMP01 biosensor cultures to 100 nM of As(III) and As(V). We found the response of lyophilized biosensor cultures to As, at concentrations representative of WHO guidelines, could be clearly distinguished from the baseline (no As added). Moreover, no significant difference between the readouts of both instruments for cultures exposed to As(III) (p=0.172) nor for cultures exposed to As(V) (p=0.869). Regardless of the instrument used, we did not, however, expect to find a significant difference in the response of the biosensors to As(III) and As(V) when exposed at the same total As concentrations (p=0.0013) (**Figure 4.2**).

This was surprising to us because, using fresh biosensor cell cultures, we have consistently observed non-significant differences in the biosensor signal output whether the cells were exposed to As(III) or As(V). To do so, we modified the exposure medium to conditions that i) minimize possible As species uptake interference, and ii) favour the intracellular reduction of As(V) to As(III) (*15*). This was achieved by removing glucose and inorganic phosphates from the growth and exposure media (*15*). The species-specific outputs that are observed in this study led us to question whether constituents of the cryoprotectant solution were interfering

with As(III)/As(V) uptake kinetics, as was previously shown with glucose and inorganic phosphate (*15*).

Both trehalose and sucrose are common lyoprotectants used in the lyophilization of bacteria (*17, 26*). Because both sugar dimers contain glucose, we were interested in testing whether their use in the cryoprotectant solution could account for the difference in As(III) and As(V) detection. Since the primary As(III) uptake facilitator channel genes (*glp*F) are sensitive to catabolite repression (*15, 23, 37*), noticeable impact on As(III) uptake would presumably require intracellular transport, sensing and hydrolysis of sucrose, into a preferred carbon source (*e.g.*, glucose). We first tested whether the DH10B biosensor chassis carried the *scr* and *csc* gene clusters required for sucrose catabolism (*22*) using the KEGG genomic database (KEGG entry T00666) (*9*); it did not. Next, we attempted to grow the DH10B biosensor chassis in an FBMS medium supplemented with sucrose as the sole carbon source (absent pyruvate). Cells grew poorly and did not reach the exponential phase even after a 48-hour incubation at 37ºC in neither aerobic nor fermentative conditions (data not shown). These experimental findings supported genomic analysis suggesting that DH10B was incapable of metabolizing sucrose which would lead to the presence of glucose in the media. We therefore find it unlikely that supplementation of sucrose to FBMS medium would interfere with As(III) uptake, thus be responsible for the species-specific response observed in **Figure 4.2**. It is possible that the difference in As(III) and As(V) detection resulted from differences in As uptake kinetics and this is what we tested in a subsequent series of experiments.

4.4.3 Data analysis.

Practical use of biosensors requires calibrating bacterial response at known contaminant concentrations. Whether automated or not, numeric quantification of toxic metal(oid)s are often achieved using calibration curves. Like many biosensor assays, its fluorescent response is dynamic and tends to increase throughout the incubation period until a "plateau" is reached (ca. 18 to 20 h following exposure) (*15,*

16). In response to As, we have found the endpoint fluorescence of pMP01 biosensor cultures is maintained over prolonged periods (~48 h at 37ºC) (data not shown). mCherry's highly stable nature (*25*), has allowed us to build reliable datasets using calibration curves that only consider culture fluorescence at a single time point, typically soon after reaching the "plateau" phase (Chapter 3, **Figure 3.2**). Unfortunately, incubation of the biosensors in the new FBMS medium provides a reduced growth rate when compared to our original MGP medium (**SI Table A1.1**). How and if this translates to changes in the time required for the signal to stabilize remains unclear. It is also possible that a reduced doubling time could be affecting As uptake kinetics and therefore causing the species-specific differences observed in **Figure 4.2**. In a follow-up series of experiments, we were interested in assessing the effect of incubation time on the detection of As species (**Figure 4.3**).

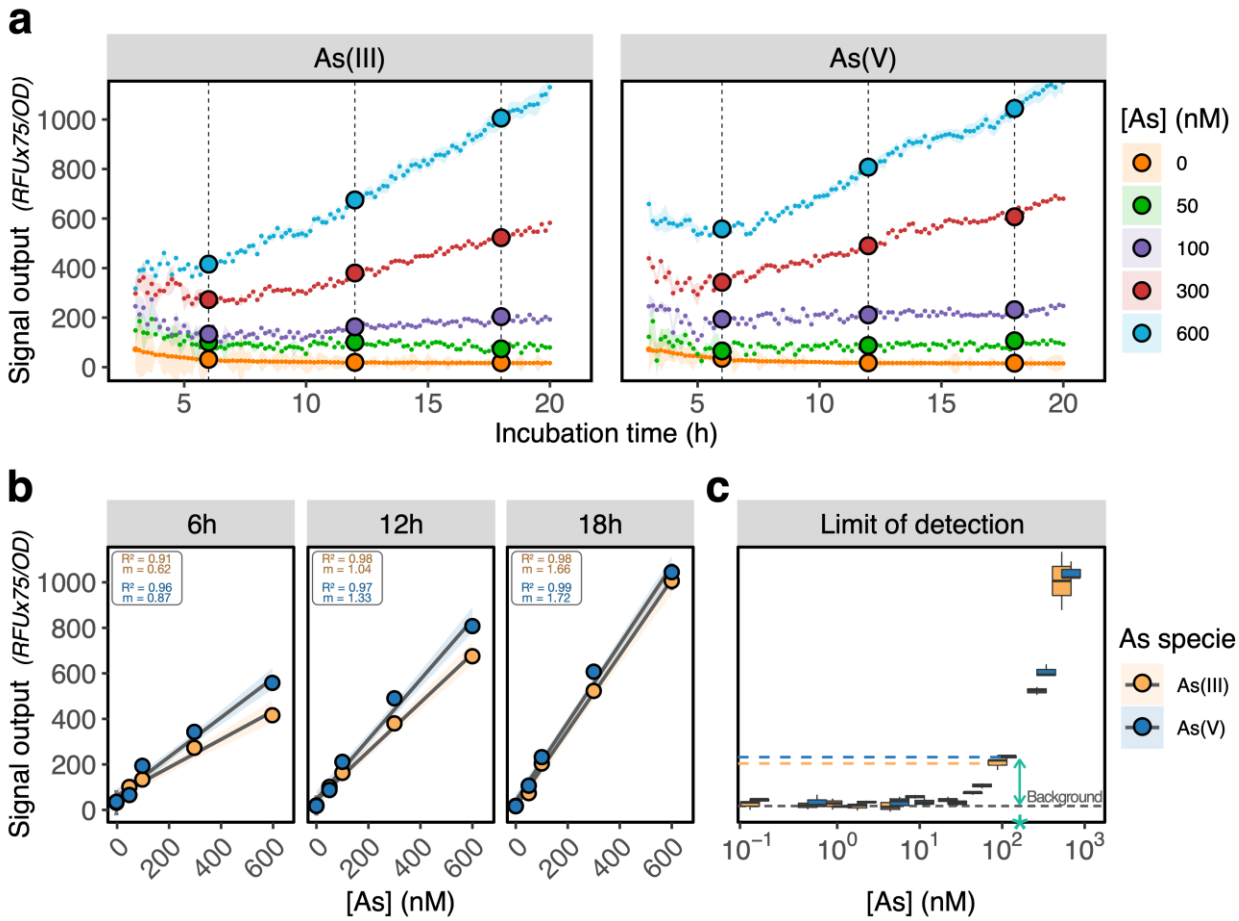

Figure 4.3 | Numeric conversion of biosensor signal to arsenic concentration involves capturing endpoint fluorescence at a specified time point. Fluorescent output (RFU) and optical density (OD) of the biosensor cultures were captured every 10 minutes using a BioTek plate reader. The normalized output signal (y-axis) is the same used throughout the study and includes 75x instrument conversion factor that is elsewhere used to align plate reader measurements with those of the FB spectrometer. Data points are then collected at specific incubation times (x-axis) (**a**) and plotted over known arsenic concentration (**b**). The linear range of the bacterial response to As(III) and As(V) (**c**) is determined using measured outputs at the 18 h time point. Current WHO and Canadian drinking water guidelines (**cyan star**) are set at 10 µg/L (or 133 nM) arsenic (*38*). The mean and standard deviation of triplicate exposures are presented. In panel b, error bars are smaller than the symbol size. Linear regressions (y~x) are presented by the lines and 95% confidence intervals by the shadings. In panel c, boxplot-present median response and quartile deviation of biological triplicates.

To test As species uptake kinetics, we exposed the pMP01 biosensor cultures to various As(III) and As(V) concentrations and extracted/plotted fluorescent output across various time points (**Figure 4.3**). We used a BioTek plate reader to capture biosensor output every 10 minutes (**Figure 4.3**a), filtered the dataset to 3 time points (6 h, 12 h and 18 h), and then plotted the normalized fluorescent response

over the spiked As concentration (**Figure 4.3**b,c). Using regression analysis, we found the most pronounced differences between As(III) and As(V) regression slopes to be at [As] <300 nM (**Figure 4.3**a), and for exposure times ≲12 hours (**Figure 4.3**b).

Here, the nature of As uptake pathways may be responsible for these differences. For instance, As(V) is thought to enter the cells through active Pi transporters (*21, 39*) rather than by osmotic gradient as shown for As(III) (*40*). Under our exposure conditions, bacterial cells were deprived of inorganic phosphates and of a carbon source favouring *glp*F induction (i.e., glycerol). It is possible that the difference between As(III) and As(V) uptake were caused by i) upregulation of Pi transport systems (As(V) transport), ii) the absence of GlpF inducers (As(III) transport) in the exposure media, iii) activation of As resistance pathways (*e.g.*, *ars*B efflux pump) (*28, 31*), or iv) to the differential interactions of As(III) and As(V) with yet unidentified cell wall components that may contribute to differential availability of As species over time. Because the fluorescent response tends to eventually stabilize to similar values, the marked differences in the first hours are therefore likely a result of differential uptake kinetics.

Recognizing that additional research is required to understand the mechanisms involved in the differential uptake kinetics of As(III) and As(V), we have found, in practice, that these differences were not affecting the accuracy of the measurements especially at ca. 18-20 hours following exposure. Using the FBMS minimal medium, the pMP01 fluorescent biosensor (*ars*R-*ars*R-mCherry) offered a broad linear detection range from 25 nM to 600 nM (or ~1.9–45 µg/L), that fully covers current WHO and Canadian drinking water guidelines (133 nM or 10 µg/L) (**Figure 4.3**c).

4.4.4 Environmental monitoring.

In this study, we highlight four ways environmental matrices could alter biosensor response, thereby affecting output consistency. These include changes to i) host

fitness/physiology, ii) baseline (background) signal, iii) As uptake kinetics, and iv) As bioavailability. It is important to highlight the implications of this last point since the control measures presented until now do not mitigate the potential impact of the sample's matrix on the bioavailability of As in these waters. Here, As transporter expression/availability, As complexation/exchange with ligands and the impact of ions on the outer membrane porosity/charge of the host chassis are just a few ways environmental waters could influence As bioavailability. How and if these factors combine to enhance or suppresses the analytical response, is better known as the "matrix effect" and is typically quantified through standard additions.

In analytical chemistry, standard additions are frequently used to eliminate rotational (Δ slope) but not translational matrix effects (Δ baseline or background) (*5*). In the context of environmental As biomonitoring, this calibration technique could be used as a quality control measure by allowing the user to assess the impact of the sample's matrix on the biosensor's performance. Take for instance a sample where the biosensor's response to the added As was 60% lower than the measured response in the external control. It would then be reasonable to expect a proportional decrease in the biosensor's response to the nominal (or historical) As content in those samples. Surprisingly, this was not the case when analyzing the waters of historically contaminated lakes in Northern Canada (*15*). Those findings are suggesting that rotational matrices (Δ slope) are only representative of the biosensor's response to newly added As. In a final series of experiments, we tested whether newly added As(III) and As(V) standards can be used as a quality control measure to eliminate rotational matrix effects in As biosensing (**Figure 4.4**).

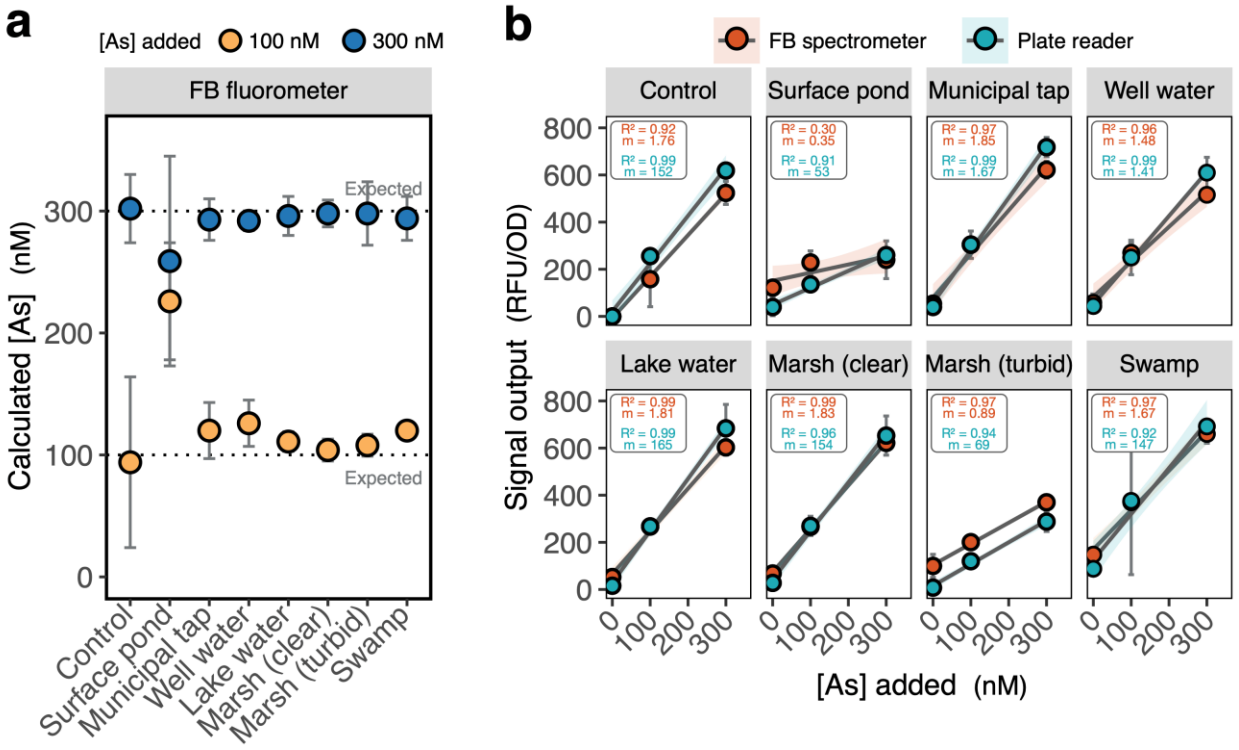

Figure 4.4 | Using As standard additions to characterize biosensor response in environmental matrices. The FB spectrometer's digitization process (**orange**) is compared to the analogue to digital conversion process of a BioTek microplate reader (**cyan**). Displayed are the average output (**points**) and standard deviation of 3 individually lyophilizes and rehydrated biosensor cultures as determined by both instruments using the same normalization algorithms. Plate reader measurements include a 75x instrument conversion factor to match FB spectrometer scale (y-axis). The slope and intercept of the linear regressions (y~x) (**b**) were used to predict the added As content (**a**). The dotted line is the expected response of the biosensors to the spiked arsenic.

Our sampling sites include water samples collected from a swamp, two marshes, surface water from Charleston Lake Provincial Park, a groundwater fed pond located in Chelsea, QC, groundwater from a private well in Ottawa, ON, and tap water from the city of Tottenham, ON (**Figure 4.4)**. Using the slope (m=1.76) and intercept (b=-8) of the external calibration curve (in FBMS medium only), we can convert bacterial response into a numeric As concentration. Using ICP-MS, we found all samples contained very low naturally occurring As levels (<1 µg/L or <12 nM) (**SI Table C1.2**). Since these concentrations are below the biosensor's limit of detection, we cannot cross-validate this response to the nominal As content of the samples. We

can, however, confirm an almost complete recovery of the newly added As content (**Figure 4.4**a) despite large differences in response curves (**Figure 4.4**b slopes).

Biosensors are analytical instruments that are sensitive to environmental factors that would typically not affect traditional analytical instruments. If the water samples were to impact the bioavailability of As, we expect the effect would manifest as a muted slope. This is because physiological and translational matrix effects are mostly accounted for in the normalized steps, and because this exposure medium was derived from a control platform with an estimated As bioavailability of ca. >94% (*15*). When using standard additions to predict nominal [As] concentration in environmental waters, it is vital to achieve a highly linear response curve (*5*).

The trade-off to using standard additions is the tripling of the samples required to test a sample. But this calibration technique does offer valuable insights into the validity of the readout. In the Surface Pond sample, the biosensor's response did not correspond to the of the nominal [As] added, nor the value obtained by the ICP-MS (**SI Table C1.2**). When biosensors exhibit a non-linear recovery of the added As standards, extrapolation of the calibration curve to zero should not be attempted as this could produce a false reading. Our recommendations are to reprocess any sample that i) does not meet the linearity criteria (R^2>0.9), and ii) presents a rotational matrix effect that exceeds a 60% difference relative to the external calibration slope. We recognize this process works over the small sample size presented here, and that a larger sampling effort is required to validate this mitigation procedure.

4.5 Conclusion

Achieving a single step As monitoring solution required breaking down the fundamentals of As redox chemistry, environmental ligand exchanges, and biological transport pathways. The hardware/software integration of the presented instrument drastically improved consistency of outcomes when measuring fluorescence. We then

simplified transportation of the bacterial sensors through a dehydration process. Our instrument, in combination with freeze-dried biosensors, was shown to accurately quantify As at concentrations that fully cover the WHO set guidelines for safe water consumption. The lyophilized biosensor cells produce a detectable signal at 100 nM As(III) and As(V) roughly 18-21 hours following rehydration. Although this time-sensitive constraint is not ideal, collection of a water sample with an overnight turnaround to measure it's As content does not seem prohibitive to its use. Moreover, our system does not produce toxic waste nor potentially expose the user to toxic chemicals.

We found the highest level of uncertainty increases as the concentration of naturally occurring As levels approach the biosensor's limit of detection. That said, there are a number of tests that can be performed to determine if such an event has occurred. These include standard additions, normalized for background fluorescence, autofluorescence, and optical density before converting to As concentration. Although standard addition may help assess the validity of the calculated [As], this calibration technique does triple the number of tests required by the user, and requires a more advanced understanding of its limitations. Going forward, implementation and automation of quality control measures such as this one into the core algorithms of portable instruments could make it fairly easy for users to predict the likelihood of producing false readings. Finally, we are hopeful that a speciation protocol described in our previous publication will be compatible with this instrument in the near future.

4.6 Acknowledgements

We would like to thank Dr. Emmanuel Yumvihoze for providing water chemistry analysis data using ICP-MS. We would also like to thank Carolyn Pothier, Tom Murphy, Laurie Chan and Kim Irvine, for assisting in the collection of the environmental water samples. This work was funded by an NSERC discovery grant,

an Early Researcher Award from the Province of Ontario, and an NSERC Accelerator Grant funding to AJP.

4.7 Author contributions

MPP, EJK, AJP conceptualized the project; MPP, EJK, BS initiated initial design and construction of the instrument; MPP, AJP and KP carried out the experiments; EJK and MPP wrote the Arduino codes that controls the instrument; MPP wrote the R scripts for data analyses; MPP wrote the manuscript with support from AJP, EJK, and BS; AJP, EJK and BS supervised the project. All authors have given approval to the final version of the manuscript.

4.8 Appendix A. Supplementary data

FBMS minimal medium constituents, water chemistry profiles, FB spectrometer concepts and construction, optical bandpass filtration, FB spectrometer Cambodian field validation.

4.9 Abbreviations

ADC, analog to digital converter; **As(III)**, arsenite; **As(V)**, arsenate; **BMS**, battery management system; **DOM**, dissolved organic matter; **EDTA**, Ethylenediamine-tetraacetic acid; **EM**, Electromagnetic; **FBMS**, field biosensor mixed salts; **HPLC**, high-performance liquid chromatography; **ICP-MS**, inductively coupled mass spectroscopy; **LB**, lysogeny broth; **MGP**, mops glycerophosphate; **MIP**, mops inorganic phosphate; **PCB**, polychlorinated biphenyl; **PLA**, polylactic acid; **pMP01**, Arsenic biosensor; **RFU**, relative fluorescent units; **TIA**, transimpedance amplifier; **WHO**, World Health Organization.

4.10 Declaration of interest statement

Authors declare no competing financial interest.

4.11 Bibliography – Chapter 4

1. P. Bhattacharya *et al.* (Elsevier, 2007).
2. S.-Y. Chen *et al.*, Development of a highly sensitive whole-cell biosensor for arsenite detection through engineered promoter modifications. *ACS synthetic biology* **8**, 2295-2302 (2019).
3. C. C. Conrad, K. G. Hilchey, A review of citizen science and community-based environmental monitoring: issues and opportunities. *Environmental monitoring and assessment* **176**, 273-291 (2011).
4. A. Date, P. Pasini, S. Daunert, Construction of spores for portable bacterial whole-cell biosensing systems. *Analytical Chemistry* **79**, 9391-9397 (2007).
5. S. L. Ellison, M. Thompson, Standard additions: myth and reality. *Analyst* **133**, 992-997 (2008).
6. S. Fendorf, H. A. Michael, A. van Geen, Spatial and temporal variations of groundwater arsenic in South and Southeast Asia. *Science* **328**, 1123-1127 (2010).
7. I. W. G. o. t. E. o. C. R. t. Humans, W. H. Organization, I. A. f. R. o. Cancer, *Some drinking-water disinfectants and contaminants, including arsenic*. (IARC, 2004), vol. 84.
8. A. Ivask *et al.*, Fibre-optic bacterial biosensors and their application for the analysis of bioavailable Hg and As in soils and sediments from Aznalcollar mining area in Spain. *Biosensors and Bioelectronics* **22**, 1396-1402 (2007).
9. M. Kanehisa, S. Goto, KEGG: kyoto encyclopedia of genes and genomes. *Nucleic acids research* **28**, 27-30 (2000).
10. A. Kuppardt, D. Vetterlein, H. Harms, A. Chatzinotas, Visualisation of gradients in arsenic concentrations around individual roots of Zea mays L. using agar-immobilized bioreporter bacteria. *Plant and soil* **329**, 295-306 (2010).
11. J. Li, S. S. Pawitwar, B. P. Rosen, The organoarsenical biocycle and the primordial antibiotic methylarsenite. *Metallomics* **8**, 1047-1055 (2016).
12. B. C. Matlock, D. Wilmington, Differences in bacterial optical density measurements between UV-Visible spectrophotometers. (2017).
13. D. Melamed, Monitoring arsenic in the environment: A review of science and technologies with the potential for field measurements. *Analytica Chimica Acta* **532**, 1-13 (2005).
14. S.-i. MIYASHITA *et al.*, Action is Needed on Chemicals of Major Public Health Concern. (2010).
15. M. P. Pothier, A. J. Hinz, A. J. Poulain, Insights Into Arsenite and Arsenate Uptake Pathways Using a Whole Cell Biosensor. *Frontiers in Microbiology* **9**, (2018).
16. M. P. Pothier *et al.*, Dissolved organic matter controls of arsenic bioavailability to bacteria. *Science of The Total Environment*, 137118 (2020).
17. S. Prévéral *et al.*, A bioluminescent arsenite biosensor designed for inline water analyzer. *Environmental Science and Pollution Research* **24**, 25-32 (2017).
18. E. Revesz, D. Fortin, D. Paktunc, Reductive dissolution of scorodite in the presence of Shewanella sp. CN32 and Shewanella sp. ANA-3. *Applied Geochemistry* **63**, 347-356 (2015).
19. E. Revesz, D. Fortin, D. Paktunc, Reductive dissolution of arsenical ferrihydrite by bacteria. *Applied Geochemistry* **66**, 129-139 (2016).
20. A. Roda *et al.*, Bioengineered bioluminescent magnetotactic bacteria as a powerful tool for chip-based whole-cell biosensors. *Lab on a Chip* **13**, 4881-4889 (2013).
21. H. Rosenberg, R. Gerdes, K. Chegwidden, Two systems for the uptake of phosphate in Escherichia coli. *Journal of bacteriology* **131**, 505-511 (1977).
22. S. Sabri, L. K. Nielsen, C. E. Vickers, Molecular control of sucrose utilization in Escherichia coli W, an efficient sucrose-utilizing strain. *Appl. Environ. Microbiol.* **79**, 478-487 (2013).

23. O. I. Sanders, C. Rensing, M. Kuroda, B. Mitra, B. P. Rosen, Antimonite is accumulated by the glycerol facilitator GlpF in Escherichia coli. *Journal of bacteriology* **179**, 3365-3367 (1997).
24. M. C. Sforna *et al.*, Evidence for arsenic metabolism and cycling by microorganisms 2.7 billion years ago. *Nature Geoscience* **7**, 811 (2014).
25. N. C. Shaner *et al.*, Improved monomeric red, orange and yellow fluorescent proteins derived from Discosoma sp. red fluorescent protein. *Nature Biotechnology* **22**, 1567-1572 (2004).
26. K. Siegfried *et al.*, Field testing of arsenic in groundwater samples of Bangladesh using a test kit based on lyophilized bioreporter bacteria. *Environmental Science and Technology* **46**, 3281-3287 (2012).
27. K. Siegfried *et al.*, Introducing Simple Detection of Bioavailable Arsenic at Rafaela (Santa Fe Province, Argentina) Using the ARSOlux Biosensor. *International Journal of Environmental Research and Public Health* **12**, 5465 (2015).
28. S. Silver, D. Keach, Energy-dependent arsenate efflux: the mechanism of plasmid-mediated resistance. *Proceedings of the National Academy of Sciences* **79**, 6114-6118 (1982).
29. M. T. Smith, S. D. Berkheimer, C. J. Werner, B. C. Bundy, Lyophilized Escherichia coli-based cell-free systems for robust, high-density, long-term storage. *Biotechniques* **56**, 186-193 (2014).
30. B. Stenzler, A. Hinz, M. Ruuskanen, A. J. Poulain, Ionic strength differentially affects the bioavailability of neutral and negatively charged inorganic Hg complexes. *Environmental science & technology* **51**, 9653-9662 (2017).
31. L. S. Tisa, B. Rosen, Molecular characterization of an anion pump. The ArsB protein is the membrane anchor for the ArsA protein. *Journal of Biological Chemistry* **265**, 190-194 (1990).
32. M. Tramier, M. Zahid, J. C. Mevel, M. J. Masse, M. Coppey‐Moisan, Sensitivity of CFP/YFP and GFP/mCherry pairs to donor photobleaching on FRET determination by fluorescence lifetime imaging microscopy in living cells. *Microscopy research and technique* **69**, 933-939 (2006).
33. P. T. K. Trang, M. Berg, P. H. Viet, N. Van Mui, J. R. Van Der Meer, Bacterial bioassay for rapid and accurate analysis of arsenic in highly variable groundwater samples. *Environmental Science and Technology* **39**, 7625-7630 (2005).
34. F. Truffer *et al.*, Compact portable biosensor for arsenic detection in aqueous samples with Escherichia coli bioreporter cells. *Review of Scientific Instruments* **85**, (2014).
35. A. Van Geen *et al.*, Promotion of well-switching to mitigate the current arsenic crisis in Bangladesh. *Bulletin of the World Health Organization* **80**, 732-737 (2002).
36. X. Wan *et al.*, Cascaded amplifying circuits enable ultrasensitive cellular sensors for toxic metals. *Nature chemical biology* **15**, 540 (2019).
37. D. L. Weissenborn, N. Wittekindt, T. J. Larson, Structure and regulation of the glpFK operon encoding glycerol diffusion facilitator and glycerol kinase of Escherichia coli K-12. *Journal of Biological Chemistry* **267**, 6122-6131 (1992).
38. *Guidelines for drinking-water quality: recommendations* (9241546387, 2004).
39. G. R. Willsky, M. H. Malamy, Effect of arsenate on inorganic phosphate transport in Escherichia coli. *Journal of Bacteriology* **144**, 366-374 (1980).
40. R. Wysocki *et al.*, The glycerol channel Fps1p mediates the uptake of arsenite and antimonite in Saccharomyces cerevisiae. *Molecular microbiology* **40**, 1391-1401 (2001).
41. Y.-G. Zhu, X.-M. Xue, A. Kappler, B. P. Rosen, A. A. Meharg, Linking genes to microbial biogeochemical cycling: lessons from arsenic. *Environmental Science & Technology*, (2017).

Annex C – Chapter 4 SI

SUPPLEMENTARY MATERIALS

Design and application of a portable spectrometer to detect As at nanomolar levels

***Martin P. Pothier*[1], *Eric J. Kitchen*[1], *Bill Sinclair*[2], *Kongkea Phan*[3], *Alexandre J. Poulain*[1]**

[1] *Biology Department, University of Ottawa, 30 Marie Curie, Ottawa, ON, K1N 6N5, Canada*

[2] *Independent Consultant, Ottawa, ON, Canada*

[3] *Faculty of Science and Technology, International University, Phnom Penh, 12210, Cambodia*

List of supplementary materials:

The following Supplementary Materials contains confidential information that has must be revised by uOttawa Innovation Support Services before submission for publication.

Annex C1 Supplementary table

SI Table C1.1 | Constituent concentration in the FBMS medium.

Reagents	Salt	[Constituents] in stock solution (M)	[Constituents] in FBMS medium (M)	[Constituents] upon biosensor exposure (M)
Field buffer (pH=7.150)	$C_7H_{14}NO_4S$ (acid)	0.352	0.0350	0.0315
	$C_7H_{14}NNaO_4S$ (base)	0.348		
	KCl	0.300	0.0150	0.0135
	$(NH_4)_2SO_4$	0.640	0.0320	0.0290
	EDTA	$1x10^{-5}$	$5.00\ x10^{-7}$	$4.50\ x10^{-7}$
	$FeCl_2 \cdot 4H_2O$	$1x10^{-5}$	$5.00\ x10^{-7}$	$4.50\ x10^{-7}$
Magnesium sulphate	$MgSO_4$	2.0	$1.25x10^{-3}$	$1.40x10^{-4}$
Pyruvate	$CH_3COCONa$	0.100	0.030	0.0150
Fumarate	NaOOCCH=CHCOONa	1.000	0.030	0.0110
β-glycerophosphate	$(HOCH_2)_2CHOP(O)(ONa)_2 \cdot H_2O$	0.400	0.001	$9.00x10^{-4}$
Amino acids	L-Leucine	0.075	$2.28x10^{-4}$	$2.05x10^{-4}$
	L-Isoleucine	0.075	$2.28x10^{-4}$	$2.05x10^{-4}$
	Valine	0.075	$2.28x10^{-4}$	$2.05x10^{-4}$
Trace elements #1 (0.1M H_2SO_4)	$NiCl_2 \cdot 6H_2O$	$6.25x10^{-3}$	$1.25x10^{-5}$	$1.25x10^{-6}$
	$CoCl_2 \cdot 6H_2O$	$3.25x10^{-3}$	$6.50x10^{-6}$	$6.50x10^{-7}$
	$ZnSO_4$	$5.00x10^{-4}$	$1.00x10^{-6}$	$1.00x10^{-7}$
	$MnSO_4$	$1.00x10^{-2}$	$2.00x10^{-5}$	$2.00x10^{-6}$
Trace elements #2 (0.1M NaOH)	H_3BO_3	$5.00x10^{-3}$	$1.00x10^{-5}$	$1.00x10^{-6}$
	Na_2SeO_4	$1.50x10^{-3}$	$3.00x10^{-6}$	$3.00x10^{-7}$
	$Na_2MoO_4 \cdot 2H_2O$	$6.50x10^{-4}$	$1.30x10^{-6}$	$1.30x10^{-7}$

SI Table C1.2 | Chemical profiles and coordinates of the water samples collected in **Figure 4.4**.

	As (Bio[1])	As (Bio[2])	As (ICP[3])	Fe	Cu	Mn	Ca	Mg	Na	K	P	Coordinates
Sample ID	(nM)	(nM)	(nM)	(µg/L)	(µg/L)	(µg/L)	(µg/L)	(µg/L)	(µg/L)	(µg/L)	(µg/L)	Lat, Long (DD[4])
Surface pond	90	15	1.32	2.7	2.1	0.25	36.4	2.1	3.1	0.99	<0.000	Chelsea, QC
Municipal tap	50	53	4.62	1.6	145.7	2.16	14.7	7.8	18.1	0.63	<0.000	Tottenham, ON
Well water	52	43	1.13	1.7	26.7	2.04	35.6	2.3	21.6	1.35	<0.000	Ottawa, ON
Lake	42	43	3.40	2.6	0.9	0.25	7.9	3.1	2.1	0.17	<0.000	44.517, -76.028
Marsh (clear)	47	48	5.94	18.0	2.4	0.30	35.5	10.9	194.7	1.80	0.001	44.393, -76.018
Marsh (turbid)	64	33	11.61	5.7	2.2	0.50	40.7	9.0	23.0	2.00	0.079	44.394, -75.922
Swamp	101	96	2.54	146.8	2.5	0.83	13.9	3.0	2.2	1.24	0.133	44.516, -76.018

[1] Biosensor predictions for As concentrations in water.

[2] Corrected biosensor predictions using a bioavailability correction factor.

[3] As concentrations as calculated using ICP-MS

[4] DD = decimal degrees coordinates.

Annex C2 Supplementary figures

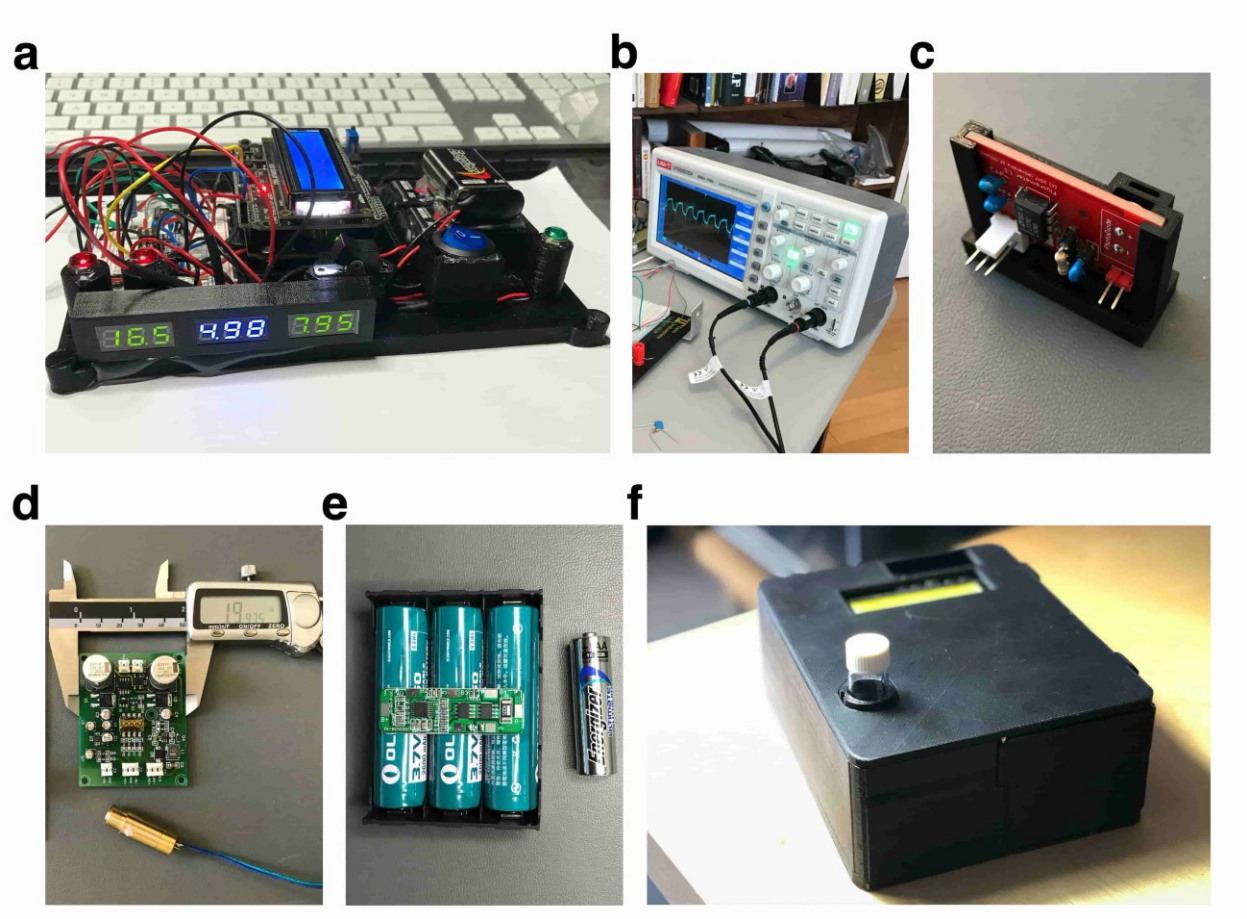

SI Fig. C2.1 | Construction of the FB spectrometer required integration of components onto custom printed microcircuit boards to reduce EM interference.

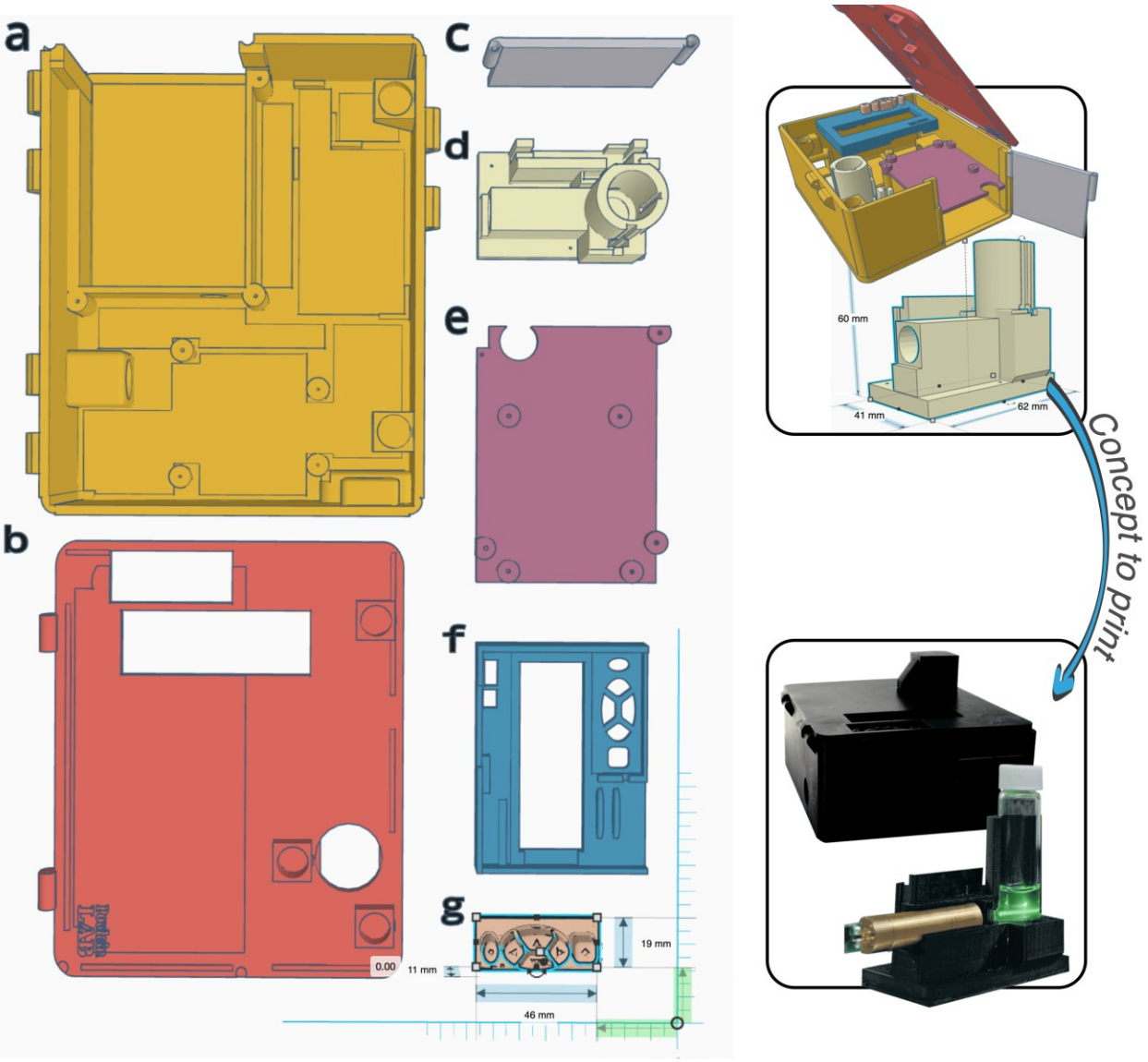

SI Fig. C2.2 | Concept and design of the FB spectrometer. Final assembly parts include **a)** main case/outer shell, **b)** case lid with integrated hinges, **c)** hinged battery compartment access door, **d)** vial/photodiode holder, **e)** battery compartment cover, **f)** Arduino LCD shield cover, and **e)** LCD shield button cover. All assembly parts were designed using Tinkercad and printed using PLA plastic with exception of part g that was printed using flexible thermoplastic polyurethane.

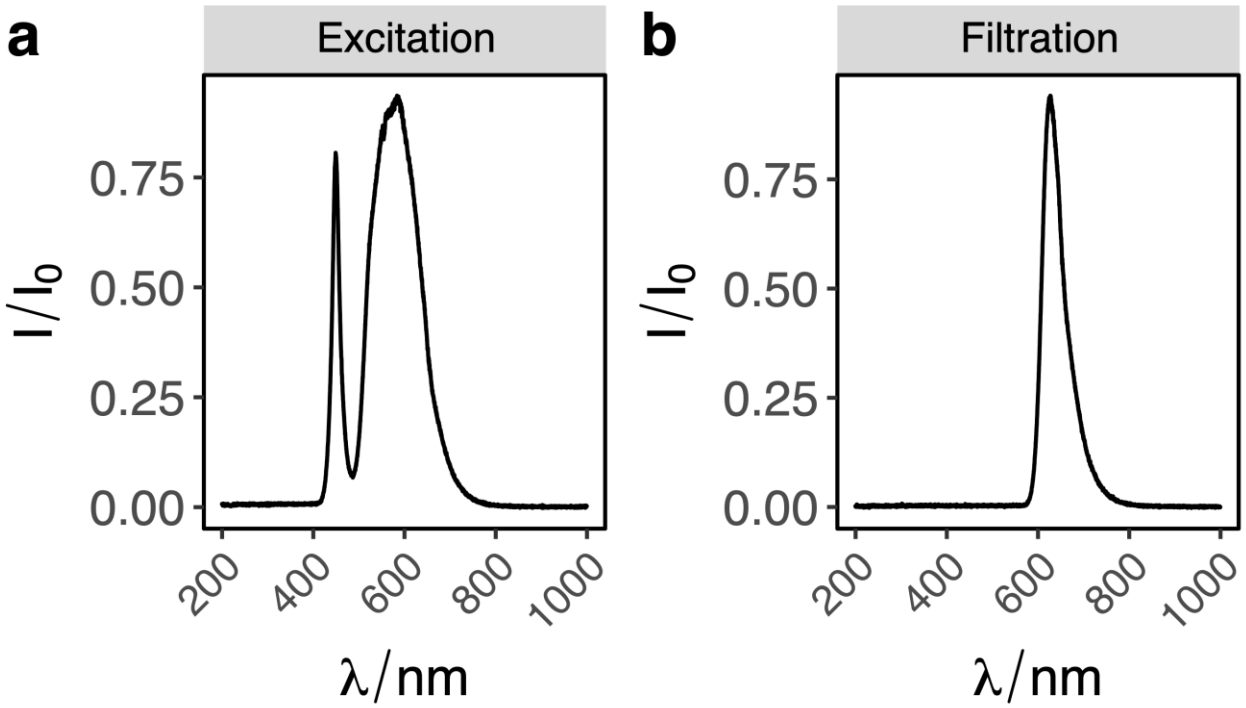

SI Fig. C2.3 | Removal of excitation wavelengths using a 590-640 nm optical density filter. Emission spectrum of a smartphone's rear facing light emitting diode is presented before (a) and after (b) the optical bandpass filter.

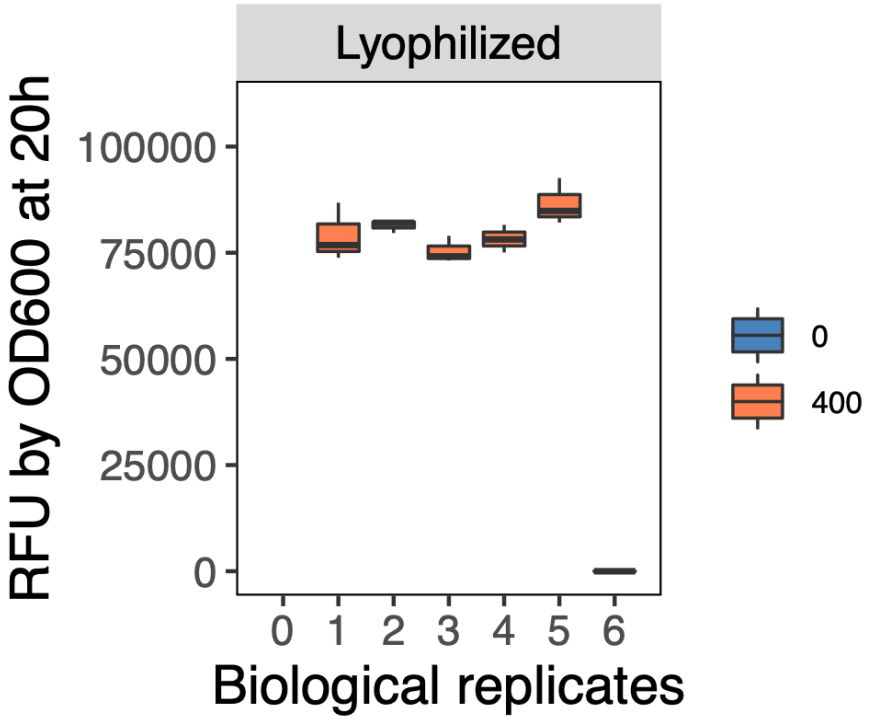

SI Fig. C2.4 | Comparison of lyophilized biosensor culture response to 0 and 400 nM As(V). Each lyophilized biosensor vials were hydrated then divided into three separate wells and cultured using a microplate reader. The group's quartiles and median are displayed (boxes).

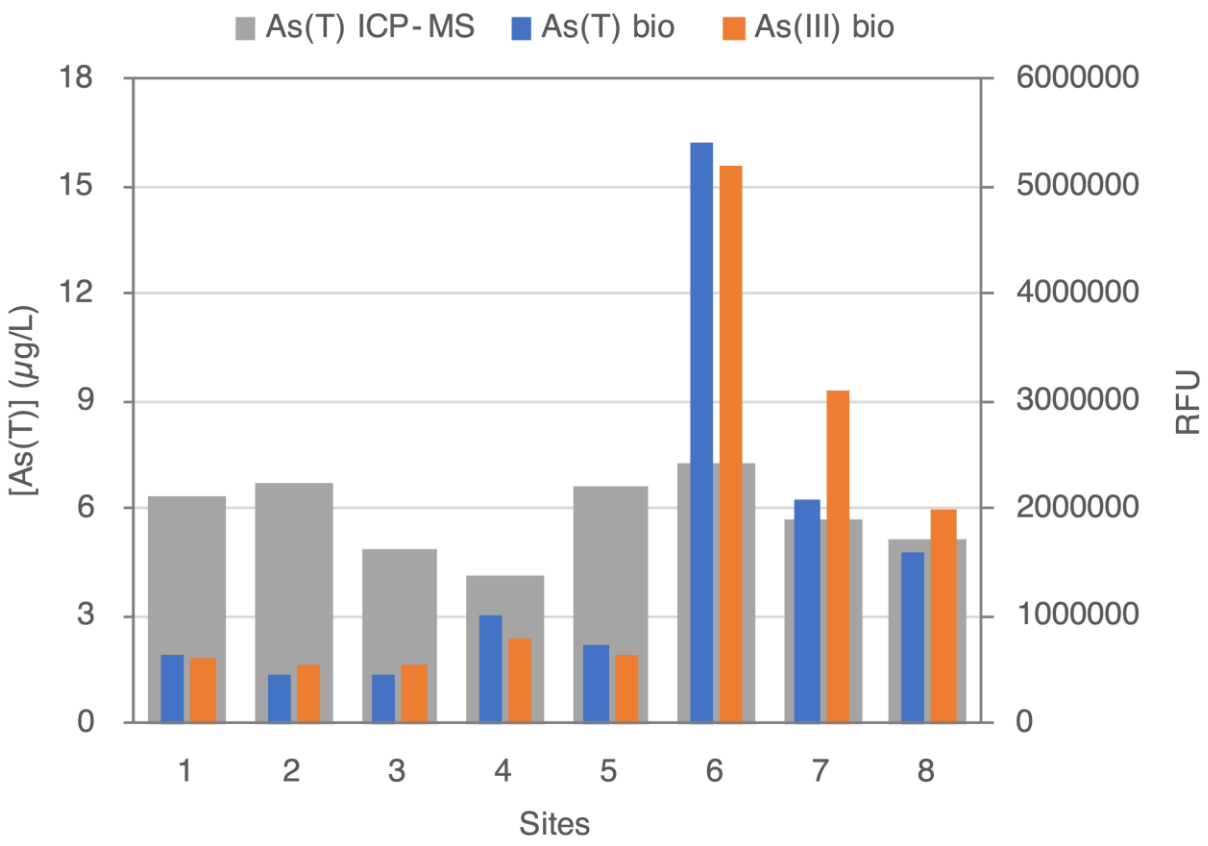

SI Fig. C2.5 | Field validation of a prototype version of the FB spectrometer using lyophilized biosensor cultures. Naturally occurring As concentration were determined using HPLC-ICP-MS (**grey bars**). The response of a single lyophilized biosensor culture is presented with (+) inorganic phosphate (**orange bars**) and without (-) inorganic phosphate (**blue bars**). Addition of 10 mM phosphate to the cultures produces a biosensor response that is proportional to As(III) concentration in the sample (Chapter 2). Raw RFU values are presented (y-axis) that has not been corrected for background fluorescence, background noise nor for culture yield.

Chapter 5 – Research synthesis

5.1 Summary of research contributions

The goal of my thesis research was to develop, validate and test a new bioanalytical instrument and associated protocol to assess the bioavailability of inorganic As species in the environment. At its core, my thesis research achieved a simple As monitoring solution using dehydrated bacterial sensors and a compact spectrometer. With it, I established a platform that allowed me to answer knowledge gaps in the fields of biology and engineering in the context of As biogeochemistry.

5.1.1 In the field of Biology

In Chapter 2, I addressed the inconsistencies among *ars*R-based biosensors that have prevented their widespread use. These included i) improving lower limit sensing performance, ii) addressing biosafety concerns, and iii) determining whether the heterogeneity among As biosensor exposure conditions were responsible for the variability in As(V) detection reported so far. I tested the hypothesis that inorganic phosphate controls cytoplasmic As(V) concentration. I also tested whether the presence of glucose in exposure media limited uptake of As(III) into the cytoplasm.

I developed a biological exposure assay that, for the first time, is capable of detecting As(V) at the same concentration and signal intensity as As(III). I further tested the hypothesis by reintroducing competing agents (10 mM Pi salts) in the medium and found drastic decrease in biosensor response to As(V) even within a mixture of As(III) and As(V). I used a combination of wildtype and mutant biosensors

to determine what constituents of environmental waters can interfere with As uptake by monitoring for changes in biosensor signalling. Overall, this assay offers a control platform on which I also gained insights into: i) the role of central carbon metabolism on As(III) uptake, ii) the importance of *ars*-independent reduction pathways in detection of As(V) by ArsR, and iii) the bioavailability of legacy As contamination in environmental samples where DOC was highlighted as a possible driver.

In Chapter 3, I was interested in identifying potential drivers of As bioavailability in environmental waters. Here, I tested the hypothesis that DOM controls both As(III) and As(V) bioavailability. More specifically, this study was the first to explore the nature of As-DOM interactions through cation amendments and photoirradiation experiments. It established an environmentally relevant baseline and identified conditions that dictated As-DOM bond strength and provided insights into DOM's photoreactive nature and its influence on As(III) redox in solution.

Studying this topic required that I develop an As biosensor exposure assay and a series of algorithms that normalizes and isolates biosensor response to As within the complex environmental matrices. Using R programming language, I conceptualized a data normalization framework that i) extracts pertinent information directly from a Tecan F200 Pro plate reader datasheet, ii) compiles datasets from multiple assays, and iii) standardizes biosensor output in a format that best represents bacterial response to As, with minimal influence from the sample's matrix. Each step encoded by these algorithms have been illustrated in **Figure 3.2**, of Chapter 3.

5.1.2 In the field of Engineering

In Chapter 4, I was interested in building a compact, easy-to-use, and customizable instrument to enable deployment of the bioassay outside of the laboratory. For this last research objective, I assembled a multidisciplinary team of experts in the fields of physics, mechanical engineering, programming and microcircuit design. The initial

objective was to miniaturize expensive and fragile plate reader hardware into a robust and inexpensive casing, made of open source microelectronics and 3D printed parts. Once built, I quickly realized that integration of the normalization algorithms into the core processes of the portable fluorometer was necessary and essential to overcome the constraints that have historically hindered market reach of biosensor solutions.

Through a lengthy development process, I amended the fluorescent detection components with hardware and software that now adds the ability to normalize fluorescent signals to culture yield (OD_{600}). This inexpensive and portable spectrometer can now also account for translational and physiological matrix effects on biosensor signalling. In this study, I also presented a possible way we could use standard additions to account for rotational matrix effects, but a larger sample collection effort will be required to validate this approach. Although these findings are promising, achieving a market-ready solution will require a commercialization push that goes beyond my expertise and the scope of this thesis. I am therefore actively looking for partnership opportunities so that all code and plans of this instrument can be used to produce this technology.

5.2 Applications

As described in **Section 1.2.2**, microbes can greatly affect mineral stability and therefore the concentration and speciation of As in water. Microbes used as sensory probes (biosensors) offer a practical and cost-effective alternative to current analytical methods.

5.2.1 Development of a field-ready As speciation technique

In-situ quantification of bioavailable As species is key in determining immobilization methods and mitigating health risks. Currently, the use of traditional As speciation techniques are costly, not easily portable, and require tedious sample preservation

steps that are inconsistent among studies. Thus, speciation is rarely undertaken unless required by risk management.

Use of biosensors as As monitoring probes is a solution that has lacked suitable instruments capable of measuring the signals produced by these biosensors outside of the laboratory environment. There is now an increasing push for connected devices to support citizen science. The bioassay and associated hardware technology presented here now present a safe, cost-effective and scalable solution that could be used to support critical, evidence-based decision-making on choosing irrigation and drinking water sources. Through a scaled commercialization effort, this instrument could be used to assess and to monitor water quality of those affected by historical mining activities, or farmers in choosing irrigation water sources.

5.2.2 Fluorescence detection beyond biosensors

Until now, I have developed hardware and software technology to measure biological signals that originate from the whole cell As biosensing systems. Portable technology development for the sensitive detection of biological signals is a booming field. With its small footprint, this compact spectrometer provides a portable interface that can be adapted for applications outside of As biosensing. Now at the end of my doctoral research, I am in the process of adapting this technology for the detection of nano-sized DNA aptamers. One possible application is to support deployment of aptasensors as ultrasensitive and rapid diagnostic test for COVID-19. Achieving this goal will require collaboration with industrial partner(s) well-versed in plastic injection molding, low-cost photonics, iOS/android app design, and microcircuit manufacturing.

5.2.3 Uncovering fundamentals of As biogeochemical cycling

Through a number of collaborations, I have used these biosensors to quantify the bioavailable fraction of As in the interstitial waters of sea- and fresh-water sediments (**Figure 5.1**). It has also been used for paleo-ecotoxicology purposes (collaboration

with C. Cheney and J. Blais), and as a means to study seasonal fluctuations of As release in historically contaminated lake sediments (collaboration with M. Palmer and J. Chetelat). I also cloned the biosensor plasmid into a halotolerant *E. coli* strain (NEB 5α) to evaluate As bioavailability in the pore waters of a sediment core collected in the Mediterranean Sea (*unpublished*). Finally, in a collaboration Prof. Reid at Cornell University, we are using the biosensor together with synchrotron-based X-ray absorption spectroscopy technique to further explore how the structure of DOM affect its reactivity with As (*in progress*).

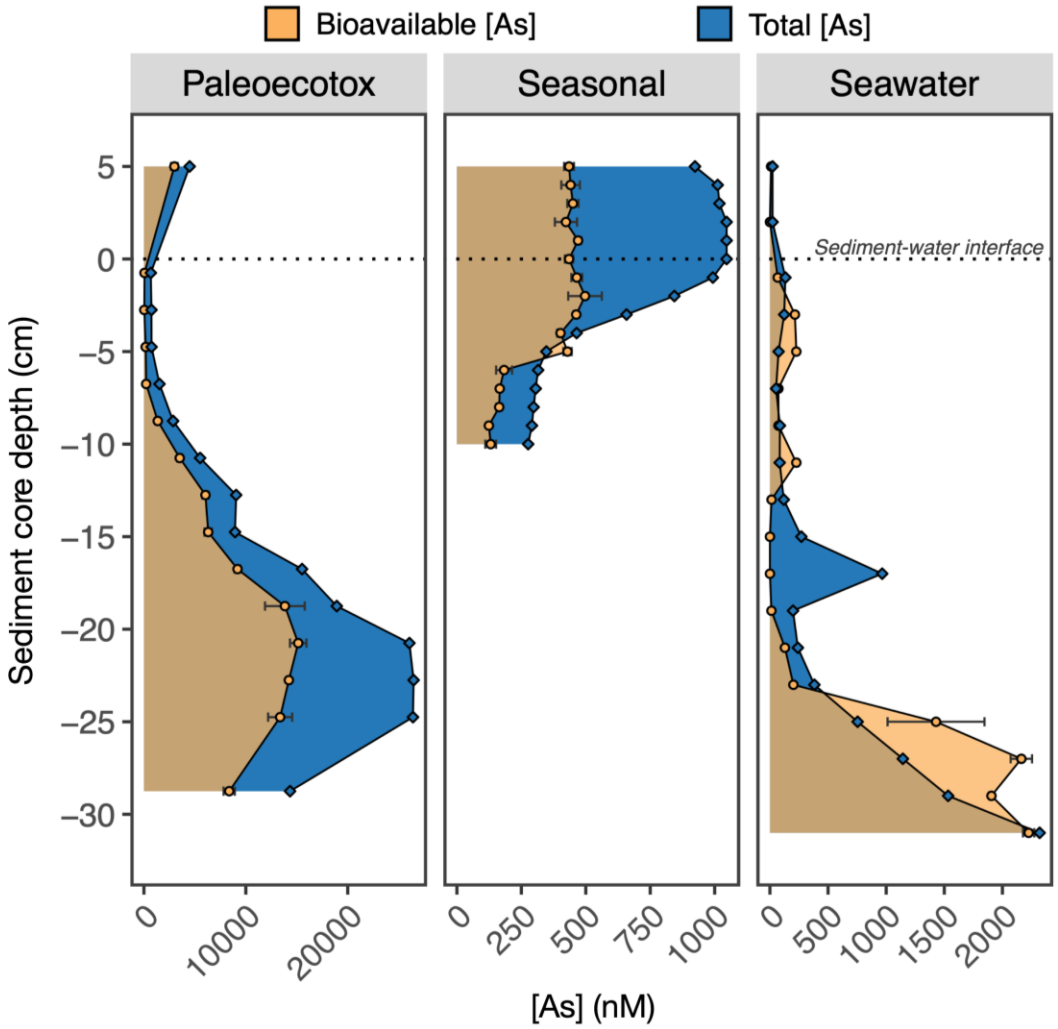

Figure 5.1 | Use of biosensors to study the drivers of As bioavailability between groundwater and sediments. The biosensor signal (X-axis) can be cross analyzed with a number of instruments all along the sediment core (Y-axis). Possible study sites include freshwater and seawater. Current collaborations include paleoecotoxicology, seasonal drivers, and marine drivers in sediment porewaters.

The use of bacterial sensors in this work has revealed that a large fraction of geogenic As is labile and is bioavailable fraction comprised of both unbound As, and As that is weakly complexed to DOM. This fraction was found to be sensitive to i) complexation time (age), ii) [As]/[DOM] ratio, iii) As-DOM bond strength, and iv) ionic competitive desorption. This ubiquitous sorbent of As is also photoreactive and seems to evoke a protective effect on maintaining As(III) speciation during photoirradiation. Overall, these findings have challenged the notion of DOM-bound metal(oid)s being inaccessible to microbes.

The role that DOM plays on the bioavailability of As to microbes is often invoked but had remained untested experimentally. In addition to organic carbon, I have also found inorganic phosphate cations to be major drivers of environmental As bioavailability. Going forward, there are many more environmentally relevant questions that have yet to be answered. An interesting follow-up study would be to test the hypothesis that microbes can indirectly affect As-DOM bond strength. An idea would be to add spent culture supernatant to an As-DOM solution. Here, I predict that the microbes' growth conditions (*e.g.*, Pi or Fe starvation) would influence the extent of As release through external cell controls (*e.g.*, siderophores, extracellular e- transfer, etc.).

5.3 Limitations

One of the more challenging aspects of environmental As biogeochemical cycling is determining the contributions of each environmental variable within the complex environmental matrix. By isolating and individually testing environmental variables, I managed to derive a number of insights regarding how these can impact As bioavailability under defined and simplified exposure conditions. But the environment presents a far more complex system with a number of synergies among variables that equal to an effect that can be much larger than the sum of its parts (i.e., its emergent properties). When exposed directly to environmental waters, whole-cell

biosensors do present a biologically relevant signal. That being said, it is important to note that the research presented in this thesis was mostly performed under controlled laboratory conditions using a bacterial chassis that underwent numerous genetic modifications. While the reasons for choosing this model organism were detailed in each chapter, they mostly revolve around high output signalling, biosafety, and well-defined genetic determinants.

Going forward, it would be important to adapt this bioassay for conditions that best represent the environment where microbially-mediated mineral dissolution mostly occurs. Future work should therefore consider working under strict anaerobic conditions and also consider using a more environmentally relevant biosensor chassis (*e.g.*, *Shewanella* sp.). It would also be important to expand the field monitoring effort to include a wider range of environmental waters and drinking water sources. The insights presented in this work serve as a baseline and are important for guiding future investigations into the environmental drivers of As bioavailability.